KU LEUVEN

FACULTY OF SCIENCE

Humanized yeast models to study aggregation of the Parkinson's Disease related proteins α-synuclein and synphilin-1

Jordi DOIJEN

Supervisor: Prof. Dr. J. Winderickx
KU Leuven
Mentor: Dr. V. Franssens
KU Leuven

Thesis presented in
fulfillment of the requirements
for the degree of Master of Science
in the biochemistry and biotechnology

Academic year 2014-2015

Preface

First of all I would like to thank my daily mentor Vanessa for her overall assistance and guidance during my project, both in lab as for the writing part. Additionally, I want to thank her for the time she took to explain me how to perform certain experiments and for teaching me important aspects concerning the research topic. I couldn't have hoped for a better mentor and I wish you the best.

Furthermore, I would like to thank my supervisor, head of the Functional biology lab, Joris Winderickx for the opportunity to perform this research project in his lab and for providing me with all required tools to give the best of myself. Furthermore, I want to thank him for his guidance and the time he took for discussing results.

Moreover, I would like to thank the current and former PhD students Tobias, Tine, Gernot and Katrien and the postdoc Erwin for the helpful conversations concerning the project but also for making my time at the Functional Biology lab a pleasant and educative journey. Further, I want to thank Joelle and Cat for their assistance during the experimental work and for always being positive.

A special thanks to Tobias for suggesting the idea of using an alternative approach i.e. myc-tagged ubiquitin, for studying SY1 ubiquitination. This approach appeared to be very helpful. I want to thank the lab of Prof. Thevelein for providing me with the myc-tagged ubiquitin expressing plasmid.

I also want to thank my friends for giving me a great year with a lot of fun and laughter. This helped me to stay optimistic and to put everything into perspective.

A big thank you to Pieter, a former fellow student and good friend, for his assistance according some problems I experienced with Latex.

My sincere gratitude also goes to my parents and brother and the rest of my family for supporting me over the past year. I consider myself very lucky for having you all.

Jordi Doijen

List of Abbreviations

α-syn	α-synuclein
AADC	aromatic amino acid decarboxylase
ALP	Autophagosome-Lysosome Pathway
APS	Ammonium persulfate
Amp^R	Ampicilin resistance marker
Atg8	Autophagy-related protein 8
ATP	Adenosine Triphosphate
BBB	Blood brain barrier
BLAST	Basic Local Alignment Searching Tool
CCD	Coiled-coil Domain
CHAPS	3-[(3-Cholamidopropyl)dimethylammonio]-1-propanesulfonate
COMT	Catechol-O-methyltransferase
CMAC	7-amino-4-chloromethylcoumarin
Ctrl.	Control strain/condition
DAPI	4'-6-Diamidino-2-phenylindole
DHE	Dihydroethidium
DMSO	Dimethylsulfoxide
DNA	Deoxyribonucleic acid
DUBs	Deubiquitinating enzymes
ECL	Enhanced Chemiluminescence
EDTA	Ethylenediaminetetraacetic acid
EGFP	Enhanced Green Fluorescent Protein
ERAD	endoplasmic reticulum associated protein degradation
EtOH	Ethanol
GTP	Guanosine triphosphate
H_2O	Water
HEPES	2-[4-(2-hydroxyethyl)piperazin-1-yl]ethanesulfonic acid
HIS	Histidine
HRP	Horseradish Peroxidase
Hsp104	Heat shock protein 104
IPOD	Insoluble protein deposit
JUNQ	Juxtanuclear quality control
LB	Lewy bodies
L-Dopa	Levodopa
LEU	Leucine
LiAc	Lithium acetate

MET	Methionine
MilliQ	'ultrapure' water (Millipore Corporation)
NaF	Sodium fluoride
NaOH	Sodium hydroxide
NEM	N-ethylmaleimide
NH_4SO_4	Ammonium sulphate
OD	Optical Density
PBS	Phosphate buffered saline
PCR	Polymerase Chain Reaction
PD	Parkinson's Disease
PEG	Polyethylene glycol
PI	Propidium iodide
PQC	Protein quality control
PVDF	Polyvinylideenfluoride
RING	Really Interesting New Gene
ROS	Reactive oxygen species
rpm	Revolutions per minute
SCF	Skp, Cullin, F-box
SD	Synthetic Dextrose
SDS	Sodium dodecyl sulphate
SNARE	Soluble NSF Attachment Protein Receptors
ssDNA	single-stranded Deoxyribonucleic Acid
StDev	Standard Deviation
SQC	Spatial Quality Control
SY1	Synphilin-1
TEMED	Tetramethylethyleendiamine
TBS	Tris-buffered saline
TPI	Triosephosphate isomerase
Tris	2-Amino-2-hydroxymethyl-propane-1,3-diol
Tween 20	Polysorbaat 20
Ubi	Ubiquitin
UCH-L1	Ubiquitin C-terminal hydrolase L1
UPR	Unfolded protein response
UPS	Ubiquitin proteasome system
URA	Uracil
WT	Wild type
YPD	Yeast extract Peptone Dextrose

Contents

Preface i

List of Abbreviations iii

Samenvatting viii

Abstract ix

1 Introduction 1

2 Literature Survey 2

2.1 Protein homeostasis . . . 2

2.2 Quality control mechanisms . . . 2

2.2.1 Protein folding . . . 2

2.2.2 Protein degradation . . . 3

2.3 The link between PQC and disease . . . 5

2.3.1 Parkinson's Disease . . . 7

2.4 Aggregation management . . . 11

2.4.1 Subcellular SQC compartments . . . 12

2.4.2 Assymetrical damage segregation . . . 13

2.5 Yeast models to study aggregation management of disease proteins . 15

2.5.1 Importance of humanized yeast models to study Parkinson's Disease . . . 16

3 Objective 18

4 Materials and methods 19

4.1 The *S. cerevisiae* strains used during the study and their function . 19

4.2 Growth media . . . 20

4.3 Plasmids . . . 21

4.4 Antibodies . . . 22

4.5 Primers . . . 22

4.6 Transformation . . . 23

4.7 Protein isolation . . . 23

4.8 Western blotting . . . 23

4.9 Stripping immobilon-P membranes . . . 24

4.10 Growth analysis in liquid cultures . . . 24

4.11 Fluorescence microscopy . . . 24

4.11.1 Nuclear staining . . . 24

4.11.2 Vacuolar staining . . . 25
4.12 Immunoprecipitation . . . 25
4.12.1 Protein extraction . . . 25
4.12.2 Pierce assay . . . 26
4.12.3 Immunoprecipitation . . . 26
4.13 Fluorescence activated cell sorting . . . 27
4.13.1 Procedure . . . 27
4.14 Preparing double deletion strains . . . 27
4.14.1 Tetrad analysis . . . 28
4.14.2 Phenol-chloroform extraction . . . 28
4.14.3 PCR . . . 28
4.14.4 Agarose gel electrophoresis . . . 29

5 Results **30**
5.1 Influence of protein degradation components on synphilin-1 biology in yeast . . . 30
5.1.1 Validation of SY1 expression in yeast . . . 30
5.1.2 Quantification of the SY1 expression in the different mutant strains . . . 31
5.1.3 Immunoprecipitation to investigate the ubiquitination status of SY1 in the different strains . . . 32
5.1.4 Growth analysis of cells expressing synphilin-1 . . . 43
5.1.5 Growth analysis of the different deletion strains in the presence of inhibitors . . . 46
5.1.6 Synphilin-1 inclusions formation . . . 49
5.1.7 Synphilin-1 inclusion localization . . . 51
5.1.8 Synphilin-1 inclusion localization in the presence of inhibitors 54
5.1.9 The effect of the PR-619 inhibitor on SY1 inclusion formation 54
5.1.10 Creation of the *ubc4*Δ*ubc5*Δ double deletion . . . 57
5.1.11 SY1 inclusion formation in the alternative strains . . . 60
5.2 Humanized yeast models to study α-synuclein toxicity and inclusion formation . . . 62
5.2.1 Validation of α-synuclein expression . . . 62
5.2.2 The effect of α-synuclein on the growth of yeast . . . 63
5.2.3 The influence of α-synuclein on the ROS level and cell necrosis 64
5.2.4 Inclusion localization of α-synuclein inclusions . . . 66

6 Discussion **69**

7 Conclusion **76**

Bibliography **77**

A Addendum **A.1**
A.1 Materials . . . A.1
A.1.1 *S. Cerevisiae* growth media . . . A.1
A.1.2 Alternative *S. Cerevisiae* media . . . A.1
A.1.3 buffers . . . A.2

A.2 Solutions A.5
A.2.1 Transformation A.6
A.2.2 Protein extraction A.7
A.2.3 Immunoprecipitation A.7
A.2.4 Fluorescence-activated cell sorting A.7
A.2.5 Agarose gel electrophoresis A.7
A.2.6 Fluorescence microscopy A.8
A.2.7 Western blotting A.8
A.2.8 Tetrad analysis A.9
A.2.9 PCR A.9
A.3 Risk analysis A.10
A.4 Statistics using Prism 6 . . . . . A.11

Samenvatting

Voor ongeveer één derde van alle genen, gerelateerd aan humane ziekten, bestaat er een gist ortholoog. Dit maakt dat gist een krachtig model is om ziekte-gerelateerde processen te bestuderen. In het gastlaboratorium werden gistmodellen geconstrueerd om de rol van α-synucleine (α-syn) en synphilin-1 (SY1) in de ontwikkeling van de ziekte van Parkinson te bestuderen. Deze modellen zijn in staat om belangrijke ziekte-gerelateerde eigeschappen zoals aggregaatvorming te reconstrueren waardoor ze ideale studie-objecten zijn voor onderzoek naar de mechanismen die betrokken zijn bij aggregaatvorming. Recent onderzoek heeft aangetoond dat inclusievorming en aggregatie een actief proces is waarbij de cel pogingen onderneemt om proteïne homeostase te herstellen. Op deze manier worden kleine aggregaten getransporteerd, met behulp van componenten van het cytoskelet, naar subcellulaire compartimenten zoals JUNQ (Juxta-Nuclear Quality Control) en IPOD (Insoluble Protein Deposit). JUNQ inclusies zijn gelokaliseerd bij de nucleus en bevatten geubiquitineerde proteïnen die oplosbaar en geaggregeerd zijn. Daarentegen zijn de proteïnen die zich in het vacuolair gelokaliseerde IPOD bevinden, onoplosbaar, inert en niet geubiquitineerd. In deze thesis werd onderzocht of α-syn en SY1 inclusies van het JUNQ of IPOD type zijn door inclusievorming, lokalisatie, ubiquitinatie en toxiciteit te bestuderen. Naast wild type (WT) gistcellen werden ook mutanten met defecten in het ubiquitine proteasoom systeem (UPS) (*pre9*Δ, *ltn1*Δ, *ubc4*Δ en *ubc5*Δ) toegevoegd aan de experimenten. Groeianalyse toonde aan dat de expressie van SY1 een kleine groeireductie veroorzaakt in alle UPS mutanten. In de stammen waarin *UBC4* en *PRE9* waren gedeleteerd was de SY1 toxiciteit toegenomen vergeleken met de WT stam. Bovendien bleek dat voor alle stammen de SY1 toxiciteit meer uitgesproken werd wanneer de cellen werden opgegroeid in de aanwezigheid van de deubiquitinating enzyme inhibitor PR-619. Verder werd voor de *ubc4*Δ stam een stijging in de hoeveelheid geubiquitineerd SY1 t.o.v de WT waargenomen. Voor geen van de andere mutanten werd er een significante wijziging in het ubiquitinatie-niveau van SY1 vastgesteld. Daarenboven, wanneer de vacuole en nucleus werden gevisualiseerd met behulp van fluorescentie microscopie, konden SY1 inclusies waargenomen worden in de nabijheid van zowel de nucleus als de vacuole. Hoewel voorheen aangetoond werd dat α-syn minder alsook kleinere inclusies vormt dan SY1, werden de α-syn inclusies ook zowel bij de nucleus als de vacuole waargenomen. Opmerkelijk is dat wanneer α-syn tot expressie werd gebracht in de *ltn1*Δ stam, er een toename in α-syn toxiciteit werd waargenomen t.o.v. de WT stam. Dit suggereert dat het Really Interesting New Gene (RING) domain ubiquitin ligase een belangrijke rol speelt in de regulatie van α-syn toxiciteit. In conclusie, geven onze resultaten een sterke indicatie dat proteïne afbraak componenten en meer specifiek ubiquitinatie mogelijk een belangrijke rol spelen in het aggregatie management van SY1 en α-syn.

Abstract

About one third of human disease related genes have a yeast orthologue. This makes yeast a powerful tool to study disease-related processes. In the host laboratory so-called humanized yeast models have been established to investigate the pathobiology of α-synuclein (α-syn) and synphilin-1 (SY1), two Parkinson's disease related proteins. These models recapitulate important disease related features such as inclusion formation, which makes them ideal tools to study aggregation management. Recent research has shown that inclusion formation and aggregation is an active process in which the cell attempts to restore proteostasis. In this respect it has been shown that small inclusions are transported along cytoskeleton components to subcellular compartments such as JUNQ (juxta-nuclear quality control compartment) and IPOD (insoluble protein deposit). JUNQ-type inclusions are located next to the nucleus and contain soluble ubiquitinated aggregated proteins. On the other hand, perivacuolar IPOD-type inclusions are insoluble and not ubiquitinated. This study investigated whether the α-syn and SY1 inclusions are from the IPOD or JUNQ type by looking at inclusion formation, localization, ubiquitination and toxicity. Besides wild type yeast cells also several strains with defects in the ubiquitin proteasome system (UPS) (*pre9*Δ, *ltn1*Δ, *ubc4*Δ and *ubc5*Δ) were included in the experiments. Growth analysis showed a minor growth reduction upon SY1 expression for all UPS mutants. Interestingly, upon deletion of *UBC4* and *PRE9* the SY1 toxicity was significicantly enhanced compared to the WT. In all strains, except for the *ubc5*Δ, the SY1 toxicity was slightly aggravated upon addition of the deubiquitinating enzyme inhibitor PR-619. Additionaly, the inhibitor increased the ratio of small to large inclusions in all different strains which suggest that small aggregates are cytotoxic. For the *ubc4*Δ cells the SY1 toxicity coincided with an increase in the ubiquitination level of full length SY1, whereas no effect on the ubiquitination status of SY1 was observed in any of the other strains. Furthermore, fluorescence microscopic visualization of the vacuole and nucleus suggested that SY1 is located to both IPOD and JUNQ. Although it has been shown previously that α-syn forms less and smaller inclusions compared to SY1, these inclusions are also found in close proximity of both the vacuole and the nucleus. Interestingly, expression of α-syn in the *ltn1*Δ strain increased the α-syn induced toxicity compared to the WT, suggesting a role for the Really Interesting New Gene (RING) domain ubiquitin ligase in the regulation of the α-syn toxicity. Overall, our results provide a strong indication that protein degradation components and especially ubiquitination might play a role in the aggregation management of SY1 and α-syn.

1. Introduction

Parkinson's disease (PD) is the most prevalent neurodegenerative movement disorder in the world, with an increased risk of incidence after the age of 60. The prevalence of this neurological disorder, and of other diseases for which age is a risk factor, is expected to increase in the following years due to the aging of the Western world. Moreover, since the disease drastically affects the quality of life and increases the susceptibility to other diseases, the impact will be enormous. Despite huge research efforts, no cure has been found thus far[1]. Hence, exploring the underlying mechanisms leading to disease onset and propagation is of major importance.

PD was long believed to be solely a sporadic neurodegenerative disorder. However, more recently monogenic hereditable forms of the disease have been discovered. This has greatly encouraged and facilitated the discovery and study of molecular pathways that lead to the disease's onset and propagation (Greggio et al., 2011). Next to the genetic factors, environmental factors also contributing to PD have been discovered and are the subject of ongoing investigation[1].

In this project, we use humanized yeast models to study cytotoxicity, ubiquitination, aggregation, and localization of two PD related proteins: α-synuclein and synphilin-1. α-synuclein is encoded by the first gene discovered to have a key role in the pathogenesis of PD (Polymeropoulos et al., 1997). Synphilin-1 was identified as an α-synuclein interacting protein. Both proteins are found together in Lewy bodies, which are protein inclusions characteristic for PD (Engelender et al., 1999).

These yeast models have already proven to be established systems for aging research and recapitulate important hallmarks of the disease such as aggregation and cytotoxicity. This makes them valuable systems for research concerning neurodegeneration (Franssens et al., 2013).

[1] Mayfield clinic, http://www.mayfieldclinic.com/PE-PD.htm

2. Literature Survey

2.1 Protein homeostasis

In order for an organism to be healthy, it must be able to fulfill its basic needs in a sufficient way. This is only possible if the cells that make up the organism are working optimally and are able to adapt to a changing environment. Therefore, important processes occur in the cells of multicellular organisms in order to keep them healthy. These biological processes make sure that the cell's protein content is in balance by determining the concentration, binding interactions, conformation and localization of individual proteins. Furthermore protein synthesis, folding, trafficking and degradation are controlled. These processes are referred to as the protein homeostasis and a healthy balance between those processes results in healthy development of the organism (Gallagher et al., 2013).

2.2 Quality control mechanisms

The combination of all control mechanisms that contribute to proteome maintainance is referred to as protein quality control (PQC). In conditions where the PQC is properly working, there is a competition between protein folding and protein degradation that together keep the cytoplasm clear from possibly harmful amyloidic proteins (Balch et al., 2008). In this way, there is a dynamic state of turnover of the cellular proteins, controlled by protein synthesis and degradation (Garrett & Grisham, 2010). In order to maintain this homeostasis, PQC mechanisms must constantly adapt to face intrinsic challenges and environmental stress (Balch et al., 2008).

2.2.1 Protein folding

The protein concentration in cells can be very high, causing proteins to constantly move and interfere with each other, so even though the protein's amino acid sequence comprises the way a protein should fold, proteins often need help to fold into the correct conformation. Many different macromolecular cellular components, such as molecular chaperones and folding enzymes, help in folding the protein polypeptide chain into the desired structure. In this way, they prevent misfolding and subsequently protein aggregation (Balch et al., 2008). Despite the help of chaperones, 30 % of the synthesised proteins are intrinsically folded incorrectly, thereby highlighting the importance of protein degradation (Takalo et al., 2013). Furthermore, the concentration, subcellular localization and distribution of chaperones differs between celltypes.

Whether a protein will fold or not is therefore also celltype-dependent. Furthermore, small ligands produced during metabolic pathways can bind folded states of proteins and thereby shift the folding equilibrium stabilizing a certain form (Balch et al., 2008).

Since development and aging changes the environment of the cell, they put a lot of stress on the proteome, hence they contribute to loss of proteostatic control (Balch et al., 2008) Furthermore, missense mutations and lack of interactions with certain oligomers can promote protein misfolding and thus contribute to loss of proteostasis (Kaganovich et al., 2008). Luckily, cells respond to loss of proteostasis by means of inducible pathways and stress sensors. One of those pathways is the unfolded protein response (UPR) by which heat shock proteins are targeted to specific proteins that in turn will be folded or unfolded (Balch et al., 2008). Unfortunately, another side effect of aging is a rise in oxidized and modified proteins that support aggregation. Therefore, proteostasis is challenged to a greater extend in older individuals. Therefore, age is a risk factor in many diseases. (Balch et al., 2008).

2.2.2 Protein degradation

The protein quality control (PQC) also involves degradation mechanisms by which proteins are broken down irreversibly. In this way, misfolded proteins are degraded when refolding is unsuccesful. Since protein degradation can have deleterious effects on cells it is compartmentalized into proteasomes or degraditive organelles such as the lysozomes (vacuole in yeast) (Garrett & Grisham, 2010).

This compartmentalization results in two different protein breakdown strategies utilized by the PQC i.e. the ubiquitin-proteasome system (UPS) and the autophagosome-lysosome pathway (ALP) (Takalo et al., 2013). The lysozomal/vacualor degradation is largely unselective, whereas proteasomal degradation only degrades certain poly-ubiquitin tagged proteins.

Autophagosome-lysosome pathway

In the autophagosome-lysozome pathway (ALP) proteins and bigger structures, such as aggregates and organelles, are enveloped within a double membrane which will form the autophagosome. Mature autophagosomes will merge with lysosomes resulting in lysosomal degradation of the autophagosomal content (Takalo et al., 2013). In yeast cells the vacuole takes over the function of the lysozome.

Ubiquitin-proteasome system

Selective degradation of proteins by the ubiquitin-proteasome system (UPS) appears to be the most common protein degradation mechanism in eukaryotes. This system utilizes ubiquitin, a highly conserved 8.5 kDa polypeptide, to label proteins for degradation (Garrett & Grisham, 2010, p. 998-1001).

The ligation of ubiquitin to proteins requires E1, E2 and E3 proteins. The E1 protein is an ubiquitin-activating enzyme that attaches to the carboxyl-terminal glycine residue on ubiquitin by means of a thioester bond with a cystein residue of its active site. This formation requires adenosine triphosphate (ATP) and an intermediary adenylated form of ubiquitin. Next, ubiquitin is transferred from E1 to an SH-group on one of many E2 conjugating enzymes. Then one of many E3 ubiquitin-ligases selects the substrate to which the charged E2 enzyme will donate its ubiquitin (Eldridge & Brien, 2009; Gallagher et al., 2013; Garrett & Grisham, 2010). The recognition and selection of proteins by the E3 ligase depends on the type of amino acid at the N-terminus of the substrate and on whether the protein contains sequence elements that promote degradation i.e. glutamate rich elements, proline, threonine and serine residues (Gallagher et al., 2013; Garrett & Grisham, 2010).

Ubiquitin is attached covalently to lysine residues (amino groups) on the substrate. Often more than one ubiquitin molecule attaches directly to the subtrate. Furthermore, ligation of a tandemly-linked chain of ubiquitin molecules to the substrate also occurs via isopeptide bonds. Next to the aminoterminal primary amine, ubiquitin has seven lysine residues that can be ubiquitinated leading to different possible polyubiquitin chain topologies. Different polyubiquitin chain topologies result in different fates of the protein, for instance in alternative degradation strategies. So it appears that isopeptide linkage of the C-terminal glycine residue of one ubiquitin to lysine 48 of the ubiquitin attached to the substrate is the most common signal for proteasomal degradation.(Garrett & Grisham, 2010; Takalo et al., 2013).

The 26S proteasome in eukaryotes is a barrel shaped structure that consists of a catalytic core (20S) and two regulatory substructures (19S) (Takalo et al., 2013). The core consists out of two times seven different α-subunits and seven different β-subunits. The two outermost rings (α_7-rings) of the core are docking sites for the 19S regulators and therefore important in the formation of the 26S proteasome. From the seven β-subunits only 3 have protease activity. The 19S regulators consist out of a base and a lid. The base, which attaches to the 20S core, is a hexameric ring built up from 6 AAA-family ATPase subunits. These subunits are important in protein unfolding and transport into the 20S proteolytic cavity. The lid covers the base and contains a subunit important for recognition and processing of the substrate's ubiquitin chain. There is a preference for proteins with four or more ubiquitin molecules attached to them. Moreover, there is a big variety of 19S regulators that can dock on the 20S. In this way, the specificity of the proteasome can be changed (Garrett & Grisham, 2010, p. 998-1001). Prior to proteasomal degradation, most of the ubiquitin molecules are removed by deubiquitinating enzymes (DUBs) and are therefore not degraded but recycled (Takalo et al., 2013). These DUBs may also counteract the E3 ligase activity by removing ubiquitin from the substrate. A schematic representation of the ubiquitin proteasome system is depicted in figure 2.1 on the following page.

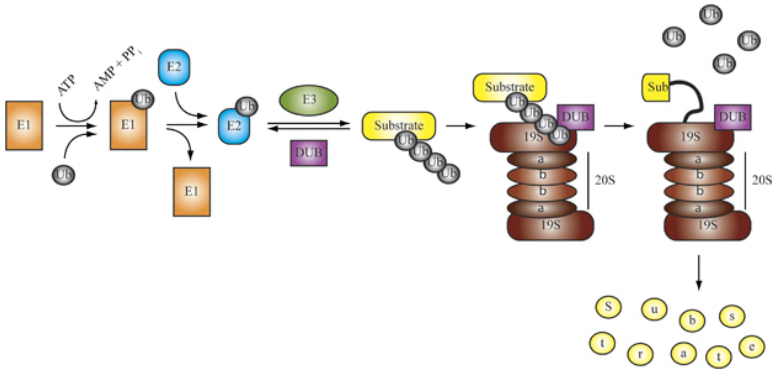

Figure 2.1: Schematic representation of the ubiquitin proteasome system (UPS). The major enzymes involved in this pathway are E1 (ubiquitin-activating enzyme), E2 (ubiquitin-conjugating enzyme) and E3 (ubiquitin ligase). DUBs (de-ubiquitinationg enzymes) are shown in purple and in brown the 26S proteasome is drawn (Eldridge & Brien, 2009). A detailed description of the mechanism is given in the text.

Besides sorting proteins for degradation, ubiquitination of proteins can have other cellular purposes. Polyubiquitination can also tag proteins for refolding (Kaganovich et al., 2008). Furthermore, ubiquitination has roles in DNA repair, chromatin remodeling, protein sorting to specific intracellular sites and so on (Garrett & Grisham, 2010, p. 998-1001).

2.3 The link between PQC and disease

There are more than 45 human degenerative diseases of which the primary hallmark is accumulation and aggregate formation of misfolded proteins (Gallagher et al., 2013). The accumulation of the misfolded proteins is related to problems in PQC. When proteins are misfolded or damaged, chaperones will try to refold and repair them. However, mutations in the protein itself or in the folding machinery can increase the amount of misfolded proteins, thereby making repair more challenging. When the proteins are damaged and beyond repair, they will be degraded by UPS or ALP. Besides protein folding problems, the homeostasis can be further impaired when degradation processes do not function properly. Malfuctioning of these processes will therefore lead to accumulation of amyloidic proteins and subsequent aggregation (Bagola & Sommer, 2008). Figure 2.2 on the next page depicts the protein quality control strategies, resulting in different fates for misfolded proteins. Many neurodegenerative diseases, such as Parkinson's disease are related to aggregation and inclusion formation of misfolded proteins and are therefore named protein folding diseases. The misfolded proteins, involved in neurodegenerative diseases often have β-sheet secondary structures, which simplifies and promotes fibril formation and aggregation. This inclusion formation typically occurs at specific areas in the brain (Takalo et al., 2013). Figure 2.3 on the following page gives a representation of the variety of diseases that arise from amyloidic protein accumulation (Kaganovich et

al., 2008; Soto, 2003).

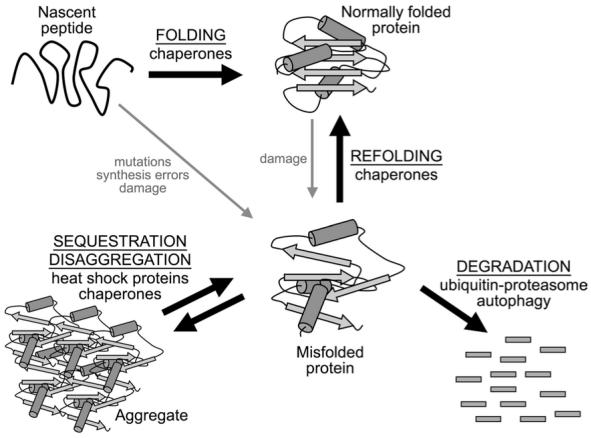

Figure 2.2: Parallel protein quality control strategies for maintainance of proteostasis in the eukaryotic cell. Misfolded proteins often result from mutations in the sequence, mistakes from the translation machinery or by physical and/or chemical stress on the nascent peptide (Gallagher et al., 2013).

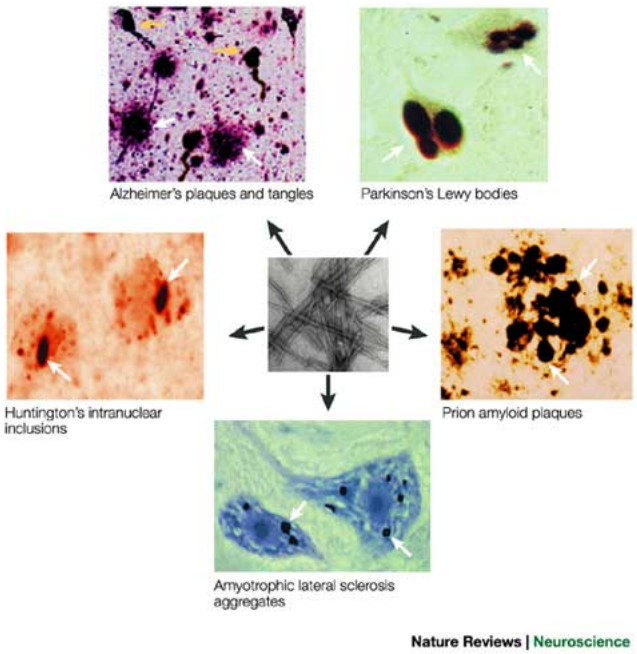

Figure 2.3: Diseases related to protein folding problems: Alzheimer's disease, Parkinson's disease, prion diseases, Amyotrophic Lateral Sclerosis and Huntington's disease (Soto, 2003).

2.3.1 Parkinson's Disease

Parkinson's disease (PD) is the second most common neurodegenerative disease. Moreover, it is the most prevalent movement disorder in elderly people (Franssens et al., 2013). The disease is characterized by a decline in normal movement and daily functions (Büttner et al., 2010; Greggio et al., 2011). Patients suffer from resting tremor, balance impairement, stifness and bradykinesia. Furthermore, there is a significant loss of autonomic and cognitive function (Greggio et al., 2011).

In PD affected brains, there is continuous and specific loss of dopaminergic neurons in the substantia nigra pars compacta, a brain section important in motor control. The reason for this decline is still unknown. When about 80 % of the dopamine producing neurons are lost, there is a shortage of dopamine and therefore messages are no longer transmitted sufficiently to the striatum. Subsequently, receptors in the striatum, important in body control, are no longer triggered adequately resulting in the aforementioned symptoms[1]. Another characteristic feauture of PD, next to this neuronal loss, is the presence of Lewy bodies (LB) in the the surviving neurons. LB are deposits of proteinaceous inclusions (Franssens et al., 2013).

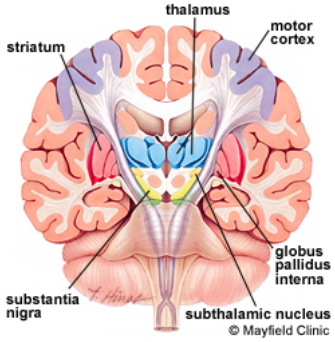

Figure 2.4: Coronal brain view. Brain areas important in motor control are indicated in the figure[1].

There are different factors that increase the risk for developing Parkinson's disease. First, the risk to develop sporadic PD increases with age. In this way, people above 60 years old have an increased risk from 2-4 %. Furthermore, the risk for PD onset can increase by certain medicines and environmental factors[1]. For example, exposure to manganese can stimulate PD pathogenesis (Racette et al., 2012).

Finally, the onset of Parkinson's disease can have a genetic cause. The discovery of PD risk genes made it possible to use modified cellular and animal models that carry the mutant gene to explore its effect on PD pathogenesis and propagation. In this way, our understanding of PD's pathobiology underwent a revolution (Greggio et al., 2011).

[1]Mayfield clinic, http://www.mayfieldclinic.com/PE-PD.htm

Treatment

In the 60's it was discovered that PD coincides with low levels of dopamine in the brain and that this is causative for the neurodegeneration of neurons in the substantia nigra pars compacta. This finding led to the development of the drug levodopa (L-Dopa). As the precursor of dopamine, L-dopa has the advantage that it can pass the blood brain barrier (BBB), allowing the dopamine level in the brain to rise again. Using this approach, PD associated symptoms such as rigidity, akinesia and tremor could be at least partly repressed. However, L-Dopa administration is not curing PD, it was the first efficient medical treatment. Unfortunately, long term use of L-Dopa has side effects such as hypotension and unvoluntary movements (Barbeau, 1969). These side effects are caused by the presence of dopamine outside the brain and can be partly counteracted by simultanous administration of an aromatic amino acid decarboxylase (AADC) inhibitor. This inhibitor prevents conversion of L-dopa into dopamine outside the brain, allowing more L-dopa to cross the BBB. Since, the AADC inhibitor itself cannot pass this barrier, decarboxylation of L-Dopa into dopamine is no longer inhibited in the brain. Unfortunately, the effectiveness of this therapy decreases overtime. More recently, it has been shown that the use of catechol-O-methyltransferase (COMT) inhibitors, as adjuvants to the aforementioned therapy, improves its efficacy since these inhibitors prevent metabolisation of L-Dopa into its metabolite 3-O-methyldopa, again allowing more L-Dopa to pass the BBB (Bonifácio et al., 2006).

All together, the discovery and optimalization of therapies is important and can improve the quality of life of PD patients. Unfortunately, despite extensive research, finding a cure for this complex neurological disorder is still a challenge.

α-synuclein

There are 18 genetic loci, PARK1-18, that are linked with PD disease onset and propagation (Franssens et al., 2013). The first gene discovered was the autosomal dominant gene, SNCA, that encodes α-synuclein (α-syn), a 140 amino acid presynaptic protein (Greggio et al., 2011; Polymeropoulos et al., 1997). Furthermore, this protein is the major component of the PD characteristic lewy bodies (LB). Three point mutations in the gene (see figure 2.5 on the next page), a duplication and a triplication of the gene are found in certain familial forms of PD. These modifications result in PD phenotypes similar to those of sporadic parkinsonism (Franssens et al., 2013; Greggio et al., 2011; Spillantini et al., 1997).

The protein is abundant and widely expressed in the brain where it interacts with a large variety of proteins, membranes and vesicles (Outeiro & Lindquist, 2003). Although, its function is still unknown, evidence suggests that excess α-syn inhibits neurotransmitter release, in this way contributing to the disease (Sidhu et al., 2004) Therefore, a role in controlling dopamine release from presynaptic vesicles has been proposed. Another study with transgenic mice, deficient in cysteine-string protein-α,

showed that human α-syn has a positive effect on the complex assembly between SNARE (Soluble NSF Attachment Protein Receptors) proteins and the plasma membrane. Therefore, it is possible that α-syn protects nerve terminals against injury. Furthermore, chaperone like activies have been reported for α-syn(Ahn et al., 2006; Chandra et al., 2005).

There is an equilibrium between an unfolded conformation of α-syn in the cytoplasma and a α-helical membrane-bound form. The amphiphatic N-terminus of the protein is important for membrane binding, whereas the acidic C-terminus is a solubilizing domain that hinders fibrillization and exhibits a chaperone-like activity. The hydrophobic core of the protein (NAC) has shown to be important for protein aggregation and fibrillization (Greggio et al., 2011). Figure 2.5 shows the domains of α-syn. Fibril formation of α-syn is facilitated by the presence of mutations and increasing protein levels. Therefore, it seems that these mutations have a gain of function effect on the protein. The β-sheet like fibrillar forms of this protein are the major components of the characteristic LB that were described earlier. Furthermore, it seems that the majority of α-syn in LB is hyperphosphorylated at two serine residues. This suggests that also phosphorylation may be an important modulator of α-syn toxicity. However, whether phosphorylation induces fibril formation or inhibits fibrilization is still unclear at this point (Greggio et al., 2011).

Next to α-syn, the inherited form of PD is also linked to Parkin and ubiquitin C-terminal hydrolase L1 (UCH-L1) (Mouradian, 2002). All three of these proteins are involved in the UPS that uses polyubiquitination as a marker for proteasomal degradation. UCH-L1 and α-syn can be ubiquitinated for their degradation while Parkin is an E3 ubiquitin ligase (Bennett et al., 1999; Choi et al., 2000; Imai et al., 2000; Zhang et al., 2000). Furthermore, UCH-L1 has been shown to create ubiquitin monomers by hydrolyzing C-terminal ubiquitin adducts (Leroy et al., 1998). Additionally, Parkin, UCH-L1, synphilin-1 and certain subunits of the proteasome system seem to be present in the PD characteristic Lewy bodies (Choi et al., 2000; Lowe et al., 1990)(Ii et al., 1997). These findings support a role for the ubiquitin proteasome system in the pathogenesis of PD (Lee et al., 2002).

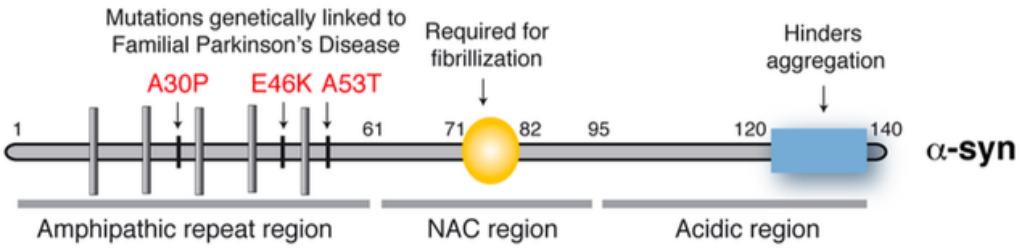

Figure 2.5: Schematic representation of the domains of α-syn. Mutations that cause familial forms of PD are indicated in red. NAC, non-amyloid β component (Greggio et al., 2011).

Synphillin-1

In 1999, the presynaptic protein synphilin-1 (SY1) was identified as an α-synuclein interacting protein, using a yeast to hybrid screen. This protein is encoded by the SNCAIP gene and promotes the formation of Lewy Bodies (Engelender et al., 1999). It consists of 919 amino acids and contains several protein-protein interaction domains such a coiled-coil domain (CCD), ankyrin-like repeats and a putative ATP, GTP-binding domain, as depicted in figure 2.6 (Engelender et al., 1999; Szargel et al., 2008). A study with human cells suggests that the central CCD of SY1 specifically interacts with the N-terminus of α-syn and in this way promotes inclusion formation (Xie et al., 2010). The interaction of the central portion of SY1 with α-syn was already suggested before by use of a yeast two hybrid assay (Neystat et al., 2002). Due to this interaction with α-syn, SY1 possibly has an important role in Parkinson's disease. The first genetic evidence suggesting a role of SY1 in PD was the mutation R621C. This mutant form was discovered in two German patients and appeared to be a susceptibilty factor for PD (Krüger, 2004; Marx et al., 2003). The funcion of SY1 is still unclear. However, since it binds to presynaptic vesicles in the presynaptic terminal, a similar role in dopamine release as for α-syn has already been suggested (Szargel et al., 2008). Furthermore, roles as adaptor protein have been suggested (Engelender et al., 1999).

The possible link of SY1 with PD is further encouraged by the fact that Lewy bodies are often intensely ubiquitinated and that the aforementioned Parkin protein seems to be the E3 ubiquitin ligase that both mono and polyubiquitinates SY1 (Li & Guo, 2009; Lim et al., 2005). Even though it was suggested that Parkin is required for both ubiquitination and inclusion formation of SY1 (Chung et al., 2001), additional research showed that SY1 is also polyubiquitinated and able to form inclusions when Parkin is not overexpressed (Lee et al., 2002). Furthermore, SY1 appears to be a relatively long-lived protein in HEK293 cells, with a half life of 16 hours. When these cells were treated with proteasome inhibitors such as MG-132, SY1 degradation was attenuated resulting in accumulation of high molecular weight SY1 and increased perinuclear inclusion formation. Finally, HEK293 cells appeared to be more susceptible to proteasomal dysfunction when SY1 was overexpressed. These findings indicate that SY1 is ubiquitinated and undergoes proteasomal degradation (Lee et al., 2002). Moreover, when using a SY1 isoform (synphilin-1A) that spontaneously aggregates, a clear toxic effect was seen on cells. However, when the proteasomal function was inhibited in these cells there was an accumulation of ubiquitinated proteins and concurrently a decrease in toxicity (Eyal & Engelender, 2006). This suggest that the formation of SY1A inclusion bodies works cytoprotective and prevents itself from causing damage. Thus, when proteasomal degradation is impaired ubiquitinated SY1 accumulates in the cell and forms inclusion bodies. Apparantly, glycogen kinase 3β phosphorylates SY1 and thereby decreases the amount of SY1 that is ubiquitinated and degraded. This shows that phosphorylation of SY1 also has an important role in the SY1 function and processing (Avraham et al., 2005). Furthermore, Seven in absentia homolog (SIAH), a ubiquitin ligase that ubiquitinates both SY1 and α-syn,

might be an important regulator of SY1's function (Szargel et al., 2009). It appears to be more efficient than Parkin in promoting UPS dependent SY1 degradation (Nagano et al., 2003). In addition, another E3 ubiquitin ligase Dorfin was shown to be able to ubiquitinate SY1 but not α-syn. When normal SY1 was overexpressed in cultured cells, large non-cytotoxic junxtanuclear inclusions were found in which Dorfin, ubiquitin and other proteasomal compounds were found. In contrast, when only the central region of SY1 was expressed, small foci were seen throughout the cytoplasm in which neither Dorfin nor ubiquitin were present. In addition, these small foci were cytotoxic. These findings suggest that the central domain of SY1 is important for aggregate formation while also having a role in the proteotoxicity (Ito et al., 2003).

Figure 2.6: Representation of the SNCAIP gene and its domains. The Ankirin-like repeats, the coiled-coil domain (CCD) that interacts with α-syn, and the putative ATP, GTP-binding domain are shown (Szargel et al., 2008).

2.4 Aggregation management

As mentioned before, PQC consists out of protein folding and proteins degradation strategies. When one or more of these strategies are impaired, misfolded proteins can accumulate more easily in the cytoplasm. Since, neurodegenerative diseases often coincide with accumulation of harmful proteins, they have a higher chance of developing in organisms that already suffer from impaired protein management processes. Furthermore, is believed that the non-native soluble intermediates of misfolded proteins are the harmful cytotoxic components. This is because they can interact with other proteins, organelles or the PQC machinery in an undesirable way and thereby stimulate pathogenesis (Takalo et al., 2013).

More recently, a well organized machinery was discovered that sequesters harmful proteins in different intracellular compartmens in order to minimize their toxic effects (Kopito, 2000; Nyström & Liu, 2013; Takalo et al., 2013). This cytoprotective mechanism is referred to as the spatial quality control (SQC) (Kaganovich et al., 2008).

Notice that the assymetric inheritance of damage between mother and daughter cells, as will be discussed in section 2.4.2, is also defined as a spatial quality control mechanism (SQC).

2.4.1 Subcellular SQC compartments

Misfolded proteins are sequestered actively into different intracellular compartments by means of the SQC. These compartments are found both in mammals and in yeast, indicating that the mechanisms by which harmful proteins are compartmentalized are evolutionary conserverd. Therefore, by gaining insight in these spatial quality control mechanisms in yeast, we can get a better understanding of protein folding diseases in humans (Bagola & Sommer, 2008).

One of the compartments harbors mainly soluble misfolded proteins that can still exchange with the cytoplasmic pool (Kaganovich et al., 2008). This compartment is named juxtanuclear quality control (JUNQ) because it is found in close proximity of the nucleus. A second compartment lies next to the vacuole and contains mainly non-diffusing aggregated proteins. Therefore, this compartment was named insoluble protein deposit (IPOD) (Kaganovich et al., 2008). Additionally, certain proteins are sequestered into so called aggresomes, perinuclear insoluble inclusions formed by dynein-dependent protein transport (Kaganovich et al., 2008; Liu et al., 2010). Not only aggresomes but also the formation of JUNQ and IPOD depend on the microtubule network. This was shown by experiments with microtubule depolimerizing drugs (Bagola & Sommer, 2008; Kaganovich et al., 2008). Finally, there is another compartment that lies in close proximity to both JUNQ and the nucleus. This compartment contains soluble ubiquitinated endoplasmic reticulum associated protein degradation (ERAD) substrates (Kaganovich et al., 2008). Hence, it is referred to as Endoplasmatic Reticulum Associated Compartment (ERAC). The different compartments are depicted in figure 2.7 on the next page.

Both JUNQ and IPOD contain Hsp104, a chaperone important in refolding misfolded proteins. Furthermore, this chaperone solubilizes aggregates in order to make them accesible for degradation or refolding (Bagola & Sommer, 2008; Zhou et al., 2011). In contrast with Hsp104, 26S proteasomes only co-localize with JUNQ and not with IPOD (Kaganovich et al., 2008; Nyström & Liu, 2013). This implies that UPS-dependent degradation of terminally misfolded proteins only occurs in JUNQ. This is in agreement with findings that suggest that protein aggregates delivered to IPOD undergo facilitated degradation via the ALP (Kaganovich et al., 2008). Moreover, it was shown that harmful amyloidogenic proteins are sequestered only in IPOD and that this sequestration even occurs in unstressed cells. Interestingly, Kaganovich et al. (2008) discovered that when ubiquitination of normal misfolded proteins is blocked they are also sequestered into IPOD. On the other hand, it was possible to change the fate of prion like proteins from IPOD to JUNQ by polyubiquitinating them. This suggests that proteins must be ubiquitinated in order for them to be sequestered into JUNQ. Hence, not only the solubility but also the ubiquitination status seems to determine the partitioning of the proteins to different subcellulular compartments. Finally, whether a protein becomes ubiquitinated or not seems to depend on interactions with molecular chaperones. This means that also chaperones determine the fate of proteins (Kaganovich et al., 2008).

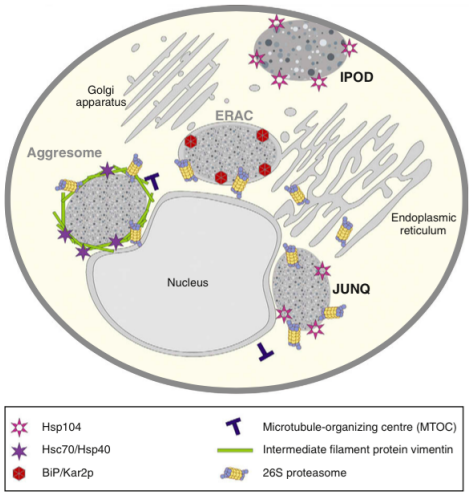

Figure 2.7: Compartments important in the SQC of yeast and mammalian cells. IPOD has a peripherical localization harboring mainly insoluble aggregates. Juxtanuclear localized JUNQ harbors soluble ubiquitinated proteins. JUNQ co-localizes with Hsp104 and 26S proteasomes while IPOD only co-localizes with Hsp104. The ERAC and aggresomes are functionally similar to JUNQ but differ in their compartment architecture (Bagola & Sommer, 2008).

2.4.2 Assymetrical damage segregation

Damage from deleterious proteins is controlled by the PQC and the SQC. However, there is an additional mechanism, found both in unicellular and multicellular organisms, that copes with the pool of damaging proteins. This mechanism is named assymetrical damage segregation and is sometimes also referred to spatial quality control (Nyström, 2007; Nyström & Liu, 2013). This mechanisms includes damage retention in the mother cell and transport of deleterious proteins from daughter to mother cell. In this way, during every reproduction cycle, a yeast mother cell will accumulate damage resulting in non-beneficial changes. Eventually, after a certain amount of cycles, she we will be incompetent for further reproduction and therefore will stop dividing. This occurs even when conditions are optimal for reproduction (Mortimer & Johnston, 1959; Nyström & Liu, 2013).

The study of Anguilaniu et al. (2003) has indicated that aggregates are retained in the mother cell during bud development and cytokinesis. However, the mechanism behind this retention process and behind retrograde transport were still unclear.

More recently, two different mechanisms were proposed by which protein aggregates can be inherited assymetrically. Both mechanisms are shown in figure 2.8 on the following page. The factor-independent mechanism is proposed by Zhou et al. (2011) and states that assymetrical inheritance is the result of both the slow random diffusion of the aggregates and the geometry of the yeast cells and therefore is solely

passive. This means that the generation time and the diameter of the bud neck are the only determants of assymtric inheritance and therefore fully explain damage retention in the mother cell. This mechanism is based on models and experiments in which the trafficking of aggregates was followed (Zhou et al., 2011). Spokoini et al. (2012) investigated the possibility of the stochastic model and observed that the bigger aggregates from the study of Zhou et al. (2011) are non-diffusible perinuclear and juxtavacualor (IPOD and JUNQ) inclusions. Hence, they question the reliability of the proposed model.

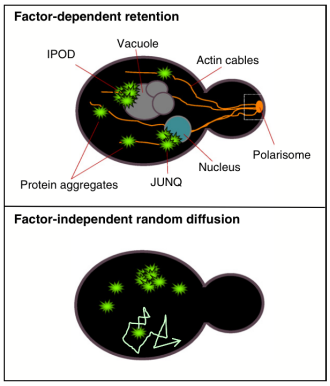

Figure 2.8: Two opposing mechanisms describing aggregate asssymetry between the mother and daughter cell during cell division. Both the factor-dependent and the factor independent retention mechanisms are described in the text (Nyström & Liu, 2013).

In contrast, the factor-dependent mechanism, proposed by Liu et al. (2010), states that assymetrical segregation depends on a properly working actin cytoskeleton and the polarisome. These structures can attach to deleterious proteins and thereby are believed to retain damage in the mother cell while also enabling retrograde transport of damage from bud to mother cell (Liu et al., 2010). Previous research already suggested that actin cables are important during polarized growth of the cell by transporting organelles, cell wall materials and other cellular content in a polarized manner (Aguilaniu et al., 2003; Pruyne et al., 2004). The polarisome is a protein complex that is located at the bud tip. It consists out of the core proteins Bni1p, Pea2p, Bud6p, and Spa2p (Liu et al., 2010). The Bni1p is one of the two formins in yeast. Previous research indicates that when bud growth occurs, an actin cable nucleates from the bni1P and elongates in the direction of the mother cell. In this way, actin substrates are believed to be transported to the mother cell via retrograde transport (Liu et al., 2010). Moreover, it has been shown that the aforementionend Hsp104 has a key function in the transport of aggregates along actin cables (Nyström & Liu, 2013). Indeed, no assymetrical inheritance was possible in mutants deficient in polarisome formation or Hsp104 function, supporting the factor-dependent mechanism (Liu et al., 2010, 2011). For example, the retention of an aggregation prone GFP-linked Huntington's disease protein (Htt103Q-GFP)

in the mother cell reduced dramatically when Bni1p was absent (Liu et al., 2011). Furthermore, it seems that tethering damaged protein aggregates onto organelle structures prevents diffusion of aggregates into the daughter cell (Kaganovich et al., 2008; Nyström & Liu, 2013).

Nystrom and Liu (2013) questioned why retention and transport of damage to the mother cell, in order to keep the daughter cell healthy, is favored over complete and transient removal of toxic material. Unfortunately, certain forms of cytotoxic damage, such as irreversible carbonylation of proteins, can't be undone. Therefore, a spatial inheritance of damaging materials is a better option. Moreover, damage segregation is less energy consuming compared to removal of irreversibly damaged proteins (Nyström & Liu, 2013). Furthermore, the assymetrical inheritance relies mainly on avoiding aggregates to enter the daughter cell in the first place and therefore the idea of retrograde transport to be the main reason for damage assymetry is probably not completely correct (Liu et al., 2010, 2011).

2.5 Yeast models to study aggregation management of disease proteins

The molecular properties of disease proteins such as α-syn and the way they induce cellular dysfunction are subject to a lot of research. Various model systems such as transgenic mice, *Drosophila melanogaster* and *Caenorhabditis elegans* have been used to study dysfunction of these proteins. These models work well for *in vivo* disease studies. However, to get a better understanding of the underlying disease mechanisms investigation of the cellular and subcellular processes and organisation is required. For this, humanized yeast models have shown to be very instrumental (Franssens et al., 2013).

Saccharomyces cerevisiae is a highly sophisticated unicellular eukaryote with complex intracellular structures. 60 % of the yeast genes are at least partly similar to human genes (Botstein et al., 1997). Moreover, 25 % of them have human orthologs (Bassett et al., 1996). In addition, a BLAST algorithm showed that about one third of the known human disease-related genes has a yeast orthologue (Foury, 1997). These properties make yeast a valuable tool to investigate human diseases. Unfortunately, nor developmental pathways of higher eukaryotes, nor the complexity of the human brain and its interactions are present in yeast. However, yeast being less complex than the human brain can have its benefits. In this way, yeast can be useful to study protein trafficking, protein degradation, PQC, protein (mis)folding, oxidative stress and mitochondrial dysfunction (Sherman, 2002). Moreover, the initial events of pathogenesis can be investigated whereas in communicating neurons it is often to difficult to investigate the disease onset. Yeast has the advantage that it has a short generation time and that it is easy to manipulate by exploiting the homologous recombination. Furthermore, human disease-related genes, with no ortholog in yeast

itself, can be investigated using humanized yeast models. Finally, the availability of deletion and overexpression libraries together with a GFP-fusion collection and a plasmid library make yeast a robust high-throughput screening system for analysis of cellular processes and genes that manipulate pathogenesis (Franssens et al., 2013; Winzeler et al., 1999).

2.5.1 Importance of humanized yeast models to study Parkinson's Disease

Over the last 15 years the normal function of α-syn and its dysfunction in synucleopathies have been succesfully investigated using *S. cerevisiae* humanized yeast models. A humanized yeast model is a yeast strain expressing a human protein that has no orthologue in yeast itself. In this way, Outeiro and Lindquist (2003) overexpressed the human α-syn in yeast and discovered that α-syn associates with the membranes. Moreover, they witnessed that it inhibits phospholipase D and promotes lipid accumulation. Additionally, they demonstrated that α-syn alters the balance between vesicular pools and causes ubiquitin accumulation. Zabrocki et al. (2005) indicated that α-syn aggregate formation occurs by means of a nucleation-elongation process that is initiated at the plasma membrane. Moreover, higher levels of phospholipids and membranes in yeast cells, induced by dimethyl sulfoxide, were shown to increase α-syn aggregation. Increasing the oxidative stress, by treating cells with ferrous ions, also resulted in enhanced aggregate formation. Furthermore, it has been evidenced that α-syn is degraded by proteasomes and autophagy (Zabrocki et al., 2005). Moreover, it has been suggested that α-syn toxicity in yeast is caused by a direct binding of α-syn to the membranes, causing loss of homeostasis (Volles & Lansbury, 2007). Another study, that explored α-syn localization, inclusion formation and toxicity in different deletion strains, suggests that α-syn toxicity in yeast is related to defects in vesicular trafficking routes. This because the toxicity is related to its endocytosis, impaired vacuolar fusion and vesicle recycling towards the plasma membrane. This points out that the characteristics of α-syn in neurons, i.e. controlling vesicular dynamics and vesicular recycling, are also present when expressed in yeast (Zabrocki et al., 2008).

As mentoined in section 2.3.1, α-syn directly interacts with SY1. This was observed using a yeast two hybrid screening and indicates that the conditions enabling this interaction are preserved in yeast (Engelender et al., 1999). Recently, a yeast model to investigate SY1 and its involvement in PD's pathobiology was established (Büttner et al., 2010). In this model, SY1 was expressed alone and co-expressed with α-syn. During exponential growth, GFP tagged α-syn was localized at the plasma membrane where inclusion formation occured in approximately 2 % of the cells. In contrast, dsRed-tagged SY1 was distributed throughout the cytoplasm and formed cytosolic inclusions in one third of the cells. The small foci formed one to two large SY1 inclusions when cells entered the stationary phase. Moreover, SY1 inclusions co-localized with lipid droplets and endomembranes. Additionally, SY1 interacted with lipid rafts to a greater extent than α-syn did. This finding, in combination with

the fact that SY1 has a greater tendency to form inclusions than α-syn, suggests that membrane interaction stimulates the formation of SY1 inclusions. Büttner et al. (2010) also demonstrated that SY1 expressing cells were less toxic than α-syn expressing cells during exponential growth. The SY1 aggregates were identified as aggresomes by a previous study (Wong et al., 2008). These aggresomes are believed to be cytoprotective since they are easily removed by autophagy. Therefore, aggresome formation might explain the lower toxicity of SY1 during exponential growth (Büttner et al., 2010). Because aging is an important factor in PD, Büttner et al. (2010) also investigated SY1 inclusion formation and toxicity in stationary and aging cultures. They discovered that SY1 is as toxic as α-syn during stationary growth and that this increased toxicity goes together with enhanced ROS production. Possibly, overpowering SY1 aggregation and aggresome formation during exponential growth causes deregulation of autophagy in response to nutrient shortage during stationary growth. Moreover, when both proteins were expressed together during stationary growth, an elevated toxicity was observed. Finally, it seems that the Sir2p (Silent Information Regulator 2), previously already identified as an anti-aging protein (Kaeberlein et al., 1999), is essential in mediating the SY1 toxicity (Büttner et al., 2010).

3. Objective

Humanized yeast models have proven to be valuable models to study neurodegenerative diseases. For research concerning PD, the host lab currently uses two types of models i.e. one in which α-syn is expressed in yeast and one in which the α-syn interacting protein SY1 is expressed. Since both proteins form aggregates when expressed in yeast, these models are excellent tools to investigate aggregation management. The first part of this study will focus on the aggregation management of SY1. Previous research showed that SY1 in yeast is present in the cytosol during exponential growth and forms small aggregates in one third of the cells. When reaching stationary phase these small aggregates transform into one or two big cytosolic inclusions often localized at the poles of the cell. Whether these big inclusions are cytoprotective or cytotoxic is still controversal. Moreover, it has been shown that protein aggregates are not random deposits of misfolded proteins but are formed through active and regulated processes involving transport along cytoskeleton components. This so-called spatial quality control includes the compartmentalization in two subcellular compartments i.e. a juxtanuclear quality control compartment (JUNQ) and an insoluble protein deposit (IPOD). Soluble ubiquitinated proteins are targetted to JUNQ whereas insoluble non-ubiquitinated proteins are guided to IPOD. Moreover, in the JUNQ compartment proteasomes are found, suggesting that the UPS dependent protein degradation is compartmentalized and mainly occurs in JUNQ. In our project we want to investigate whether SY1 is targeted to JUNQ and/or IPOD. Previous research in the host lab investigated the JUNQ or IPOD like character of SY1 inclusions by focussing mainly on SY1 inclusion localization using fluorescence microscopy. We will use a different approach i.e. investigating SY1 ubiquitination, to study whether this degradation signal has an important role in SY1 aggregation management. We will use a selection of UPS mutant strains (*ubc4*Δ, *ubc5*Δ, *pre9*Δ and *ltn1*Δ) to determine cellular readouts such as cytotoxicity and inclusion formation and especially to investigate the ubiquitination status of SY1 in these mutants. In addition to these mutant strains, the influence of biochemical inhibitors on ubiquitination, cytotoxicity, and inclusion formation will be studied. The second part will focus on the JUNQ and IPOD like character of α-syn inclusions by investigating the localization of these α-syn inclusions with fluorescence microscopy. To investigate the toxicity of α-syn we will quantify the amount of necroptotic cells and measure the cellular stress level that is linked with the amount of reactive oxygen species. In this α-syn part of our study, we will focus on the WT and *ltn1*Δ strains. Overall the proposed experiments will give us a better insight in the aggregation management of the PD associated proteins SY1 and α-syn.

4. Materials and methods

4.1 The *S. cerevisiae* strains used during the study and their function

Table 4.1: The function and phenotype of the different deletion strains

Deleted genes	**Function and phenotype of the deletion as reported by the SGD** [2]
UBC4	Stress-inducible E2 ubiquitin-conjugating enzyme, important for the degradation of misfolded, excess and cell cycle proteins via UPS. It partners with another E2 enzyme i.e. Ubc1P, interacts with the anaphase promoting complex and with the SCF E3 ubiquitin ligase complex.
UBC5	Ubc5 is a paralog of Ubc4 that arose after a genome duplication. It is heat inducible, selectively degrades short-lived, excess and misfolded proteins and is involved in the cellular stress response.
UBC4 and *UBC5*	Since Ubc4 and Ubc5 are paralogs of eachother a double deletion is expected to remove all possible complementation events present in the single deletion strains.
PRE9	This protein is the α3 subunit from the 20S core of the 26S proteasome. This protein is replaced by Pre6p (an α4 subunit) under stress conditions. This replacement results in a more active proteasome.
LTN1	Ltn1p is a Really Interesting New Gene (RING) domain E3 ubiquitin ligase, important in the ubiquitination pathway of continuously expressed proteins. Moreover, it is part of the ribosome quality control by means of degrading not completed polypeptides after the ribosome stalls during translation. Some of its mutants have already been linked to neurodegeneration onset.

[2]Saccharomyces Genome Database, http://www.yeastgenome.org

Table 4.2: The genotype of all the used strains.

Strain	Genotype	Reference
WT (BY4741)	MAT**a** *his3Δ0 leu2Δ0 met15Δ0 ura3Δ0*	Own lab
*ubc4*Δ (BY4741)	MAT**a** *his3Δ1 leu2Δ0 met15Δ0 ura3Δ0 ubc4Δ::KanMX4*	Own lab
*ubc5*Δ (BY4741)	MAT**a** *his3Δ1 leu2Δ0 met15Δ0 ura3Δ0 ubc5Δ::KanMX4*	Own lab
*pre9*Δ (BY4741)	MAT**a** *his3Δ1 leu2Δ0 met15Δ0 ura3Δ0 pre9Δ::KanMX4*	Own lab
*ltn1*Δ (BY4741)	MAT**a** *his3Δ1 leu2Δ0 met15Δ0 ura3Δ0 ltn1Δ::KanMX4*	Own lab
WT (MHY501)	MATα *his3Δ200 leu2-3, 112 ura 3-52 lys 2-801 trp1-1*	Chen et al. (1993)
*ubc4*Δ (MHY498)	MATα *his3Δ200 leu2-3, 112 ura 3-52 lys 2-801 trp1-1 ubc4Δ1::HIS3*	Chen et al. (1993)
*ubc5*Δ (MHY499)	MATα *his3Δ200 leu2-3, 112 ura 3-52 lys 2-801 trp1-1 ubc5Δ1::LEU2*	Chen et al. (1993)
*ubc4*Δ*ubc5*Δ (MHY508)	MATα *his3Δ200 leu2-3, 112 ura 3-52 lys 2-801 trp1-1 ubc4Δ1::HIS3 ubc5Δ1::LEU2*	Chen et al. (1993)

The strains with reference Chen et al. (1993) were a gift from Mark Hochstrasser's group.

4.2 Growth media

Table 4.3: The growth media used during the study

Name	Composition	Species
YPD	2% peptone, 1% yeast extract and 2% dextrose in MilliQ water. For solid medium add 1.5% agar	*S. cerevisiae*
SD	0.5% ammonium sulphate, 0.19% yeast nitrogen base without amino acids and without ammonium sulphate, a mix containing the appropriate amino acids and 2% dextrose in MilliQ water. The pH is brought to 5.5 using KOH. For solid medium 1.5% agar is added and the pH is brought up to 6.5 using KOH	*S. cerevisiae*

All media were autoclaved before use in order to make them sterile.

4.3 Plasmids

Table 4.4: The plasmids used during the study

Plasmid	Back-bone	Inserted gene	Prom.	Bact. marker	Yeast Marker	Tag	Ref.
pYX212	pYX212	none	TPI	Amp^R	URA3	none	Büttner et al. (2010)
pYX212-SY1	pYX212	synphilin-1	TPI	Amp^R	URA3	none	Büttner et al. (2010)
pYX212-dsRed	pYX212	dsRed	TPI	Amp^R	URA3	dsRed	Büttner et al. (2010)
pYX212-dsRedSY1	pYX212	dsRed + synphilin-1	TPI	Amp^R	URA3	dsRed	Büttner et al. (2010)
pUG23	pUG23	none	MET25	Amp^R	HIS3	EGFP	Zabrocki et al. (2005)
pUG23-αsyn	pUG23	α-synuclein	MET25	Amp^R	HIS3	EGFP	Zabrocki et al. (2005)
pGGE181	YEp181	none	TPI	Amp^R	LEU2	none	Zabrocki et al. (2005)
pGGE181-αsyn	YEp181	α-synuclein	TPI	Amp^R	LEU2	none	Zabrocki et al. (2005)
pYX212T	pYX212	none	TPI	Amp^R	URA3	none	/
pYX212T-αsyn	pYX212	α-synuclein	TPI	Amp^R	URA3	none	/
pMRT39-myc-Ubi	pRS423	myc- Ubiq-uitin	CUP1	Amp^R	HIS3	Myc	Van Zeebroeck et al. (2014)

The plasmid pMRT39-myc-Ubi was a gift from Johan Thevelein's group (Van Zeebroeck et al., 2014).

4.4 Antibodies

Table 4.5: The antibodies used in this study

Antibody name	Nr.	Type	Organism	Dilution	Company	Conjugate
Anti-synphilin (C-terminal)	93	Primary	Rabbit	1/4000	Sigma	none
Anti-α-synuclein (Polyclonal)	26	Primary	Rabbit	1/1000	Sigma	none
Anti-ubiquitin (P4G7 clone)	169	Primary	Mouse	1/200	Santa cruz	none
Anti-ubiquitin (P4G7 clone)	25	Primary	Mouse	1/1000	Covance	none
Anti-myc (myc-tag (9b11)	117	Primary	Mouse	1/1000	Cell signaling	none
Anti-myc (myc-tag (9b11)	160	Primary	Mouse	1/1000	Cell signaling	HRP
Goat anti-rabbit	S5	Secondary	Goat	1/1000	Santa Cruz	HRP
Goat anti-mouse	S9	Secondary	Goat	1/10000	Santa Cruz	HRP

4.5 Primers

Table 4.6: The primers used in this study

Type	Sequence	Gene
Foward	CAACAGCTCACCTTGAAAGG	upstream sequence of *UBC4*
Forward	ACGGTGTAAACTCTCGTAGC	upstream sequence of *UBC5*
Reversed	CAGTGGTGAGTAACCATGC	*KanMX4* cassette

4.6 Transformation

Transformations were performed using a previously described method (Gietz et al., 1995). Precultures were grown overnight at 30 °C and subsequently used to inoculate 50 mL YPD cultures. Cells were grown until an OD of 2 and centrifuged for 5 minutes at 3000 rpm using the Beckman centrifuge. After removal of the supernatant, pellets were resuspened in 1 mL 0.1 M LiAc and transferred to microcentrifuge tubes. These tubes were then centrifuged for 5 minutes at 3000 rpm using the table centrifuge. Subsequently, the pellet was resuspended in 100 µL 0.1 M LiAc. After an incubation period of 10 minutes, 50 µL of cell suspension was transferred to a new microcentrifuge tube. To this tube 300 µL PLI-mix (1 mL 1 M LiAc, 1 mL H_2O, 8 mL 3350 PEG 50 %), 5 µL ssDNA (10 mg mL^{-1}) and 2 µL plasmid DNA (= 1 µg) were added. The complete mixture was vortexed for 10 seconds and incubated for 30 minutes at 42 °C in a heat block. Subsequently, the suspension was centrifuged (5 minutes, 3000 rpm) and the supernatant was removed. Finally, the transformed cells were resuspended in 200 µL sterile H_2O and plated out on selective medium. After a 2 day incubation period at 30 °C, single colonies were replated on the same medium. This was again followed by a similar incubation period whereafter the single transformants were stored at 4 °C. Table 4.2 on page 20 and 4.4 on page 21 give an overview of the different strains and plasmids that were used.

4.7 Protein isolation

Cells were grown overnight in 3 mL selective medium. Subsequently, these cultures were diluted to an OD_{600nm} = 0.5 and grown again until an OD_{600nm} = 1.5-2. The cells were placed directly on ice and 1 mL of the culture was transferred to a microcentrifuge tube. Cells were collected by centrifugation (1 min, 14000 rpm, 4 °C) and the pellet was resuspended in an appropriate amount of 1x sample buffer (50 mM Tris pH 8, 2 % SDS, 0.1 % bromophenol blue, 10 % glycerol and 10 mM β-mercaptoethanol). 50 µL sample buffer was used for cells with OD_{600nm} = 2. After an incubation period of 15 minutes at 95 °C samples were spun down shortly and stored at -20 °C.

4.8 Western blotting

Protein samples, obtained from the protein isolation protocol (section 4.7), were analyzed using standard SDS-PAGE and westen blotting techniques (Towbin et al., 1979). The samples were separated on a 10 % Tris-Glycine gel whereafter they were transferred to an immobilon-P membrane (millipore). The primary antibodies and the HRP-conjugated secondary antibodies, used for immunodetection, are given in table 4.4 on the previous page. Immunodetection of the membranes was done

using the ECL detection reagents with a kit from Thermo Scientific and using the Biospectrum Multispectral imaging system, UVP®.

4.9 Stripping immobilon-P membranes

Antibodies were removed from the PVDF membranes by incubating the membrane for 20 minutes at 60 °C in stripping buffer (2 % SDS, 62.5 % Tris-HCl pH 6.8 and 100 mM β-mercaptoethanol). Stripped blots were washed two times for 10 minutes with TBST.

4.10 Growth analysis in liquid cultures

Precultures were grown in selective medium until reaching stationary phase. Stationary cultures were diluted to an OD_{600nm} of 0.01 in a microtiter plate in SD medium. The growth of the cells was measured by checking the OD_{600nm} every 2 hours using a spectrophotometer (Multiskan GO from Thermo Scientific).

4.11 Fluorescence microscopy

For the fluorescence microscopy, dsRed-SY1 expressing strains and EGFP-α-syn expressing strains were grown for 72 hours until stationary growth was reached. Subsequently, the cells were visualised using the Leica DM400 B fluorescence microscope. For localizing the aggregates, prior to visualising the cells, nuclear and vacuolar stainings were performed, as described in section 4.11.1 and 4.11.2.

4.11.1 Nuclear staining

The cyan blue fluorescent DAPI (4'-6-Diamidino-2-phenylindole) dye was used to stain double stranded DNA. Therefore, cells were grown at 30 °C for 72 hours. 100 µL of those stationary cells were transferred into a 1.5 mL centrifuge tube whereafter they were centrifuged for 5 minutes at 3000rpm in order to precipitate the cells. After removal of the supernatant, cells were washed. This was done by resuspending them in 500 µL 1x PBS followed by a centrifugation step at 3000rpm for 5 minutes and finally by again removing the supernatant. Then cells were fixed in 100 µL 50 % EtOH in 1x PBS for 20 minutes at room temperature. After the fixation step, cells were again centrifuged at 3000rpm for 5 minutes in order to remove the 50 % EtOH. Next, cells were resuspended in 1 mL PBS 1x to which 1 µL DAPI dye (1 mg mL^{-1}) was added. This was followed by an incubation period in dark of 15 minutes. To wash the cells, they were centrifuged (3000rpm, 5 minutes), the supernatant was removed and they were resuspended in 500 µL PBS. Finally, after repeating the washing step 3 times, the cells were analyzed under de fluorescence microscope. Note: For the cells with EGFP tagged α-syn, the fixation step in ethanol was omitted since it led to poor fluorescent GFP signals.

4.11.2 Vacuolar staining

The 7-amino-4-chloromethylcoumarin (CMAC) dye was used to stain the vacuolar content of cells and allows us to investigate vacuolar localization of aggregates. Cells were grown at 30 °C for 72 hours as described before. Next, 100 µL of the cell suspension was centrifuged, at 3000 rpm for 5 minutes, whereafter the pellet was resuspended in 100 µL HEPES solution (10 mM HEPES, pH 7.4 containing 5 % glucose). Next, 1 µL CMAC dye (10 mM stock) was added whereafter the cell suspension was incubated for 30 minutes in the dark. Finally, after centrifugating the suspension at 3000 rpm for 5 minutes, the CMAC containing solution was poured off and the cells where resuspended in 100 µL HEPES solution.

4.12 Immunoprecipitation

Immunoprecipitation is a technique to isolate a certain protein of interest from a protein mixture by use of a specific antibody that can attach to a solid substrate. The protocol that was used is based on previously described work (Takahara & Maeda, 2012).

4.12.1 Protein extraction

First precultures were inoculated in 3 mL selective medium and grown overnight at 30 °C. From the precultures, a certain volume was transferred into 50 mL cultures to reach an OD of 0,5. These 50 mL cultures were grown at 30 °C until an OD of 2 or higher (dependent on what one wants to investigate). The cultures were transferred to falcon tubes that were centrifuged for 5 minutes at 3000rpm (4 °C). Next, the cells were resuspended in 1 mL ice cold PBS (1x), transferred to fast prep tubes and centrifuged (2 minutes, 3000rpm, 4 °C) using a table centrifuge. The washing step was repeated by removing the supernatant, resuspending the cells in 1 mL ice cold PBS and centrifugating the tubes again. After removal of the supernatant, the pellets were flash frozen in liquid nitrogen and stored at −80 °C.

After thawing the pellet, cells were resuspended in 250 µL lysis buffer (see table A.1 on page A.3 in the appendix) whereafter glass beads were added to the tube. The suspension was shaked 4 times with MP Fastprep for 30 seconds at speed 6, with an interval of 1 minute on ice. Next, the cell debris was pelleted by centrifugation at 3500 rpm for 5 minutes at 4 °C. The supernatant was transferred to a microcentrifuge tube and centrifuged (30 minutes, 13000 rpm, 4 °C). The supernatant, which contained the protein extract, was transferred to a new microcentrifuge tube. The concentration of the protein extract was determined based on the Pierce assay whereafter the extract was diluted to 1 mg mL^{-1} in lysis buffer.

4.12.2 Pierce assay

First a standard dilution series of BSA in lysis buffer was made (0 - 0.2 - 0.4 - 0.6 - 0.8 - 1 - 2 - 4 $\mathrm{mg\,mL^{-1}}$) in a microtiter plate. Next, 10 µL of each protein sample was brought in to the microtiter plate. 150 µL of Pierce 660nm Protein assay reagent was added to all wells whereafter the plate was shaken for 1 minute. After an incubation period at room temperature of 5 minutes the absorbance of the samples was detected at 620nm (Beckman DXT 880 Multimode Detector). Based on the absorbance measurements of the BSA dilution serie, a standard curve was made to calculate the protein concentration of the samples.

4.12.3 Immunoprecipitation

The antibody of interest was added in the concentration suggested by the company (2.5 µL for anti-SY1 antibody and 1 µL for anti-myc antibody) to 500 µL 1 $\mathrm{mg\,mL^{-1}}$ protein sample. In order to let the antibody bind to the protein of interest, the mixture was rotated overnight at 4 °C on a rotating wheel. After the overnight incubation, 50 µL of dynabeads were added to an empty microcentrifuge tube and washed with 1 x PBS containing 0.02 % Tween 20. Next, 500 µL of the with antibody incubated protein solution was added to the beads. This mixture was rotated for 30 minutes at room temperature. During this incubation period, the antibody attached to the beads using its Fc region. After a short spin the samples were washed 4 times with 500 µL lysis buffer using a magnet holder. During the last washing step, the sample was transferred to a new microcentrifuge tube. After removing lysis buffer for the fourth time, the beads were resuspended in 40 µL sample buffer (50 mM Tris pH 8, 2 % SDS, 0.1 % bromophenol blue, 10 % glycerol and 10 mM β-mercaptoethanol). An incubation period of 15 minutes at 95 °C resulted in elution of the antibody bound protein. After a short spin, the eluted antibody protein solution was separated from the beads using the magnet holder. The solution was then transferred to a new microcentrifuge tube and was ready for western blotting.

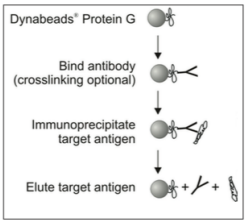

Figure 4.1: A schematic overview of the immunoprecipitation using Dynabeads protein G as described by the NOVEX® by life technologies™. In our procedure, the antibody was bound to the protein of interest before the complex was attached to the dynabeads.

4.13 Fluorescence activated cell sorting

Fluorescence activated cell sorting (FACS) is a type of flow cytometry. It can seperate cells based on differences in fluorescence and light scattering. It quantitatively records the fluorescence intensity while also physically separating the cells into different pools. The fluorescent dyes used for the FACS were dihydroethidium (DHE) and propidium iodide (PI). DHE is used to measure the amount of reactive oxygen species (ROS) which coincides with apoptosis of yeast cells. The dye is lipophilic and therefore can be oxidized by superoxide radicals, a reaction that results in the product ethidiumbromide. After being formed, ethidiumbromide will intercalate double stranded DNA resulting in a detectable red fluorescent signal proportional to the amount of apoptotic cells (Benov et al., 1998). PI gives an indication of the cell viability by identifying dead cells in the population. PI is a red fluorescent molecule that intercalates in double stranded DNA without sequence preference. After binding to the DNA the fluorescence increases 20-30 fold making it easily detectable during flow cytometry. In viable cells the PI dye cannot enter the cell because it is membrane impermeable. The function of the PI dye and guidelines for its use are described by invitrogen, life technologies^{TM}.

4.13.1 Procedure

3 mL cultures were grown and at different timepoints (12h, 36h and 60h) an amount of 100/OD µL cells was taken from the cultures and added to a microwell plate. A certain amount of 1x PBS was added in order to reach a final volume of 100 µL. A 4x final concentration solution of the dyes in 1x PBS was prepared as described in the appenidx A.2.4 on page A.7. 50 µL of a staining solution and 50 µL 1x PBS were added to the wells. For the blank, instead of adding staining solution, 100 µL 1x PBS was added. After the plate was prepared, it was shaked for 10 seconds (in a plate shaker at 1200rpm) followed by an incubation period of 10 minutes at 30 °C in dark. Next, the cells were pelleted by centrifugating the plate at 3000rpm for 10 minutes. Afterwards, the cells were resuspended in 200 µL 1x PBS. This washing step was repeated once more to remove all background staining. As a final step the cells were diluted by resuspending 20 µL of every prepared well in 200 µL 1x PBS in a new well plate. The DHE and PI values were then measured using the Guava .

4.14 Preparing double deletion strains

A double mutant strain lacking both *UBC4* and *UBC5* was created using following procedure: Single colonies of a mating type α *ubc4*Δ strain and a mating type a *ubc5*Δ strain were inoculated on a YPD plate and mixed. After overnight incubation at 30 °C, cells were plated out on minimal medium lacking lysine and methionine. In this way only diploids containing both selectable markers could grow. After an incubation period of 24h at 30 °C, single colonies were inoculated in 3 mL YPD until reaching stationary growth. Subsequently, cells were precipitated, the supernatant was removed and the cells were resuspended in the remaining liquid layer. From these

cell suspensions 20 µL was spotted on plates containing sporulation medium and were incubated at room temperature for 6 days. For the content of the sporulation medium, see section A.1.2.

4.14.1 Tetrad analysis

After tetrads were formed on the sporulation plates, the tetrad analysis was performed. Cells were incubated for 30 minutes in 45 µL H_2O containing 5 µL lyticase solution in order to digest the wall of the ascus. Next, the solution was dripped onto the side of a rich medium petri dish whereafter the spores were separated and placed in separate positions using a micromanipulator needle. After 3 days of growth at 30 °C the tetrads were analyzed. Analysis is facilitated by the fact that growth of the segregants follows mendelian rules.

For the first step of the analysis, the grown segregants were plated out on agar medium containing 150 µg mL^{-1} geneticin. In this way, only segregants in which the gene *UBC4* and/or *UBC5* was replaced by the KanMX cassette could grow. This is the case for the deletion strains and the double deletion but not for the WT.

4.14.2 Phenol-chloroform extraction

For further analysis, the genomic DNA of the different segregants was extracted using the liquid-liquid phenol-chloroform extraction. This was done by the following steps: Segregants that grew on the YPD plate with geneticin were resuspended in 150 µL 1x TE buffer pH 8 in a fastprep tube. After addition of glassbeads and 150 µL phenol-chloroform (1:1), cell lysates were obtained by shaking the suspension two times for 20 seconds with fastprep MP at speed 6. Next, the suspension was centrifuged for 10 minutes at 14000 rpm yielding a lower organic phase and an upper aqueous phase, the latter containing the genomic DNA. The upper phase was used in a PCR to identify the segregants with the double deletion *ubc4/ubc5*Δ.

4.14.3 PCR

For the PCR, the DNA containing phase was added to the PCR-mix given below. The content and amounts in the mixture were adapted from the KAPA Taq PCR Kit Kapabiosystems protocol:

Table 4.7: Polychain reaction mix

Component	**Amount (for one 20 µL reaction)**
Genomic DNA	1 µL
Primer (forward) (1 µg µL^{-1})	1 µL
Primer (reversed) (1 µg µL^{-1})	1 µL
dNTPs (10 mM)	1 µL
10x KAPA Taq reaction buffer (B)	2 µL
10x KAPA Taq DNA polymerase	0.15 µL
MilliQ H_2O	13.85 µL

The chosen primers used in this study are given in table 4.6 on page 22. The two forward primers were specific upstream sequences from the *UBC4* and *UBC5* genes, whereas the reversed primer was chosen in the KanMX4 cassette that replaces the deleted genes in the deletion strains. After the mixes were prepared the PCR was carried out with the following program. The program was executed by the PCR Thermal cycler.

95 °C	5 min
95 °C	30 sec*
56 °C	30 sec*
72 °C	90 sec*
72 °C	10 min
10 °C	∞

The steps with '*' indicate a 3-step cycle that was repeated for 35 times before preceeding to the following steps. After the PCR, the amplified DNA was detected using agarose gel electrophoresis.

4.14.4 Agarose gel electrophoresis

1 % agarose was dissolved in 0.5 X TAE buffer by boiling the solution for 5 seconds in the microwave. The heated solution was poured in the holder (comb already in place) and left for some time until the gel was solidified. In the meantime, loading dye (6x) was added to the PCR products. After the gel was solidified the comb was removed and the PCR products were loaded into the slots. To have a reference of fragment size, also a smartladder® was loaded. Finally, after a running period, the gel was incubated in ethidiumbromide for at least 15 minutes to make detection possible.

5. Results

5.1 Influence of protein degradation components on synphilin-1 biology in yeast

5.1.1 Validation of SY1 expression in yeast

To study SY1 aggregation, localization and ubiquitination the host lab utilizes humanized yeast models expressing SY1. Therefore, yeast cells of the BY4741 type were transformed with native SY1 (pYX212-SY1 plasmid) or SY1 with an N-terminal dsRed tag (pYX212-dsRedSY1 plasmid). Control strains were also prepared by transforming the corresponding empty vectors (pYX212 and pYX212dsRed). An overview of the used strains and plasmids is given in table 4.2 on page 20 and 4.4 on page 21. The native SY1 expressing cells were used to study the effect of SY1 on growth and to look into SY1 ubiquitination. In contrast, the dsRed-tagged SY1 expressing cells were used to study aggregate formation and localization using fluorescence microscopy. After the cells of the different strains were transformed, the expression of SY1 was validated. The strains were grown until mid-exponential phase after which the proteins were isolated as described in section 4.7. After performing western blot analysis (see section 4.8) on the protein extracts, immunodetection was done with an anti-SY1 antibody. For each transformation five transformants were analyzed. One of the transformant validations is given in figure 5.1 on the next page.

In addition to the strains that have been studied previously by the host lab (WT, *pre9*Δ, *ubc4*Δ and *ubc5*Δ) an extra strain was added in our research due to its interesting features. In this additional strain *ltn1*Δ, a RING domain ubiquitin ligase is deleted which disturbs the UPS. Nyström and coworkers discovered that when Htt103Q, the protein causative for Huntington's disease, is expressed in *ltn1*Δ, the cellular toxicity is enhanced compared to WT. In addition, fewer, but bigger Htt103Q inclusions were found with a higher tendency to be located at the nucleus (non published data). This makes the *ltn1*Δ an interesting study object in our research.

Yeast cells transformed with native SY1 (pYX212-SY1 plasmid) clearly express protein at the full-length height of SY1 i.e. 130kDa (see figure 5.1 on the next page). Furthermore, smaller synphilin-1 fragments are seen at 90kDa, 80kDa, 60kDa and 40kDa. This is in agreement with the literature (Büttner et al., 2010). In yeast cells transformed with the empty vector (pYX212) no such bands are seen.

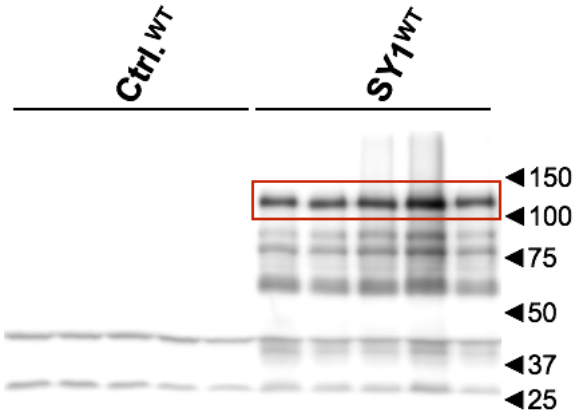

Figure 5.1: Validation of SY1 expression in transformed WT yeast strain of BY4741 type using western blot analysis. The Ctrl.^{WT} lanes represent five transformants of WT yeast with the empty vector pYX212 plasmid. The SY1^{WT} lanes represent five transformants of WT yeast with the pYX212-SY1 plasmid. The arrows at the right side of the figure indicate the molecular weight of the different fragments as determined by the protein ladder. Anti-SY1 was used as primary antibody. The secondary antibody was goat anti rabbit (see table 4.4 on page 22). The SY1 bands are indicated by a box and are present at the height of 130kDa.

All diferent strains from table 4.2 on page 20 were transformed with pYX212 and pYX212-SY1 whereafter the expression was validated in a similar way. In all transformed strains SY1 expression was verified. Therefore they could be used for growth analysis and immunoprecipitation.

5.1.2 Quantification of the SY1 expression in the different mutant strains

After verifying the SY1 expression in the different strains, we quantified the SY1 expression level. For this we determined the ratio of the immuno-response towards the SY1 antibody versus an antibody recognizing yeast Adh2, a typical yeast housekeeping gene. The SY1 expression level in the different BY4741 strains i.e. WT, *pre9*Δ, *ltn1*Δ, *ubc4*Δ and *ubc5*Δ is given in figure 5.2 on the next page.

Since the SY1 expression (see figure 5.2 on the following page) does not differ significantly between the strains we conclude that the expression levels are comparable. Unfortunately, due to a lack of data *pre9*Δ could not be compared with WT and *ltn1*Δ.

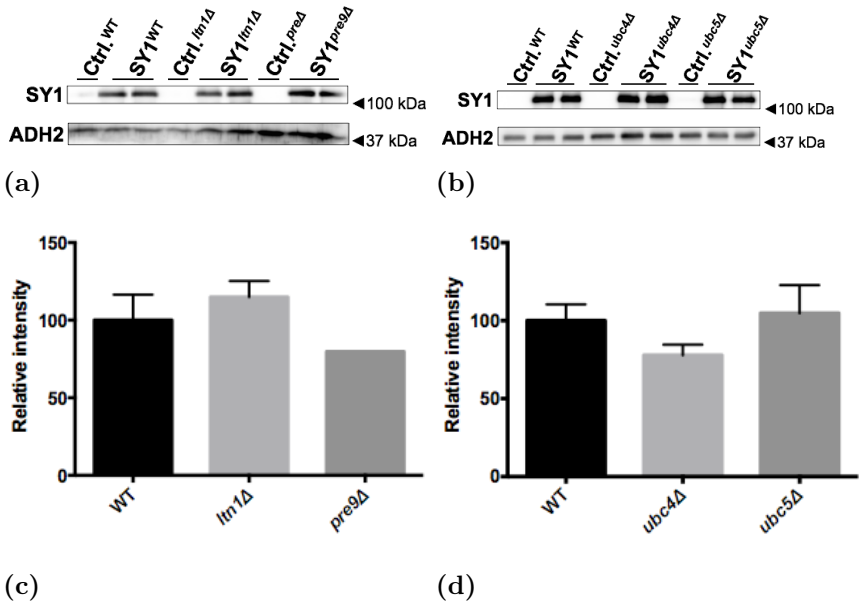

Figure 5.2: Quantification of the SY1 expression. In the upper box of figure (a) and (b) SY1 expression is analyzed. These blots were detected with SY1 primary antibody and goat anti-rabbit secondary antibody. In the lower box of (a) and (b) ADH2 expression was checked using primary anti-ADH2 antibody and secondary antibody goat anti-rabbit. Figure (c) and (d) represent the SY1 expression between the different strains based on the relative intensities (SY1 intensity/ ADH2 intensity). From each strain two transformants from the transformation with pYX212-SY1 plasmid were used whereas one transformant with the pYX212 plasmid was used. The SY1 expression did not significantly differ between the strains as determined by Welch's t-tests (α=0.05). For *pre9*Δ only one SY1 expressing transformant was used for quantification due to the quality of the blot. Hence no standard deviation (StDev) is given and no t-test was done with this strain.

5.1.3 Immunoprecipitation to investigate the ubiquitination status of SY1 in the different strains

To investigate if SY1 is ubiquitinated (for its degradation) and if the amount of ubiquitinated SY1 differs between the different strains, immunoprecipitations were performed. For each strain, transformants expressing native SY1 (pYX212-SY1) and the corresponding empty vectors (pYX212) were analyzed. The immunoprecipitation was performed using the protocol described in section 4.12. For the first immunoprecipitation, cells were grown until an OD_{600nm} of 2. The antibody used for the precipation was anti-SY1 and the antibodies used during detection were anti-SY1 and anti-Ub (stock nr. 25). The lysis buffer that was used during the immunoprecipitation protocol is given in table 5.1 on page 34.

Even though the immunodetection of SY1 (figure 5.3a and 5.3c) shows that the

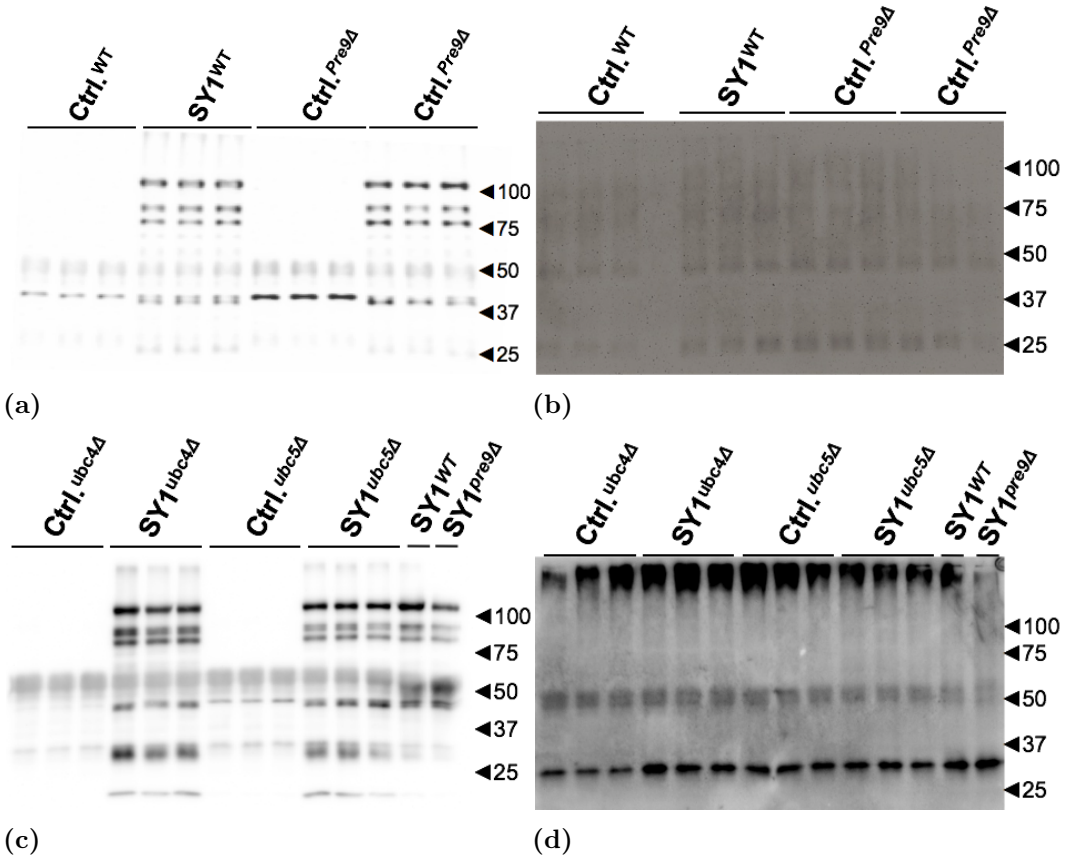

Figure 5.3: Immunoprecipitation of protein extracts from the WT, *pre9*Δ, *ubc4*Δ and *ubc5*Δ strains during exponential phase. For each strain three transformants expressing SY1 (pYX212-SY1 plasmid) and three empty vector (pYX212 plasmid) transformants were used. Blots (a) and (c) were detected with anti-SY1 and (b) and (d) were detected with anti-Ubi (stock nr. 25). The secondary antibody used for blots (a) en (c) was goat anti-rabbit. For the (b) and (d) blots this was goat anti-mouse.

Table 5.1: The content of the lysis buffer used during the immunoprecipitation protocol.

Component	**Stock concentration**	**Amount (for** 10 mL **final volume)**
HEPES-NaOH (pH 7.5)	500 mM	800 µL
NaCl	1.2 M	1 mL
EDTA	1 M	10 µL
Protease inhibitor (40 µg mL^{-1} aprotinin, 40 µg mL^{-1} leupeptin, 20 µg mL^{-1} pepstatin A)	/	1 tablet
CHAPS	3 %	1 mL
NaF	1 M	500 µL
β-glycerophosphate	1 M	100 µL
MilliQ H_2O	/	6.59 mL

immunoprecipation was succesful, we were not able to detect ubiquitinated SY1 even when the Supersignal® West Femto Maximum Sensitivity Substrate (Thermo Scientific) was used. Therefore, the immunoprecipitation was repeated and immunodetection of the blots was done using a different anti-ubiquitin primary antibody (stock number 169). The result of the immunodetection with this alternative ubiquitin antibody is shown in figure 5.4 on the following page.

When we compare the blots detected with two different anti-ubiquitin antibodies (figure 5.3 on the preceding page and figure 5.4 on the next page) we can see that the alternative ubiquitin antibody (nr. 169) gives a better result. In figure 5.4 we can clearly see small ubiquitinated fragments in the transformants expressing SY1 for all different strains. Moreover, we can see that in some of the SY1 expressing transformants of *pre9*Δ and *ubc4*Δ, there is a smear of ubiquitinated protein around the height of full length SY1 (130kDa).

Since we expected more ubiquitinated protein in stationary yeast cells, a next immunoprecipitation was performed using cultures of the same transformants grown for 48h to make sure they had reached stationary phase. In this immunoprecipitation the SY1 antibody was again used as precipitant.

As we can see in figure 5.5 on page 36, no major differences were seen when the immunoprecipitation was performed with extracts of stationary grown cells. The SY1 fragment of size 60kDa can be seen only vaguely in all different strains as was

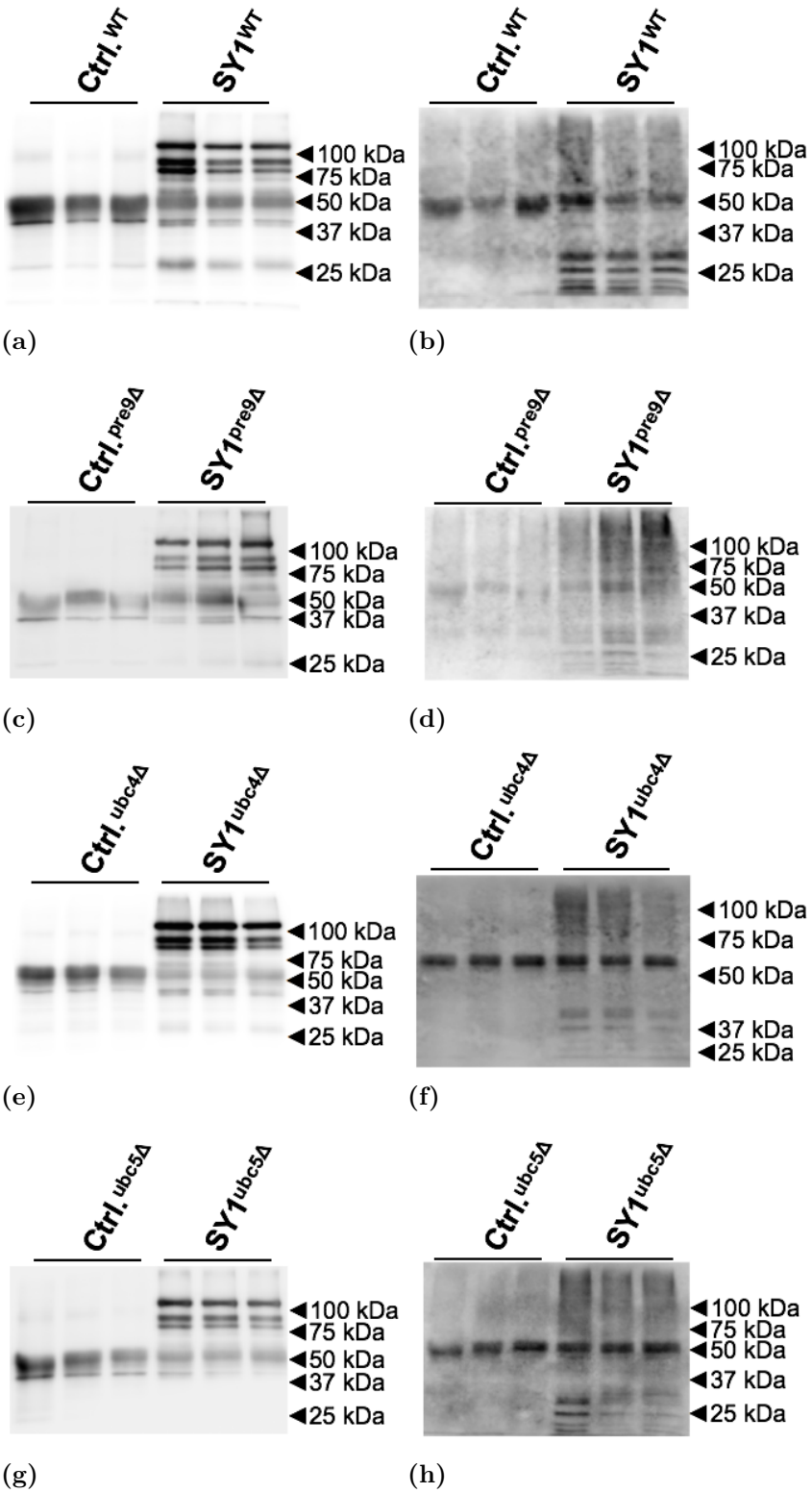

Figure 5.4: Immunoprecipitation of protein extract from the WT, *pre9*Δ, *ubc4*Δ and *ubc5*Δ strains during exponential phase. For each strain again three transformants expressing SY1 (pYX212-SY1 plasmid) and three empty vector (pYX212 plasmid) transformants were used. Blots (a), (c), (e) and (g) were detected with anti-SY1 and (b), (d), (f) and (h) with anti-ubiquitin (nr. 169). The secondary antibodies used were the same as for the immunodetection of the blots in figure 5.3 on page 33.

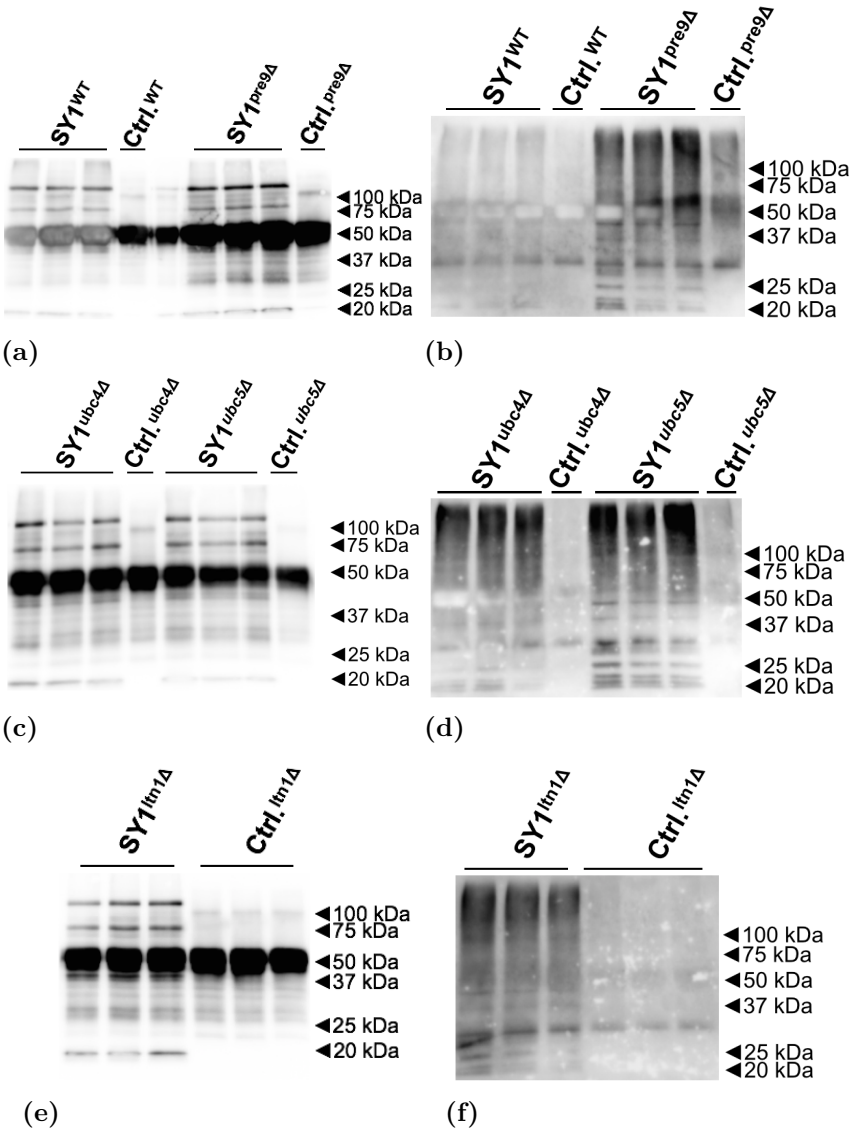

Figure 5.5: Immunoprecipitation of the protein extracts from the WT, *pre9*Δ, *ubc4*Δ, *ubc5*Δ, *ltn1*Δ strains after reaching stationary phase. For each strain, except for *ltn1*Δ, three transformants expressing SY1 (pYX212-SY1 plasmid) and one empty vector (pYX212 plasmid) transformant were used. For the *ltn1*Δ three transformants for both transformations were used. Blots (a), (c) and (e) were detected with anti-SY1 antibody and (b), (d) and (f) with anti-Ubi antibody (nr. 169). The secondary antibodies used were the same as for the immunodetection of the blots in figure 5.3 on page 33

.

the case for all previously performed immmunoprecipitations. Also no clear bands at the full length height of SY1 could be observed. However, since looking at stationary grown cells is more in line with the other experiments performed in this work we decided to perform all following immunoprecipitations with stationary cultures.

As was described in section 2.2.2, the amount of ubiquitinated protein is determined by the activity of the proteasome but also by the amount of deubiquitinating enzymes (DUBs). Ubiquitin is a relatively long-lived protein since it can be efficiently removed from its conjugate proteins by DUBs. Therefore, there is a possibility that DUBs are still active after making protein extracts from the samples and that this results in the weak signal around full length SY1 as we observed in the previous immunoprecipitations. Therefore, as a next optimalisation step we added the broad-range, reversible DUB inhibitor, PR-619 to the lysis buffer. This inhibitor of ubiquitin isopeptidases was already used in previously described work (Seiberlich et al., 2012). In addition to this small molecule inhibitor also N-ethylmaleimide (NEM) was added to the lysis buffer. This component helps preserving the ubiquitination and has been used for immunoprecipation in the past (Imai et al., 2000; Kaganovich et al., 2008). The used concentrations were based on previously described work and are give in table 5.2 (Seiberlich et al., 2012).

Table 5.2: Lysis buffer buffer content with additional inhibitors as used for the immunoprecipation given in figure 5.6 on the next page.

Component	**Stock concentration**	**Amount (for** 10 mL **final volume)**
HEPES-NaOH (pH 7.5)	500 mM	800 µL
NaCl	1.2 M	1 mL
EDTA	1 M	10 µL
Protease inhibitor (40 µg mL^{-1} aprotinin, 40 µg mL^{-1} leupeptin, 20 µg mL^{-1} pepstatin A)	/	1 tablet
CHAPS	3 %	1 mL
NaF	1 M	500 µL
β-glycerophosphate	1 M	100 µL
MilliQ H_2O	/	6.085 mL
PR-619	40 mM in DMSO	5 µL
N-ethylmaleimide	500 mM in EtOH	500 µL

During the immunoprecipitations we observed that the Dynabeads suffered from the high concentration of ethanol in the lysisbuffer that was used to dissolve the NEM. Nevertheless, the blots that were the result of the immunoprecipitation were of good quality and were used for analysis (figure 5.6). Small improvements are seen on the blots detected with anti-ubiquitin antibody. The signal around full length SY1 (130 kDa) is more or less appearing as a separate band. Unfortunately, the signal is still weak and does not allow quantification and comparison between the different strain.

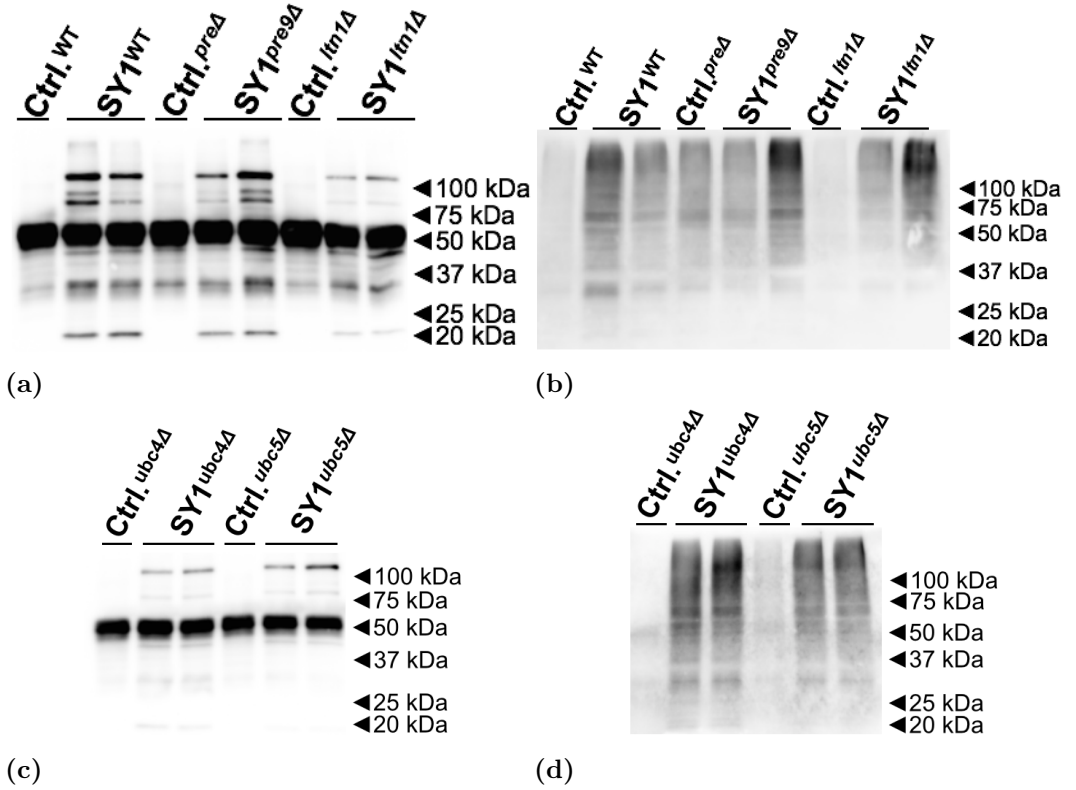

Figure 5.6: Immunoprecipitation of the protein extracts from the WT, *pre9*Δ, *ubc4*Δ, *ubc5*Δ, *ltn1*Δ strains after addition of 10 µM **PR-619 and** 25 mM **NEM.** For each strain, two transformants expressing SY1 (pYX212-SY1 plasmid) and one empty vector (pYX212 plasmid) transformants were used. Blots (a) and (c) were detected with anti-SY1 whereas (b) and (d) where detected with anti-Ubi (nr. 169). The secondary antibodies used were the same as for the immunoprecipitation of figure 5.3 on page 33.

The suffering of the dynabeads from the high ethanol concentration made it more difficult to keep a high yield. We circumvented adding NEM from a stock solution and instead added NEM powder directly to the lysis buffer. We did this until reaching a concentration of $1\,\mathrm{mg\,mL^{-1}}$ which is more or less the same as 8 mM.

The content of the adapted lysis buffer is given in table 5.3. Immunoprecipitations were performed using this optimized lysis buffer and the results are shown in figure 5.7.

Table 5.3: The content of the optimized lysis buffer used for immunoprecipitation given in figure 5.7 on the next page.

Component	**Stock concentration**	**Amount (for 10 mL final volume)**
HEPES-NaOH (pH 7.5)	500 mM	800 µL
NaCl	1.2 M	1 mL
EDTA	1 M	10 µL
Protease inhibitor (40 µg mL^{-1} aprotinin, 40 µg mL^{-1} leupeptin, 20 µg mL^{-1} pepstatin A)	/	1 tablet
CHAPS	3 %	1 mL
NaF	1 M	500 µL
β-glycerophosphate	1 M	100 µL
MilliQ H_2O	/	6.085 mL
PR-619	40 mM in DMSO	5 µL
N-ethylmaleimide	powder	0.01 g

When analyzing the blots in figure 5.7 on the next page we do not see major improvements. However, we can see in figure 5.7d that the immunodetection with ubiquitin gives a more intense signal for *ubc4*Δ than for *ubc5*Δ. Moreover, the ubiquitin signal seems more intense for *pre9*Δ than for WT and *ltn1*Δ. Unfortunately, quantification of these blots is not possible due to the weak signal around full length SY1. Even though these blots did not improve significantly compared to the blots of the former immunoprecipitation (figure 5.6 on the preceding page), we think it is better to work with the adapted lysis buffer because it facilitates working with the beads and results in a higher yield.

In none of the aforementioned immunoprecipitations we succeeded in visualising ubiquitinated SY1 clearly. Since we expect that this is due to the weak binding of the ubiquitin antibodies we tried to circumvent this by using a different approach. For this we transformed the BY4741 WT, *pre9*Δ, *ubc4*Δ, *ubc5*Δ, *ltn1*Δ strains with both the pYX212-SY1 and the plasmid pMRT39-myc-Ubi. Both plasmids are given in table 4.4 on page 21. The control strains were transformed with the corresponding plasmids (pYX212 and pMRT39-myc-Ubi). In this way, ubiquitin conjugated myc is expressed in yeast cells allowing us to detect ubiquitin indirectly. The expression

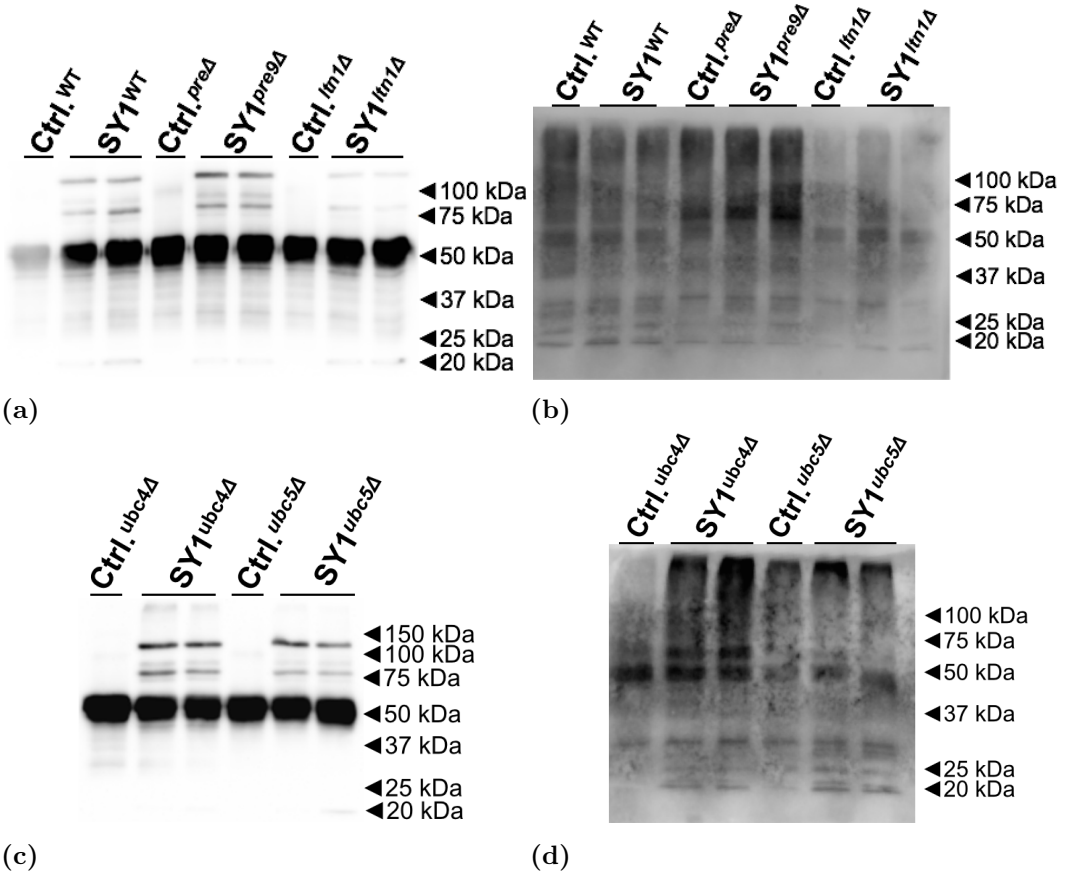

Figure 5.7: Immunoprecipitation of the protein extracts from the WT, *pre9*Δ, *ubc4*Δ, *ubc5*Δ, *ltn1*Δ strains after addition of 10 µM **PR-619 and** 1 mM **NEM.** For each strain, two transformants expressing SY1 (pYX212-SY1 plasmid) and one empty vector (pYX212 plasmid) transformants were used. Blots (a) and (c) were detected with anti-SY1 whereas (b) and (d) where detected with anti-Ubi (nr. 169). The secondary antibodies used were the same as for the immunodetection of the blots in figure 5.3 on page 33

.

of these transformed strains was verified in a similar way as the WT validation in section 5.1.

For the next immunoprecipitation the newly transformed strains were grown until stationary phase (OD 7-8). In contrast with previous immunoprecipitations, now two immunoprecipitations were done in parallel. In the first immunoprecipitation SY1 was precipitated using SY1 primary antibody. In the second immunoprecipitation myc conjugated to ubiquitin was precipitated using a anti-myc primary antibody. The lysis buffer remained unchanged (see table 5.3 on page 39). The result is shown in figure 5.8.

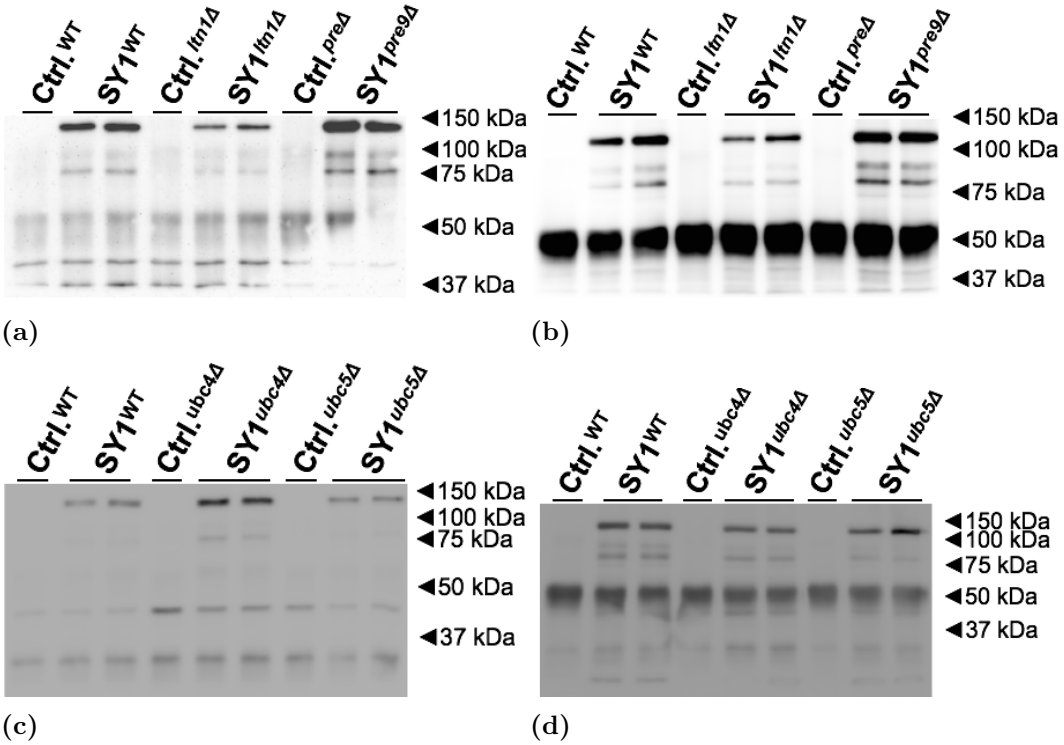

Figure 5.8: Results of two parallel immunoprecipitations of the protein extracts from WT, *pre9*Δ, *ubc4*Δ, *ubc5*Δ, *ltn1*Δ strains. Blot (a) and (c) are the result from the immunoprecipitation with myc-antibody whereas blot (b) and (d) resulted from the anti-SY1 immunoprecipitation. All blots are detected with anti-SY1 primary antibody and goat anti rabbit secondary antibody

.

The blots (a) and (c) shown in figure 5.8, which were immunoprecipitated with anti-myc and after blotting immunodetected with anti-SY1, show a clear band around full length SY1 (130kDa). This shows that SY1 is ubiquitinated in the different strains.

These findings indicate that SY1 is ubiquitaintedsuggest that SY1 is degraded by the

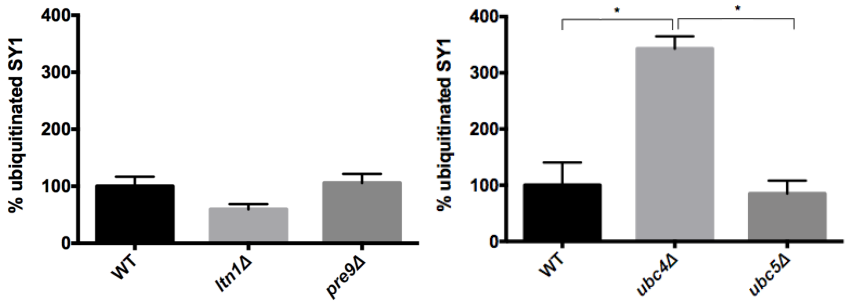

(a) (b)

Figure 5.9: The relative amount of ubiquitinated SY1 between the strains WT, *ltn1*Δ, *pre9*Δ, *ubc4*Δ and *ubc5*Δ. The amounts are based on the relative intensities of ubiquitinated SY1 (figure 5.8a and 5.8c on the preceding page) divided by the intensity of the total amount of SY1 (figure 5.8b and 5.8d). Welch's t-tests were perfromed using Prism 6. An asterisk stands for a significant difference (α=0.05). StDev are indicated in the figure.

UPS and that SY1 is probably found in JUNQ like inclusions. To determine the difference in ubiquitination of SY1 in the different strains, the amount of ubiquitinated SY1 was determined as shown in figure 5.9. These quantifications show that almost 3x more SY1 is ubiquitinated in the *ubc4*Δ strain whereas no significant difference in ubiquitinated SY1 was seen between the WT and the *ubc5*Δ, *ltn1*Δ and *pre9*Δ based on Welch's t-tests with a significance level of α=0.05. Additionaly, a significant difference was seen between *ubc4*Δ and *ubc5*Δ but not between *ltn1*Δ and *pre9*Δ.

Working independently of targetting and visualising ubiquitin directly and instead targetting ubiquitin using a myc conjugate, seems to be a better approach to detect ubiquitinated SY1. This strategy also allowed us to quantify the amount of SY1 that was ubiquitinated. Ofcourse we should keep in mind that probably more SY1 is ubiquitinated because not all ubiquitin in the cells is myc-tagged and therefore not all SY1 is detected by our approach.

The effect of different inhibitors on synphilin-1 ubiquitination

Using this approach we also studied the effect of different inhibitors on the amount of ubiquitinated SY1 in the cell. In order to do this, WT BY4741 precultures expressing myc-tagged ubiquitin (pMRT39-myc-Ubi) in combination with SY1 (pYX212-SY1) and the corresponding empty vector (pYX212) were grown overnight at 30 °C. Every preculture was grown 3 times in parallel. The next morning we diluted the three precultures from the same transformant in three different 50 mL cultures. One 50 mL culture contained 0.03 % DMSO and was used as a control, a second contained the DUB inhibitor PR-619 (10 µM) and a third contained the proteasome inhibitor MG-132 (3 µM). The 50 mL cultures were grown until stationary phase whereafter again two immunoprecipitations were performed in parallel. One in which SY1 was precipitated and one in which myc was precipitated. The lysis buffer that was used is given in table 5.3 on page 39.

In figure 5.10 on the following page we observed that there is no significant difference in ubiquitination level of SY1 between WT and the two types of inhibitor. However, there is trend suggesting that less SY1 is ubiquitinated when the inhibitors are present in the growth medium. This trend seems more pronounced for the MG-132 inhibitor than for the PR-619. This is in contrast with previous research that reported an increase in ubiquitinated proteins upon addition of the inhibitors (Seiberlich et al., 2012). Of course, our experiment should be repeated with more transformants in order to obtain more reliable results.

5.1.4 Growth analysis of cells expressing synphilin-1

In order to investigate the influence of SY1 expression on the growth of the different mutant strains, a growth analysis was performed. Therefore, WT, *ubc4*Δ, *ubc5*Δ, *ltn1*Δ and *pre9*Δ cells expressing SY1 (pYX212-SY1) and the corresponding empty vector (pYX212) were grown in selective medium as described in section 4.10. Every two hours the OD_{600nm} was checked and the average OD_{600nm} values over all transformants were plotted against time. Figure 5.11 on page 45 shows the growth of the different strains plotted against the growth of the WT strain. For the statistical analysis with the Welch's t-test all five transformants were used.

When looking at the growth of the different strains compared to the WT strain in figure 5.11 on page 45, we can see that the *pre9*Δ and *ubc4*Δ strains grow slower compared to the WT strain. Furthermore, in these two strains an additional and significant reduction in growth is observed upon SY1 expression, which is the most pronounced in the *pre9*Δ strain. In contrast, almost no difference in growth was seen when comparing *ubc5*Δ and *ltn1*Δ to the WT strain. Moreover, in these strains (WT included) SY1 expression resulted in a rather small but also significant growth reduction as indicated by single asterisks at the different timepoints.

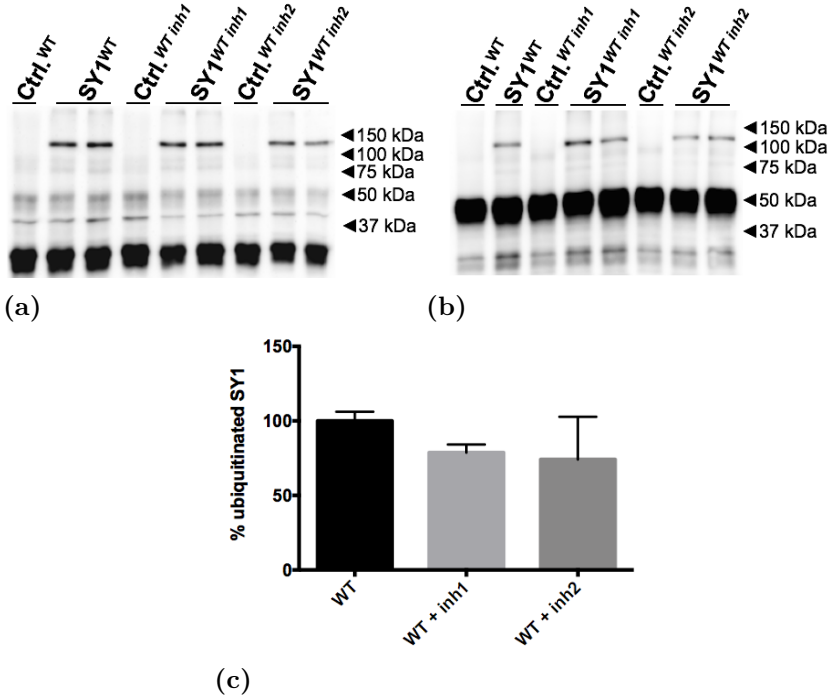

Figure 5.10: The results of two parallel immunoprecipitations of BY4741 WT strain in three different conditions. First condition (indicated with WT): Cells were grown in presence of 0.03 % DMSO. Second condition (indicated with WT^{inh1}): cells were grown in the presence of the DUB inhibitor PR-619 (10 µM). Third condition (indicated with WT^{inh2}): Cells were grown in presence of the proteasome inhibitor MG-132 (3 µM). Blot (a) is the result of the immunoprecipitation with myc-antibody whereas blot (b) resulted from the anti-SY1 immunoprecipitation. In blot (b) one sample of the first condition was lost during loading. Both blots are detected with anti-SY1 primary antibody and goat anti rabbit secondary antibody. (c) The relative amount of ubiquitinated SY1 between the three conditions. The amounts are based on the relative intensities of ubiquitinated SY1 (figure 5.10a) divided by the intensity of the total amount of SY1 (figure 5.10b). For the statistics, Welch's t-tests were performed in Prism 6. No significant differences in ubiquitination were seen between the different conditions (α=0.05). Standard deviations are indicated in the figure.

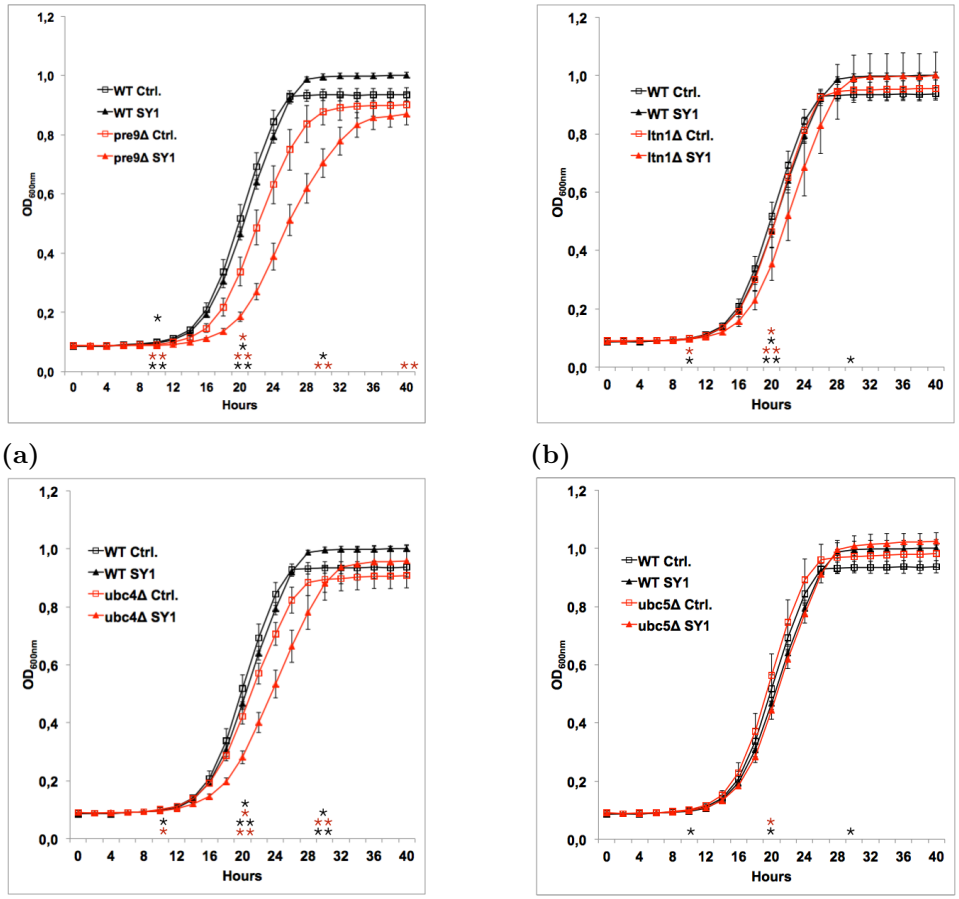

Figure 5.11: Growth analysis of SY1 expressing yeast cells. (a)(b)(c) and (d) show the growth of WT cells compared to respectively *pre9*Δ, *ubc4*Δ, *ubc5*Δ, *ltn1*Δ cells with (pYX212-SY1) or without (pYX212) SY1 expression. The asterisk is indicative for a significant difference in growth at a certain timepoint (α=0.05). At the timepoints 10, 20, 30 and 40 hours Welch's t-tests were performed on the data. The meaning of the different asterisk signs are explained in table A.2 on page A.11. The *pre9*Δ Ctrl. curve is the average over three independent transformants. For all other curves the average over four independent transformants was used. Standard deviations are indicated in the figure.

5.1.5 Growth analysis of the different deletion strains in the presence of inhibitors

Next, we studied the effect of the DUB inhibitor on the growth of the different strains in the presence and absence of SY1. Cells were grown in a similar way as under normal conditions, however now the inhibitor dissolved in DMSO was added to the selective medium to a final concentration of 10 µM. As a control the same strains were grown in the presence of a similar amount of DMSO (0.025%). The inhibitor concentration was adapted from a previous study (Seiberlich et al., 2012).

First of all, figure 5.12 on the next page again shows that the SY1 toxicity is most pronounced in the *pre9*Δ and *ubc4*Δ strains. However, the addition of the inhibitor does not cause a significant growth reduction on the strains in general, the toxic effect of SY1 was slightly aggravated in all strains (not significant for the *ubc5*Δ and *pre9*Δ) when the inhibitor was present. This suggests that SY1 toxicity is dependent on the ubiquitination machinery.

In a similar experiment the effect of the proteasome inhibitor MG-132 was investigated on the different strains. Therefore, cells were grown with and without 3 µM MG-132 in DMSO. The results are shown in figure 5.13 on page 48.

Based on the results given in figure 5.12 on the following page and figure 5.13 on page 48 we can see that the effect of the proteasome inhibitor on the growth in general is more pronounced than the effect of the PR-619 i.e. all transformed strains reach stationary phase at a lower OD when the MG-132 inhibitor is present. The toxic effect of SY1 was no longer present in the *pre9*Δ when grown in medium with MG-132. Possibly, the SY1 effect in *pre9*Δ is the same as the effect of the inhibitor. However, in the control (where no inhibitor was added) the difference between the empty vector (Ctrl.) and SY1 expressing *pre9*Δ without inhibitor is also less pronounced. In contrast with *pre9*Δ, the effect of SY1 is still present for the *ubc4*Δ but was not augmented by the inhibitor.

As an extra control experiment we evaluated the effect of DMSO on the growth of the different strains in the highest concentration used in the previous experiments (0.03%). Previous research showed that DMSO (in a concentration of 10 %) does slow down the growth of yeast cells while also increasing plasma membrane formation and the formation of intracellular membranes. Moreover, when expressed with α-synuclein it increases the amount of inclusions drastically (Zabrocki et al., 2005). It is therefore important to see to what extend our results are influenced by the presence of DMSO in the culture medium.

As we can see in figure 5.14 on page 49, no significant effect of DMSO in this low concentration is seen on the growth of the WT strain. The effect of DMSO on the growth of *pre9*Δ, *ltn1*Δ, *ubc4*Δ and *ubc5*Δ was also investigated (data not shown). For none of the strains there was a significant effect of DMSO at this concentration.

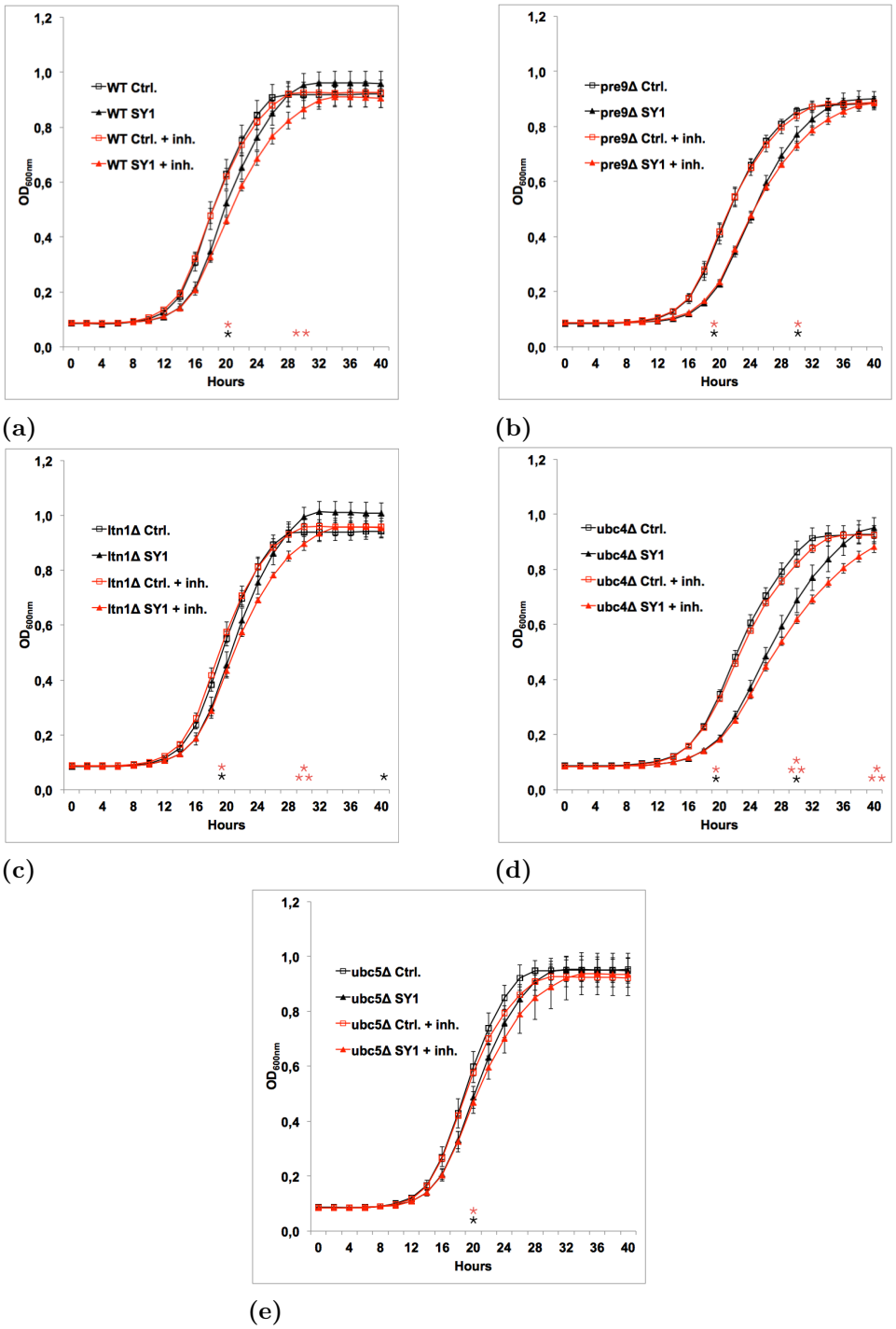

Figure 5.12: Influence of the DUB inhibitor PR-619 on SY1 expressing yeast cells. (a)(b)(c)(d) and (e) show the growth of respectively WT, *pre9*Δ, *ltn1*Δ, *ubc4*Δ, *ubc5*Δ cells with (red) and without (black) 10 µM of **PR-619 DUB inhibitor**. The condition without the inhibitor is in presence of a similar amount of DMSO (0.025%). For each strain the SY1 four SY1 expressing transformants were averaged (indicated with SY1). Furthermore, for each strain the average of four of the according empty vector transformants were plotted as well (indicated with Ctrl.). The asterisk is indicative for a significant difference in growth at a certain timepoint (α=0.05). At the timepoints 20, 30 and 40 hours Welch's t-tests were performed on the data. The meaning of the different asterisk signs are explained in table A.2 on page A.11. Standard deviations are indicated in the figure.

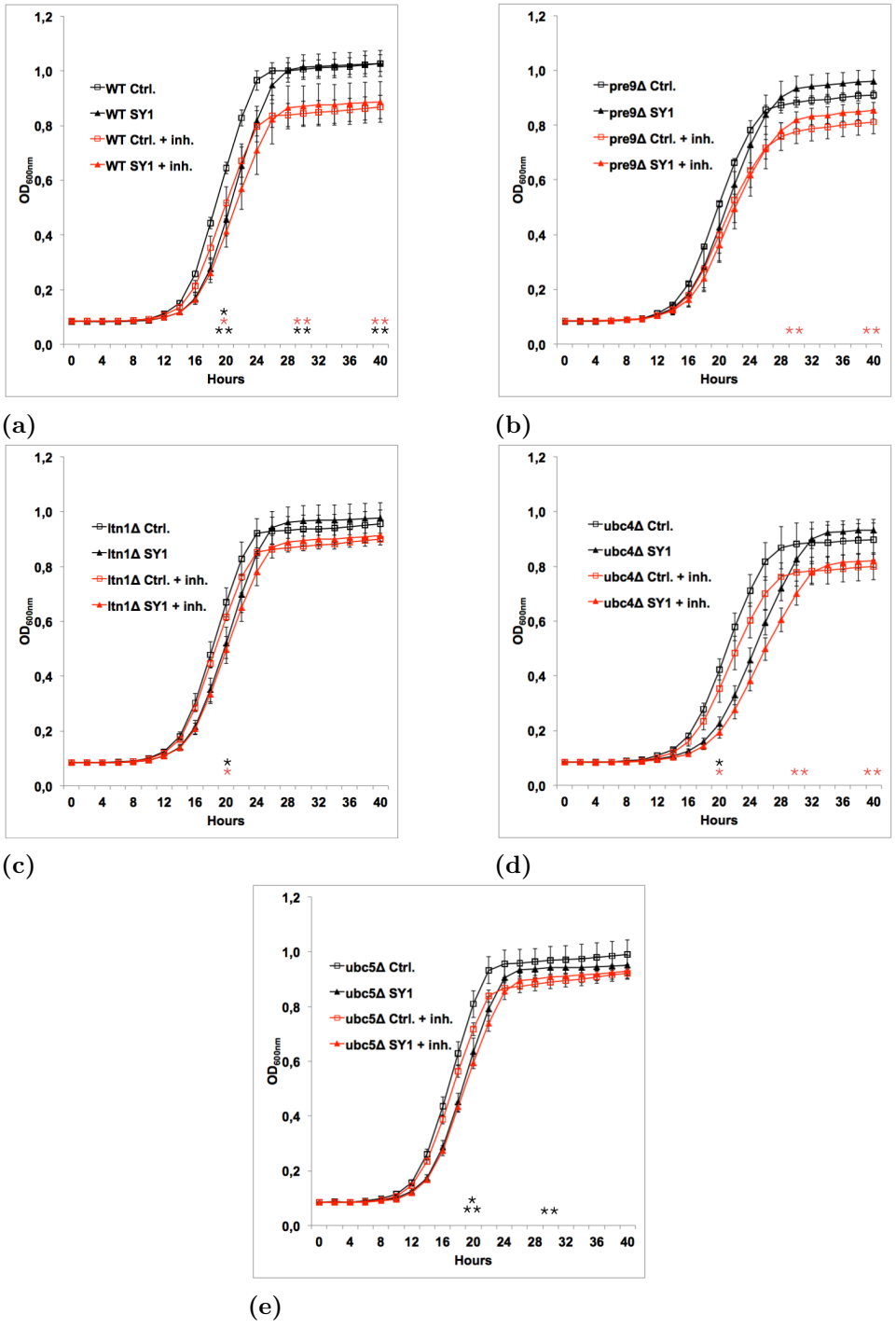

Figure 5.13: Influence of the proteasome inhibitor MG-132 on SY1 expressing yeast cells. (a)(b)(c)(d) and (e) show the growth of respectively WT, *pre9*Δ, *ltn1*Δ, *ubc4*Δ, *ubc5*Δ with (red) and without (black) 3 µM of **MG-132 proteasome inhibitor**. The condition without the inhibitor is in presence of a similar amount of DMSO (0.03%). For the *pre9*Δ Ctrl. and the *ubc5*Δ SY1 + inh. three transformants were averaged. For all other curves four transformants were used. The asterisk is indicative for a significant difference in growth at a certain timepoint (α=0.05) based on all four transformants. At the timepoints 20, 30 and 40 hours Welch's t-tests were performed on the data. The meaning of the different asterisk signs are explained in table A.2 on page A.11. Standard deviations are indicated in the figure.

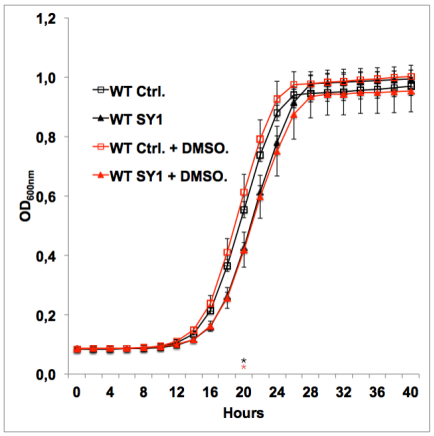

Figure 5.14: The effect of DMSO on the growth of WT BY4741. Black: Growth of WT strains in selective medium without DMSO. red: Growth of WT strains in selective medium containing 0.03% DMSO. The growth of WT cells with Synphilin-1 expression is indicated with filled triangles whereas the corresponding control strain is indicated using open squares. Asterisks are indicative for significant differences (α=0.05). More information about the signs is given in table A.2 on page A.11. For all plotted curves four independent transformants were averaged and the corresponding standard deviations are implemented on the curves.

5.1.6 Synphilin-1 inclusions formation

Yeast cells transformed with fluorescently labelled SY1 (pYX212-dsRed SY1) (see table 4.4 on page 21) were used to study SY1 inclusion formation by means of quantifying the amount of aggregates present in stationary grown cells (48h). As a control, cells transformed with the pYX212-dsRed plasmid were used. Using the fluorescence microscope, brightfield and fluorescent images were taken of the cells from three independent transformants. Next to the average amount of cells with SY1 inclusions, also the average amount of cells with small and large inclusions was determined. For each independent transformant atleast 200 cells were counted.

The quantification was done for the WT strain and the *ltn1*Δ, a strain that was included in our study because of its interesting features as described earlier. Furthermore, the *pre9*Δ strain was implemented in this study because only a limited amount of fluorescent data was available from previous studies. For the *ubc4*Δ and *ub5*Δ strains these quantifications were already performed in a previous study.

As shown in figure 5.15a on the next page we first quantified the amount of cells with inclusions. There is a significant difference between the % inclusion positive cells of the WT and the *ltn1*Δ strain as indicated by the asterisk. Moreover, a significant difference was seen between *ltn1*Δ and *pre9*Δ. No significant difference was seen

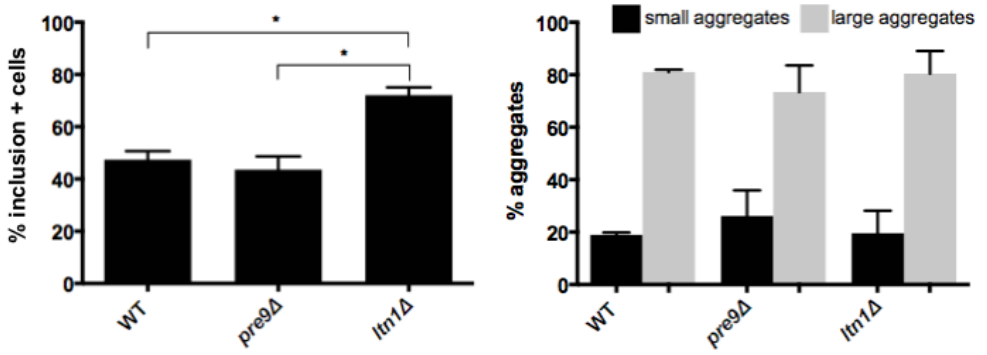

(a) **(b)**

Figure 5.15: SY1 inclusion formation in WT, *ltn1*Δ and *pre9*Δ cells. (a) The percentage of synphilin-1 inclusion positive cells for the different strains. (b) shows the percentage of small and large aggregates for each strain. For each strain three transformants were used and more than 200 cells were counted per transformant. Standard deviations are indicated in the figure. A significant difference ($\alpha = 0.05$) is indicated by an asterisk. For the statistics we used a two-sided Welch's t-tests in the program Prism 6.

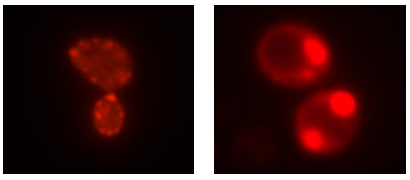

(a) **(b)**

Figure 5.16: Fluoresence microscopy images from WT BY4741 cells expressing fluorescently labelled SY1 (pYX212-dsRed-SY1). In figure (a) we see two cells with small aggregates whereas figure (b) shows cells in which the small aggregates are fused together into large inclusion. In one of the cells two large inclusions are positioned at the opposite poles.

between the WT strain and the *pre9*Δ. Subsequently, the fluorescence images were used to determine the amount of cells with large and small inclusions. Quantification of the amount of small and large inclusion (see figure 5.15b) showed no significant differences between the different strains. Figure 5.16 shows representative images of cells with small and large inclusions.

Previous research in the host lab reported a small increase in cells with inclusions for all UPS mutants (*pre9*Δ, *ubc5*Δ, *ubc4*Δ). Since we do not see an increase in inclusion positive cells in the *pre9*Δ, our results are in conflict with these findings. Furthermore, we report about 50% inclusion positive cells for the WT which is a little higher than the previously reported 33%. (Büttner et al., 2010). Moreover, the ratio of large to small inclusions was determined earlier as being 90 to 10 for the

WT while we report an 80 to 20 ratio for WT. These differences can be due to the subjective nature of determining the ratios. The previous study further showed that the ratio large over small inclusions does not change for *pre9*Δ and *ubc4*Δ compared to the WT. However, for *ubc5*Δ a small increase in large inclusions was found (95%) compared to the WT. We see a small but not significant increase in small aggregates for the *pre9*Δ and no difference for the *ltn1*Δ.

5.1.7 Synphilin-1 inclusion localization

Previous research suggests that compartmentalization of proteins depends on the degree of ubiquitination and their solubility. In 2008 the group of Kaganovich described two subcellular compartments i.e. IPOD and JUNQ. JUNQ lies in close proximity to the nucleus and contains mainly soluble ubiquitinated proteins. Furthermore, proteasomes are found in this compartment. On the other hand, IPOD is localized close to the vacuole and mainly insoluble non-ubiquitinated proteins are directed to this compartment (Kaganovich et al., 2008). Using a nuclear staining (DAPI) and a vacuolar staining (CMAC) we investigated whether SY1 has a tendency to be present in close proximity to the vacuole and/or the nucleus. SY1 localization was already investigated in the host lab for the strains *pre9*Δ, *ubc4*Δ and *ubc5*Δ. Non-published data showed that SY1 was located near the nucleus and vacuole for all these UPS mutants. Moreover, it was discovered that small inclusions occurred more often close to the nucleus while large inclusions were found more often close to the vacuole. In the different UPS mutants less aggregates were found close to the nucleus than in the WT. We have to keep in mind that these results are ambiguous and therefore more data should be analyzed with more steady and precise techniques that accurately identify certain compartments. For instance, the autophagy-related protein 8 (Atg8) and the endoplasmic reticulum marker Sec63 can be used as markers respectively for IPOD and JUNQ (Kaganovich et al., 2008).

In this study we looked into the localization of SY1 inclusions in the WT and the *ltn1*Δ strain. Figure 5.17 on the following page and 5.18 on page 53 show nuclear and vacuolar staining images of respectively the WT and *ltn1*Δ strain.

In these fluorescent pictures we see that for both WT and *ltn1*Δ the SY1 inclusions are located close to the nucleus and the vacuole. These results suggest that both JUNQ and IPOD like inclusions are found in both strains. However, at this point it is to early to draw reliable conclusions. In order to do this, further research has to be done using additional markers. For example the markers Sec63 and Atg8 co-localize respectively with JUNQ and IPOD and therefore they can provide extra proof on whether an aggregate is actually IPOD or JUNQ.

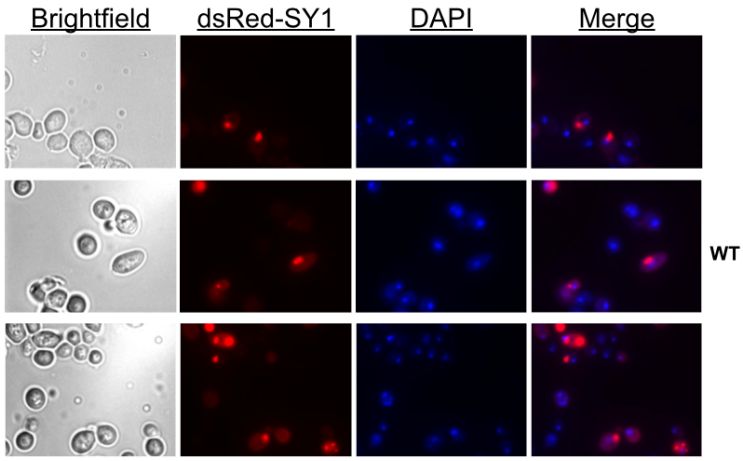

(a)

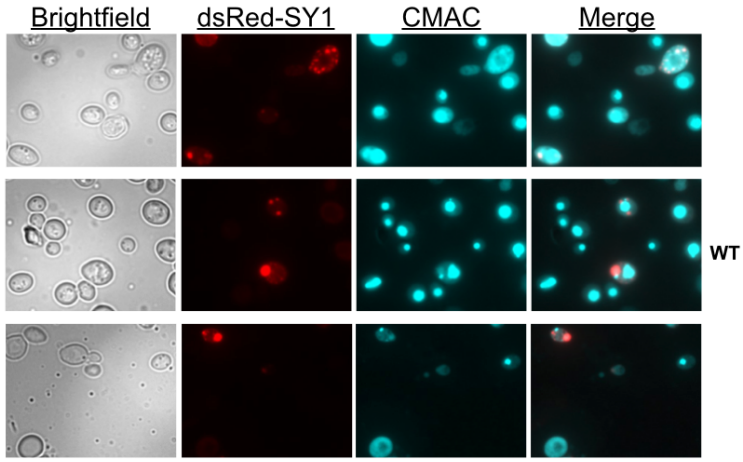

(b)

Figure 5.17: Fluorescence microscopy images of WT yeast cells after 48 hours of growth showing SY1 inclusion formation (red). In (a) the SY1 localization relative to the nucleus (DAPI) is shown whereas (b) shows the localization relative to the vacuole (CMAC). The first channel shows the brightfield image, the second SY1 inclusion formation (red), the third the nuclear/vacuolar staining and the last channel is an overlay of both fluorescent channels.

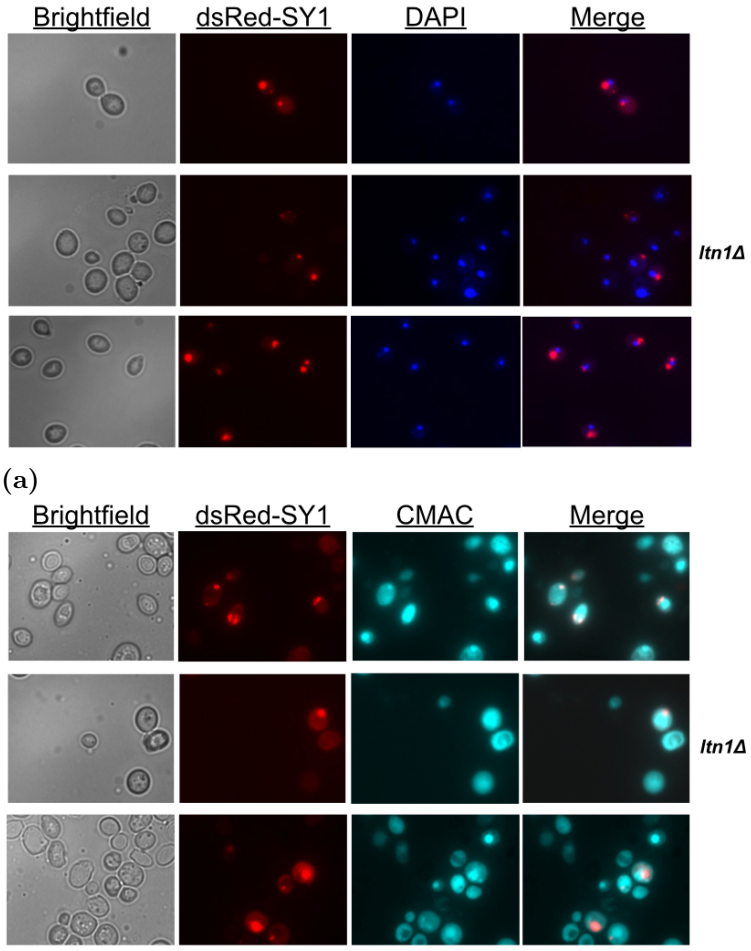

Figure 5.18: Fluorescence microscopy images of *ltn1*Δ yeast cells after 48 hours of growth showing synphilin-1 inclusion formation (red). In (a) the synphilin-1 localization relative to the nucleus (DAPI) is shown whereas in (b) shows the localization relative to the vacuole (CMAC). The first channel shows the brightfield image, the second SY1 inclusion formation (red), the third the nuclear/vacuolar staining and the last channel is an overlay of both fluorescent channels.

5.1.8 Synphilin-1 inclusion localization in the presence of inhibitors

In addition to the growth analysis of the BY4741 WT strain in the presence of different inhibitors we also looked at the inclusion localization of the SY1 expressing strains (pYX-dsRed-SY1) under similar conditions i.e. in the presence of 0.025% DMSO, 10 µM PR-619 in DMSO, 0.03% DMSO and 3 µM MG-132 in DMSO. Using a nuclear staining (DAPI) we investigated whether SY1 has a tendency to be present in close proximity to the nucleus. Therefore, three SY1 expressing transformants of each BY4741 strain were incubated for 48 hours in selective medium of each condition whereafter the staining was performed as described in sections 4.11.1. In figure 5.19 on the following page and figure 5.20 on page 56 we can see the result of the stainings.

For all different strains SY1 inclusions are often localized near the nucleus. Furthermore, when we see two aggregates at opposite poles in one cell, often one of them is situated close to the nucleus. We would expect this aggregate to be the JUNQ like inclusion. It seemed that upon addition of either one of the inhibitors, fewer cells with two large inclusions were found. This could mean that only IPOD is present in these cells since the UPS present in JUNQ like inclusions is impaired. However, these aggregates are sometimes found close to nucleus, which is in conflict with this idea. As mentioned before, additional experiments should be performed (e.g. using additional markers that co-localize with JUNQ and IPOD) before conclusions can be drawn.

5.1.9 The effect of the PR-619 inhibitor on SY1 inclusion formation

To see if the deubiquitinating enzyme inhibitor had an effect on the inclusion formation of SY1, we let SY1 expressing cells (pYX212-dsRed-SY1) from WT and all UPS mutants grow for 48h in the presence of PR-619 (10 µM) whereafter we analyzed the inclusions using the fluorescence microscope. The results are shown in figure 5.21 on page 57.

As can be seen in figure 5.21 on page 57, the percentage of inclusion positive cells does not change significantly when the inhibitor is present compared to the condition where there is no inhibitor in the growth medium. However, the percentage of small aggregates increased upon addition of the inhibitor in all different strains (not signficicant). Previous research states that DUB inhibition using PR-619 results in a stress response, an increase in ubiquitinated cytoplasmatic proteins and inclusions typically found in aggregopathies (Seiberlich et al., 2012). The observed increase in small aggregates possibly represents the previously described increase in toxic proteins. Since an enhanced SY1 toxicity was seen for all strains upon addition of PR-619 (see figure 5.12 on page 47), we assume that small aggregates are cytotoxic.

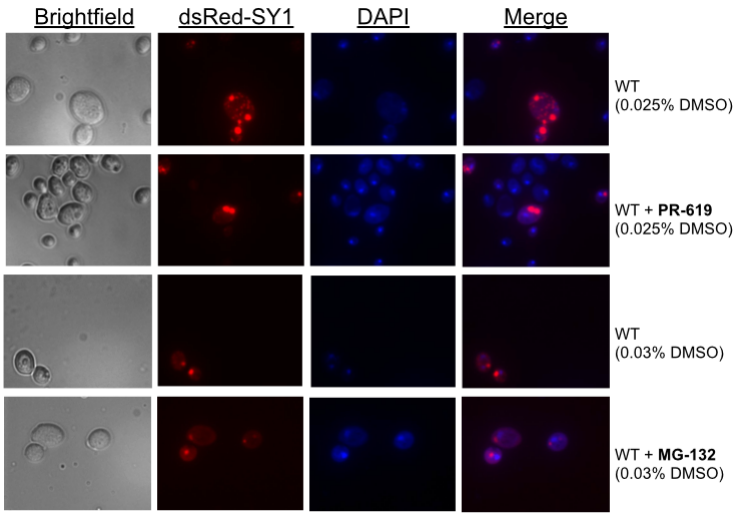

(a)

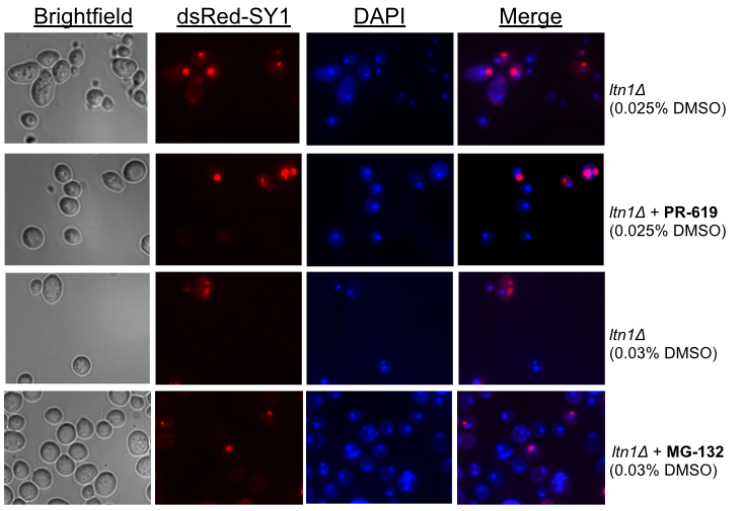

(b)

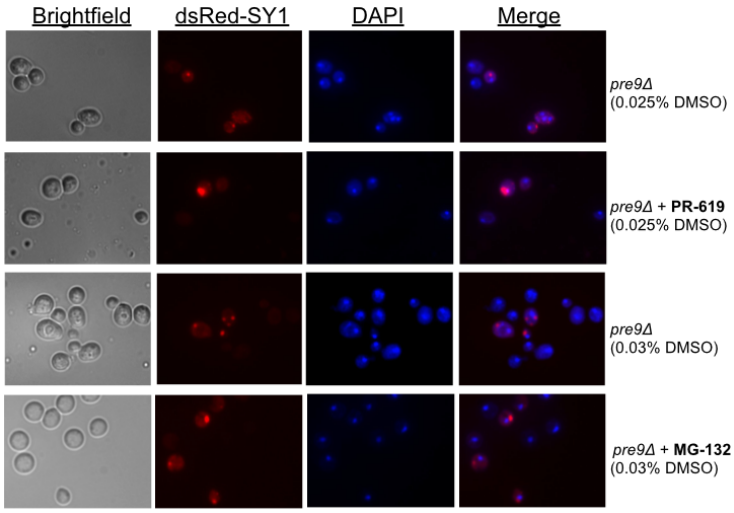

(c)

Figure 5.19: Fluorescence microscopy images after 48h of growth of respectively the WT (a), *ltn1*Δ (b) and *pre9*Δ (c) strain expressing dsRed tagged synphilin-1. The first channel shows the brightfield image, the second synphilin-1 inclusion formation (red), the third the nuclear staining (DAPI) and the last is an overlay of both fluorescent channels. The different growth conditions are indicated on the right side of the figure.

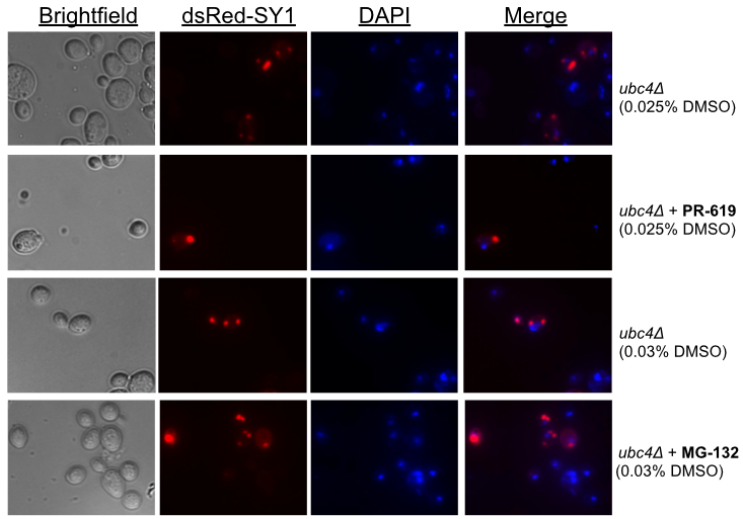

(a)

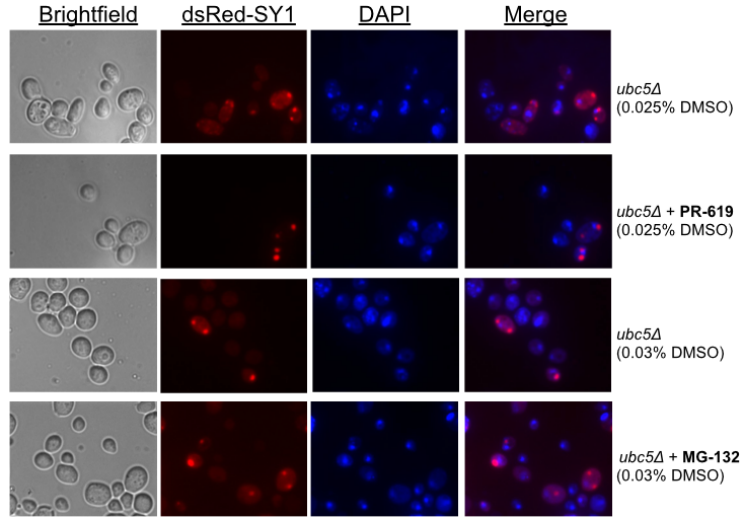

(b)

Figure 5.20: Fluorescence microscopy images after 48h of growth of respectively the *ubc4*Δ (a) and *ub5*Δ (b) strain expressing dsRed tagged synphilin-1. The first channel shows the brightfield image, the second synphilin-1 inclusion formation (red), the third the nuclear staining (DAPI) and the last is an overlay of both fluorescent channels. The different growth conditions are indicated on the right side of the figure.

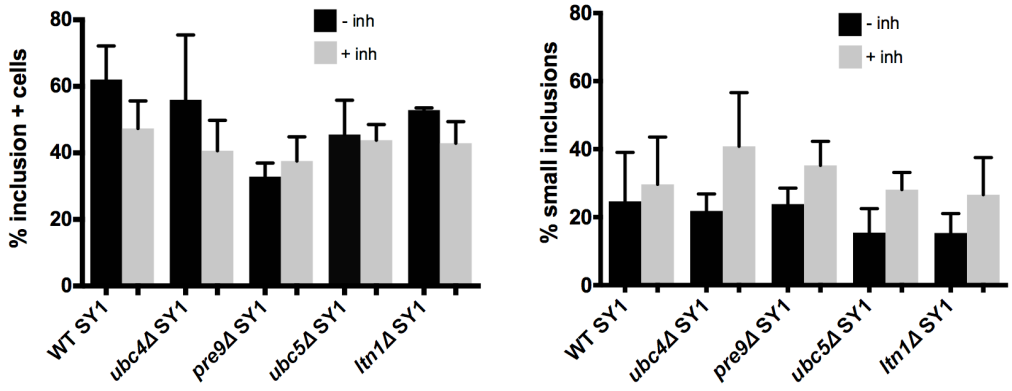

(a) (b)

Figure 5.21: SY1 inclusion formation in WT, *ubc4*Δ, *ubc5*Δ, *pre9*Δ, and *ltn1*Δ cells. (a) The percentage of SY1 inclusion positive cells for the different strain with (grey) and without (black) 10 µM PR-619. (b) The percentage of small inclusions in the different strains with (grey) and without (black) the inhibitor. For each condition at least 200 cells were counted. The standard deviations are indicated in the graphs. No significant differences were seen between the two conditions using Welch's t-tests (α=0.05).

5.1.10 Creation of the *ubc4*Δ*ubc5*Δ double deletion

As described in table 4.1 on page 19, *UBC4* and *UBC5* are paralogs and can atleast partly complement eachother. When no complementation of these genes is possible, additional knowledge can be gathered about their importance and influence on the toxicity of SY1. In order to do this, we tried to make the double deletion strain *ubc4*Δ*ubc5*Δ.

As depicted in method section 4.14, we used the *ubc4*Δ and *ubc5*Δ strains with the BY4741 background to gain a double mutant *ubc4/ubc5*Δ. After sporulation of the diploids and separating the tetrad using the micromanipulator, the four spores from one ascus were grown on a YPD plate as can be seen in figure 5.22.

Figure 5.22: YPD plate on which subsequently 4 spores of the diploid strain (made from *ubc4*Δ mating type α and *ubc5*Δ mating type a) were plated out horizontally.

From figure 5.22 on the previous page it can be seen that in none of the rows four segregants were able to grow. This means that one of the genotypes is lethal. The most logical explanation would be that this is the double deletion segregant. A tetrad can grow as non-parental ditype, meaning that you have two WT spores and two double mutants (deletions) in one tetrad. Another possibility is tetratype, meaning that all four possible spores are present (mutant 1 and 2, wild type and the double mutant). To analyze the tetrads we plated them out on medium containing $150\,\mu g\,mL^{-1}$ geneticin. Since, WT genotypes miss the KanMX4 cassette they cannot grow on this medium. In this way, WT segregants could be identified. This experiment strengthened the hypothesis that the double mutant is lethal in the BY4741 background (result not shown).

To be sure of the fact that none of the segregants was a double mutant, they were analyzed using PCR as described in method section 4.14.3. After the PCR, for neither one of the segregants a band appeared for both primer combinations which indicates that none of the segregants possessed both the *ubc4*Δ and the *ubc5*Δ deletion. Therefore, we conclude that the double mutant is lethal in the BY4741 background.

Fortunately, we were able to receive a viable double mutant strain in a different background as a gift from the group of Mark Hochstrasser (Chen et al., 1993). In addition to the double mutant we also received the corresponding WT, *ubc4*Δ and the *ubc5*Δ strains with the alternative background. An overview of the alternative strains (MHY series) is given in table 4.2 on page 20.

After receiving these alternative strains (WT, *ubc4*Δ, *ubc5*Δ and *ubc4*Δ*ubc5*Δ) they were transformed with native SY1 (pYX212-SY1 plasmid). Additionally, the corresponding empty vector strains were prepared by transformation with the control plasmid (pYX212). SY1 expression was validated for these strains in a similar way as described in section 5.1.1 on page 30.

Growth analysis of synphilin-1 expressing cells in the alternative background

Cells expressing SY1 (pYX212-SY1) and the empty vector (pYX212) from the different strains were grown in selective medium and the OD_{600nm} was measured every two hours as described in section 4.10. Since, the *ubc4*Δ*ubc5*Δ did grow much slower, the growth was followed over a longer period of time. The results of the growth analysis are give in figure 5.23 on the following page.

When comparing the growth of the alternative strains (figure 5.23 on the following page) with the growth of the strains in the BY4741 background (figure 5.11 on page 45) we can see that the WT, *ubc4*Δ and *ubc5*Δ grow slower in the alternative background than in the BY4741. Moreover, when looking at the timeline in 5.23c on the following page we see the significantly diminished growth of the *ubc4*Δ*ubc5*Δ

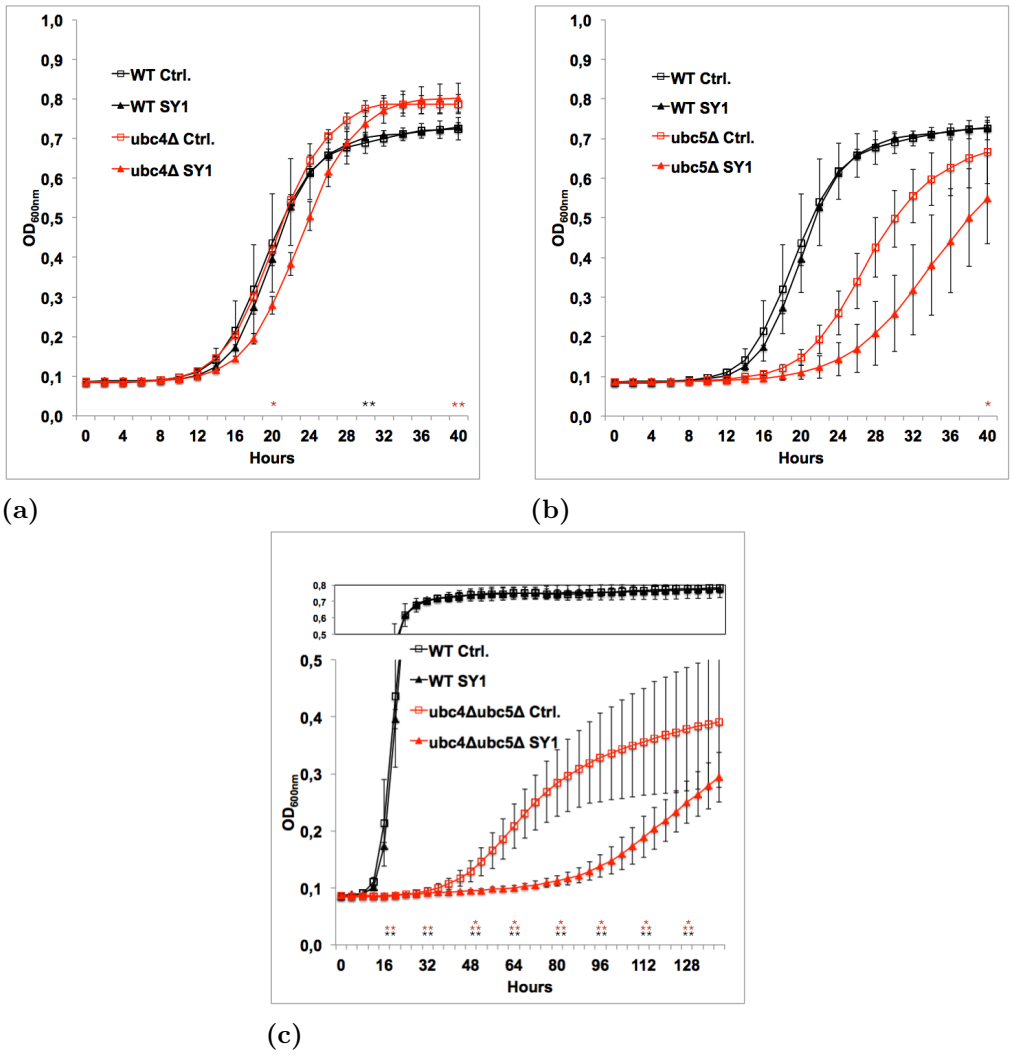

Figure 5.23: Growth analysis of the WT (MHY501) strain (black) together with respectively (a) *ubc4*Δ (MHY498), (b) *ubc5*Δ (MHY499) and (c) *ubc4*Δ*ubc5*Δ (MHY508) strains in red. For each strain the average of the SY1 expressing transformants (pYX212-SY1) and the average of the corresponding empty vector transformants (pYX212) are plotted. Except for the WT cells expressing SY1 or the empty vector (Ctrl.), at least three independent transformants were used to calculate the average. For the WT only two transformants were included in the calculation. StDevs are implemented on the curves. The asterisk symbol for significance is used as described in table A.2 on page A.11. For (a) and (b) Welch's t-tests were performed at timepoints 20, 30 and 40 hours. For (c) the t-tests were performed at timepoints 16, 32, 48, 64, 80, 96, 112, and 128 hours.

compared to the WT. In contrast with the results in the BY4741 background, the *ubc5*Δ(MHY498) seems more toxic than *ubc4*Δ in this background. Furthermore, also the toxic effect of SY1 seems more pronounced in the *ubc5*Δ (MHY499). However, when looking at the standard deviations one can understand that there was a lot of variation between the different transformants of both the empty vector and the SY1 expressing *ubc5*Δ cells. Moreover, at none of the timepoints significant differences were seen between WT and *ubc5*Δ while only the 40 hour timepoint gives a significant difference between control and SY1 expressing *ubc5*Δ cells. It should be taken into account that also in the WT and the *ubc4*Δ*ubc5*Δ a lot of variation was seen in growth of the independent transformants. The variation in growth can be due to the formation of suppressors. Possibly, these suppressors partly reduce the toxic effect. Hence, an altered growth pattern is seen which makes the results less reliable. Another downside of these alternative strains is that the cells precipitate very easily which makes it more challenging to get correct OD_{600nm} measurements. Finally, the *ubc4*Δ*ubc5*Δ grows extremely slow which makes it very difficult to perform certain experiments in a similar way as before. For example, fluorescence microscopy has to be done at a later timepoint. Furthermore, for future experiments concerning the ubiquitination level of SY1, it will be challenging to obtain a sufficient amount of cells to make the protein extraction and subsequent immunoprecipitation possible.

5.1.11 SY1 inclusion formation in the alternative strains

When investigating a certain feature, it is possible that the observed phenotype is dependent on the genetic background (Franssens et al., 2010). Therefore, it is also important to study the inclusion formation of SY1 in the alternative strains i.e. the WT (MHY501), *ubc4*Δ (MHY498), *ubc5*Δ (MHY499) and *ubc4*Δ*ubc5*Δ (MHY508) strains. In order to do this, these strains were transformed with the pYX212-dsRed-SY1 plasmid (see table 4.4 on page 21). As control, the same strains were transformed with pYX212-dsRed. After the transformation, independent transformants were grown for 48 hours and 96 hours in selective medium at 30 °C.

Based on figure 5.24b and 5.24d on the following page, we can conclude that the ratio of small and large inclusions is more or less switched compared to the BY4741 background resulting in a much higher occurrence of small aggregates in the alternative strains. Furthermore, after 48 hours of growth almost no aggregates were seen in the very slowly growing double mutant strain. Compared to the WT there is a significant increase in small aggregates in the *ubc4*Δ after 48 hours of growth. A smaller and not significant trend can be seen for the *ubc5*Δ. These trends are still present after 96 hours, however there were no more significant differences with the WT strain. Interestingly, in the *ubc4*Δ*ubc5*Δ inclusion positive cells were present after 96h of growth however only in 9% of the fluorescence positive cells. Moreover, the ratio small over large aggregates was unexpected i.e. 45% small and 55% large aggregates.

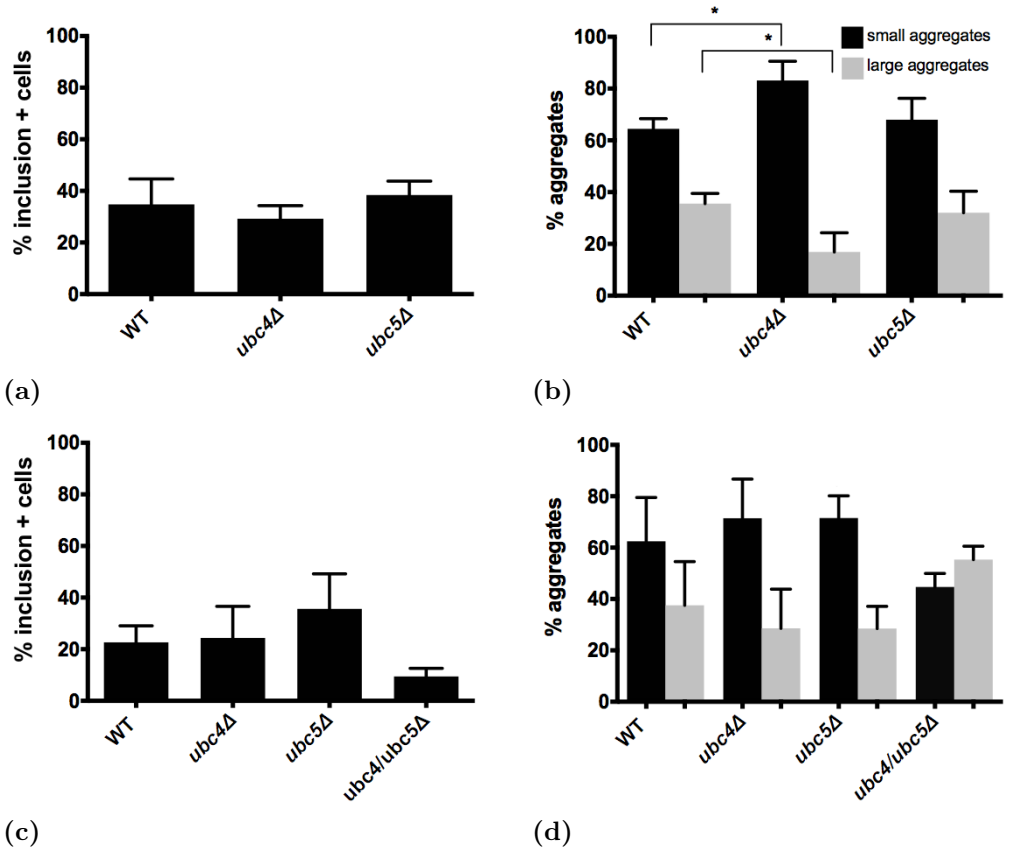

Figure 5.24: Quantification of the SY1 inclusions. (a) and (c) show the amount of SY1 inclusion positive cells in the different SY1 expressing (pYX212-dsRed-SY1 plasmid) alternative strains respectively after 48h and 96h of growth. Figure (b) and (d) show the amount of small (black bars) and large (gray bars) aggregates present in the same strains respectively at 48h and 96h. Over 200 cells from each of three independent transformants were counted per strain. The standard deviations are indicated in the graphs. An asterisk indicates a significant difference based on a Welch's t-test (α=0.05).

A trend that we see over the performed experiments is that a higher incidence of small aggregates seems to be linked to a higher cytotoxicity. Therefore, we expected to see an even higher ratio of small over big aggregates in the double mutant strain. However, this was not the case, as we can see in figure 5.24d on the previous page. Possibly, only cells that were able to form suppressors due to mutations can grow and are therefore not really showing the effect of the double mutant strain on aggregate formation. This explanation is strengthened by the fact that the amount of inclusion positive cells is very low and that this strain grows very slowly.

5.2 Humanized yeast models to study α-synuclein toxicity and inclusion formation

5.2.1 Validation of α-synuclein expression

In a similar way as we studied SY1 in yeast, we investigated the PD related protein α-syn. For this, BY4741 WT cells were transformed with native α-syn (pGGE181-α-syn) or the corresponding empty vector (pGGE181) or with fluorescently labelled α-syn (pUG23-α-syn) and the corresponding empty vector. For an overview of the plasmids see table 4.4 on page 21. After the transformations were complete, the expression of α-syn was verified. The cells were grown until mid-exponential phase after which the proteins were isolated as described in section 4.7. After performing western blot analysis (see section 4.8) on the extracts, immunodetection was done with anti-α-syn antibody. For each transformation five transformants were analyzed. The validation of the WT strain expressing native α-syn is shown in figure 5.25. The validation was also done for the BY4741 strains *ubc4*Δ, *ubc5*Δ, *ltn1*Δ and *pre9*Δ (not shown) both for native α-syn expression as for the expression of GFP-tagged α-syn.

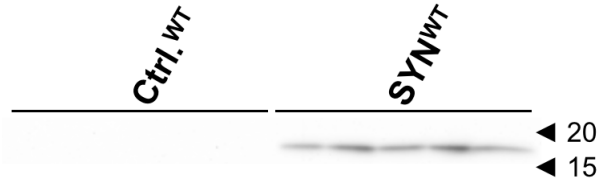

Figure 5.25: Validation of the expression of native α-syn in WT yeast strain (BY4741 type) using western blot analysis. The Ctrl.^{WT} lanes represent five transformants of WT yeast cells with the empty vector pGGE181 plasmid. The SYN^{WT} lanes represent five transformants of WT yeast cells with the pGGE181-SYN plasmid. The arrows at the right side of the figure indicate the molecular weight of the different fragments as determined by the protein ladder. Anti-α-syn was used as primary antibody. The secondary antibody was goat anti rabbit (see table 4.4 on page 22). The α-synuclein band is found at a height of 17kDa.

Yeast cells transformed with native α-syn (pGGE181-α-syn) clearly express protein at a height corresponding to the molecular weight of α-syn (see figure 5.25 on the previous page). In yeast cells transformed with the empty vector (pGGE181) no such protein band is seen.

5.2.2 The effect of α-synuclein on the growth of yeast

Previous studies already revealed that α-syn has a deleterious effect on the growth of yeast cells (Büttner et al., 2010; Outeiro & Lindquist, 2003; Zabrocki et al., 2005). In the host lab the growth of WT, *ubc4*Δ, *ubc5*Δ and *pre9*Δ transformants expressing native α-synuclein has already been studied previously (unpublished data). However, for the *ltn1*Δ strain no growth analysis was performed before and therefore the strain was included in this study. For this, transformants expressing SY1 or the empty vector (pGGE181-SYN and pGGE181) of both WT and *ltn1*Δ were grown in selective medium and every two hours the OD_{600nm} was measured. The growth curves are given in figure 5.26.

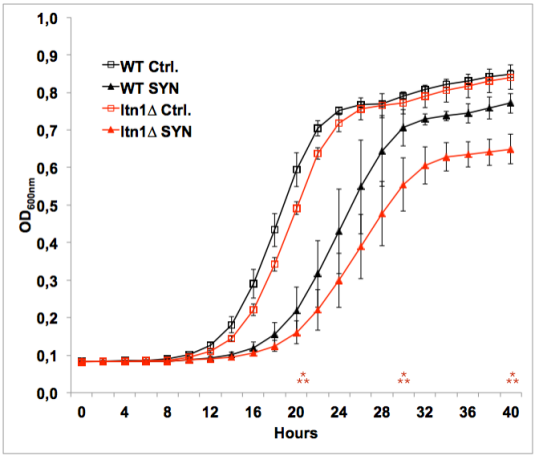

Figure 5.26: Growth analysis of the *ltn1*Δ strain (red) and the WT BY4741 strain (black). The empty vectors (pGGE181) are indicated with empty squares whereas the α-syn expressing strains (pGGE181-SYN) are indicated with closed triangles. For the WT control the average over four transformants was taken. For the α-syn expressing WT transformants the average of two transformants was used. For both types of *ltn1*Δ transformants five transformants were averaged and plotted. Standard deviations are included in the figure. Statistics were done using Prism 6. Welch's t-tests were performed at 20, 30 and 40 hours using all five independent transformants. An overview of the different asterisk types is given in table A.2 on page A.11.

As observed in figure 5.26, α-syn expression in WT yeast has a negative effect on the growth. This negative effect is not significant when performing Welch's t-tests using all five transformants of both the control and the α-synuclein expressing strain. Since the α-synuclein expressing *ltn1*Δ grows signficantly slower than the WT (pGGE-

181-SYN) we can conclude that the toxic effect of α-syn is enhanced in the *ltn1*Δ. The deleterious effect of α-syn that we see for the WT strain is in agreement with previous research performed by the host lab. Moreover, the host lab discovered similar α-syn induced growth reductions for the UPS mutants *ubc4*Δ, *ubc5*Δ and *pre9*Δ than for the WT. Therefore, the discovery of the enhanced toxic effect of α-syn in the *ltn1*Δ is interesting and should be investigated in more detail.

5.2.3 The influence of α-synuclein on the ROS level and cell necrosis

To investigate whether this growth defect caused by α-syn is correlated with an increase in cytosolic stress and cell necrosis, as already suggested by previous research, we performed DHE and PI stainings (see method section 4.13) (Swinnen et al., 2011). During a first experiment, cells transformed with native α-syn (pGGE181-SYN) and the corresponding control transformants (pGGE181) were grown in selective medium and after 36 hours the DHE and PI levels were measured. We saw that the control cells had a higher amount of PI and DHE positive cells than the α-syn expressing ones (not shown). A possible explanation for this could be that the cells lost α-syn toxicity overtime and therefore that the toxicity had to be studied at an earlier timepoint.

Therefore, cells transformed with native α-syn (pGGE181-SYN) and the corresponding control transformants (pGGE181) were grown in selective medium. In addition, we also transformed the WT with alternative plasmids i.e. the pYX212T-SYN and its corresponding control (pYX212T) to see if the toxic effect of α-syn was more stable in these transformants. After 12, 36 and 60 hours, DHE an PI stainings were performed using fractions of the cultures in order to follow the ROS level overtime. The results of the DHE and PI staining are given in figure 5.27 on the next page

In this figure we can see that the % DHE and PI positive cells is lower for the empty vectors (pGGE181 and pYX212T) than for the α-syn expressing cells (pGGE181-SYN and pYX212T-SYN) at the first two timepoints. This means that indeed α-syn expression results in a more toxic phenotype. Furthermore, at the 60h timepoint the % DHE and PI positive cells is higher in the empty vector (pGGE181) than in the α-syn expressing transformants (pGGE181-SYN). This is not the case for the plasmid with the pYX212T backbone. Therefore, we can conclude that in cells transformed with the pGGE181-SYN plasmid, α-syn toxicity is less stable. Possibly, suppressors can be formed more easily when these plasmids are used. Therefore, we recommend using the pYX212T-SYN plasmid for future research concerning α-syn toxicity.

At the start of the incubation of the FACS cultures, a small amount was used to perform growth analysis as a parallel experiment. Every two hours the OD_{600nm} was measured and the resulting data was plotted in figure 5.28 on page 66.

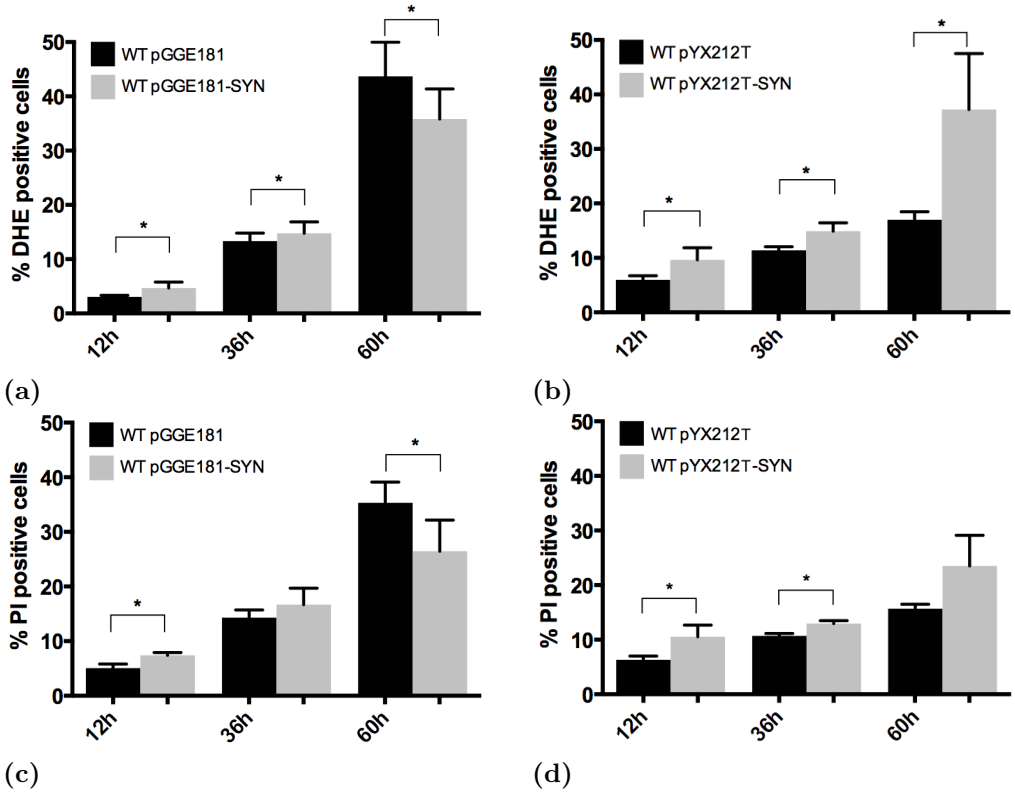

Figure 5.27: The effect of α-syn expression on DHE and PI levels. The results of the DHE staining (a, b) and PI staining (b, d) at the timepoints 12, 36 and 60 hours. In (a) and (c) the WT transformants expressing native α-syn (pGGE181-SYN) and the corresponding control (pGGE181) were used. In (b) and (d) the transformants with the plasmids pYX212T-SYN for native α-syn expression and pYX212T as control were used. At all timepoints, for both DHE and PI measurements, the values of atleast three independent transformants were averaged. Standard deviations are implemented on the boxes. Welch's t-tests were performed at all three timepoints to see if the difference in PI/DHE positive cells was significant between the control and the α-syn expressing transformants. An asterisk is indicative for a significant difference (α=0.05).

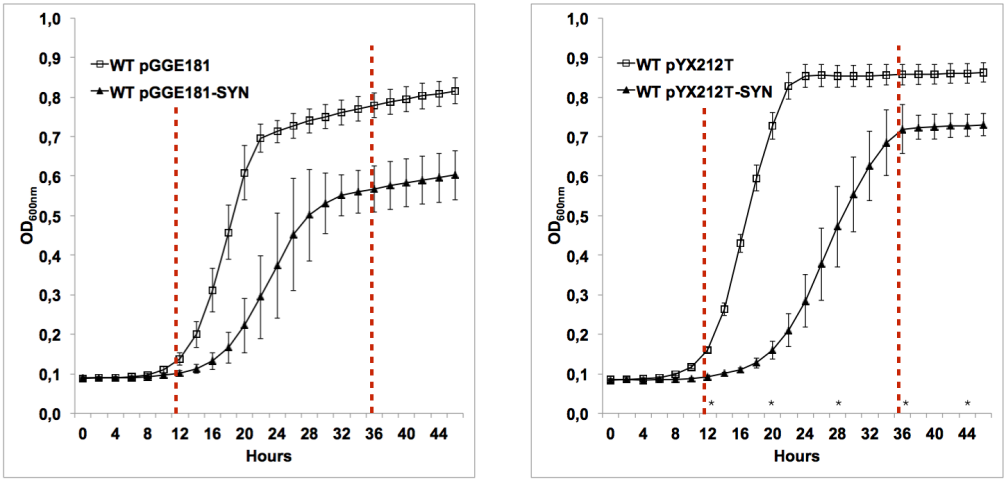

(a) **(b)**

Figure 5.28: Growth analysis of α-syn expressing yeast cells. (a) growth of the native α-synuclein (pGGE181-α-syn) expressing transformants (closed triangle) and the corresponding controls (pGGE181) (open squares). (b) growth of the transformants expressing native α-synuclein (pYX121T-α-syn) (closed triangle) and the corresponding control (pYX212T) (open squares). The points at which DHE and PI stainings were performed are indicated with red broken lines. For WT pGGE181 and pGGE181-SYN respectively five and three independent transformants were averaged and plotted. For the WT pYX212T and pYX121T-SYN respectively five and three independent transformants were used. Standard deviations are implemented in the graphs. Welch's t-tests were performed at timepoints 12, 20, 28, 36 and 44 hours and indicate (using asterisks) at which timepoint the five control and five α-syn expressing transformants differ significantly.

By looking at figure 5.28, we again see that α-syn expression causes a reduction in growth. Using the information of figure 5.27 on the preceding page we can say that this reduction in growth upon α-syn expression is linked to higher amounts of ROS and cell death. Consistent with the finding that the toxic effect of α-syn is more stable in cells transformed with pYX121T-SYN, we see in figure 5.28 that the reduction in growth upon α-syn expression is more pronounced when cells are transformed with the pYX121T-SYN plasmid.

The results are in agreement with previous research and therefore we know this working model is a good starting point for future research concerning α-syn toxicity (Swinnen et al., 2011).

5.2.4 Inclusion localization of α-synuclein inclusions

To investigate α-syn inclusion localization in WT and *ltn1*Δ strains, cells of both strains were transformed with the pUG23-SYN plasmid. As a control, cells were

transformed with the corresponding empty vector pUG23. The expression of EGFP-tagged α-synuclein was verified as described in section 5.2.1. Next, three independent transformants of each strain were grown for 48h in selective medium containing one fifth of the normal amount of methionine. Methionine shortage causes derepression of the MET25 promotor thereby stimulating EGFP-tagged α-synuclein expression. After 48h of growth DAPI and CMAC stainings were performed as described in method sections 4.11.1 and 4.11.2.

When looking at figure 5.29 on the following page, we see that α-syn inclusions can be found both close to the nucleus and vacuole. This finding suggest that α-syn is directed both to JUNQ and IPOD like compartments. In the WT often one big aggregate is located close to the periphery sometimes in concert with additional small aggregates. This is the same for *ltn1*Δ. However, a small increase in small aggregates was seen for the *ltn1*Δ. Proper cell counting should be performed on the images in order to get more exact results but the available data is not sufficient to do this. Also here it is important that the experiments are repeated using markers that co-localize with the compartments. This will allow us to identify the compartments more clearly.

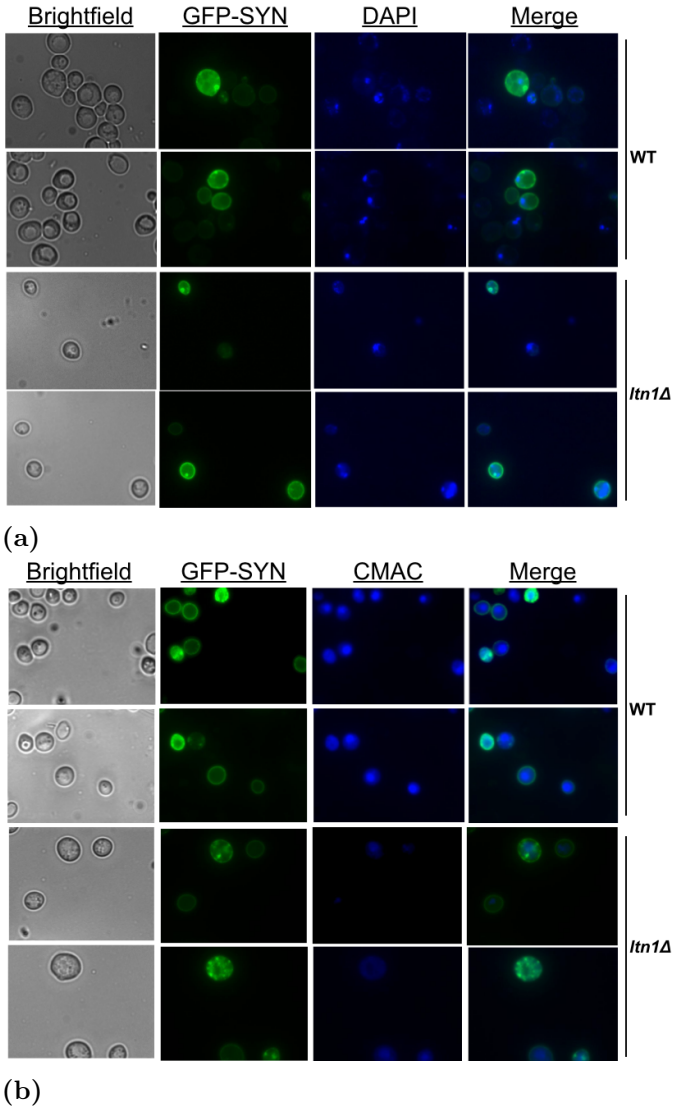

Figure 5.29: Fluorescence microscopy images after 48 hours of growth of WT and *ltn1*Δ yeast cells transformed with the pUG23-SYN plasmid (see table 4.4 on page 21). Fluorescent images of EGFP-tagged α-syn are shown in column two. In column three nuclear stainings (a) and vacuolar stainings (b) are shown. The last image of each row is an overlay of both fluorescent channels and shows the α-syn localization relative to the nucleus (a) or vacuole (b).

6. Discussion

Due to its high impact on the aging western population and its increasing prevalence, PD has been subjected to many studies. The neurodegenerative disorder is characterized by progressive loss of dopaminergic neurons in the substantia nigra and by intracellular protein deposits (Lewy bodies) in which α-syn and SY1 can be found. Despite, numerous studies, the underlying mechanisms concerning inclusion formation of these proteins and the formation of these Lewy bodies are still poorly understood. Hence, whether the inclusions are cytoprotective or cytotoxic is still controversal. A decade ago humanized yeast models were established for α-syn research (Outeiro & Lindquist, 2003; Zabrocki et al., 2005). More recently, also a model was developed expressing SY1 (Büttner et al., 2010). These models have proven to be valuable tools for PD research since they are able to recapitulate important disease-related features such as inclusion formation of α-syn and SY1. In this study we further explore the inclusion formation and localization of α-syn and SY1 while also investigating their cytotoxicity and ubiquitination, the latter possibly being important for LB formation.

In a first step of our study we transformed WT BY4741 cells and the UPS mutants *ltn1*Δ, *pre9*Δ, *ubc4*Δ and *ubc5*Δ with a plasmid that allows SY1 expression. When performing growth analysis on the WT transformants we witnessed a minor but signficant decrease in growth upon SY1 expression. This is in agreement with previous research (Büttner et al., 2010). When looking at the different UPS mutants we saw that the growth of the *pre9*Δ and *ubc4*Δ strain were reduced compared to the WT. This was not the case for *ubc5*Δ and *ltn1*Δ. This indicates that in general *pre9*Δ and *ubc4*Δ are more toxic. Possibly, a less efficient UPS in the *pre9*Δ and *ubc4*Δ is causative for more stress and therefore results in a diminished growth. Upon expression of SY1 we saw that *ubc5*Δ and *ltn1*Δ showed a similar growth reduction as when SY1 was expressed in the WT, whereas the toxic effect of SY1 was enhanced in the *pre9*Δ and *ubc4*Δ. Therefore, we conlude that SY1 is more toxic in the *pre9*Δ and *ubc4*Δ. Ubc4p and Uc5p are two similar E2 ubiquitin conjugating enzymes that interact with the proteasome more strongly under stress conditions to clear the cytoplasm from misfolded and excess proteins (Tongaonkar et al., 2000). Possibly, the Ubc4p-proteasome interaction is more efficiently induced as stress response upon SY1 expression than the Ubc5p-proteasome interaction, explaining the increased toxicity in the *ubc4*Δ strain. Interestingly, it has also been described that under stress conditions the deletion of *PRE9*, encoding the α3 subunit from the 20S core of the proteasome can be replaced by the α4 subunit, resulting in a more active proteasome (Kusmierczyk et al., 2008). However, if this is the case for SY1 expressing cells and how this could result in a reduction in the growth of the cells is still unknown and should be investigated in more detail. A possibility is that

the growth reduction is caused by energy loss as a result of the more active proteasome.

In line with previous research, we observed that initially small cytoplasmic SY1 foci transform into one or two big aggregates, often localized at opposite poles when entering stationary phase (Büttner et al., 2010). It is unclear whether these inclusions are cytoprotective or cytotoxic. However, based on their nuclear localization, it has been suggested that these inclusions resemble aggresomes (Swinnen et al., 2011). These aggresomes have shown to be cytoprotective because they store proteins which in turn facilitates their removal by autophagy (Zaarur et al., 2008). We saw that in the WT about 50 % of the SY1 expressing cells had inclusions, which is higher than the 33% reported earlier (Büttner et al., 2010). This difference can be due to the fact that different transformants were used and to the subjective nature of determining the ratios. Moreover, for *pre9*Δ about 43% inclusion positive cells were counted. However the decrease was not significantly different from the WT, it could be explained by the fact that this mutation possibly results in a more active proteasome and therefore a lower amount of aggregates is present in the cell. Our findings are in conflict with earlier research in the host lab for which a small increase in inclusions was reported for all UPS mutants (*pre9*Δ, *ubc4*Δ and *ubc5*Δ). In addition to these UPS mutants , we also included the *ltn1*Δ strain in our study. Quantification of the inclusion positive cells in this strain showed a significant increase in the cells with inclusions (72%) compared to the WT. This can be explained by the idea that this mutant has an impaired UPS and therefore less SY1 is degraded resulting in more aggregates. The ratios of small versus large aggregates in our study was 20% - 80% for the WT. However, in the *pre9*Δ a small elevation in small aggregates was present (up to 26%), this was not a significant change, which is in agreement with previous research in the host lab. Also for the *ltn1*Δ the ratio did not change compared to the WT. In addition, the inclusion localization was studied for WT and *ltn1*Δ, and we observed that SY1 inclusions are often localized near the nucleus and the vacuole. This suggest that both IPOD and JUNQ like compartments are present. When two aggregates were present often one of them was localized at the nucleus, which is a possible indication that this is a JUNQ like compartment. Double stainings or stainings with compartment characteristic markers such as Atg8 and Sec63, have to be performed in the future to provide extra proof when identifying certain compartments.

In a following experiment the effect of the deubiquitinating enzyme inhibitor (PR-619) was checked on the growth of the UPS mutants. As observed in the growth analysis without inhibitor, we again witnessed that mainly in *pre9*Δ and *ubc4*Δ strains SY1 expression is toxic. The SY1 toxicity was slightly enhanced in the presence of the inhibitor for all strains except for *ubc5*Δ. When the proteasome inhibitor MG-132 was added to the medium a general reduced growth was seen for all strains. This effect was significant for all strains expect for the *ltn1*Δ. SY1 expression again had a significant toxic effect on the growth of *ubc4*Δ. However, no additional effect of the inhibitor was observed. Interestingly, the toxic effect of SY1, observed previously in the absence of the inhibitor, was no longer present in the *pre9*Δ when the inhibitor was added. It must be said that in this experiment the difference between the control

and SY1 expressing *pre9*Δ cells without inhibitor was also less pronounced. Moreover, the effect of the deubiquitinating enzyme inhibitor on SY1 inclusion formation was investigated using the fluorescence microscope. Upon addition of the inhibitor, a non-significant increase in the ratio of small to large inclusions was seen for all UPS mutants. Since previous research suggests that PR-619 induces a stress response, increases the amount of ubiquitinated cytoplasmatic proteins and deleterious inclusions, the small aggregates are possibly ubiquitinated toxic inclusions (Seiberlich et al., 2012). This is in agreement with the enhanced SY1 toxicity that was discovered for all strains upon addition of PR-619. In the future it would be interesting to also perform similar experiments with the proteasome inhibitor, MG-132.

Since previous research has shown that SY1 is ubiquitinated in Lewy bodies, and can induce Lewy body formation, it is interesting to study the ubiquitination of SY1 in the different UPS mutant strains (Engelender et al., 1999; Lim et al., 2005). Therefore, first SY1 was precipitated from protein extracts of the different mutant strains after which the presence of ubiquitin was checked with immunodetection. We repeatedly performed this type of immunoprecipitation in order to optimize the procedure and the lysis buffer until finally the protocol was sufficient to quantify ubiquitination of SY1 for the different strains. As described during the optimalization, even though an alternative ubiquitin antibody improved the detection, this was still not sufficient. Moreover, deubiquinating enzyme inhibitor (PR-619) was added to the lysis buffer in order to avoid ubiquitin release from SY1 during the immunoprecipation. Also N-ethylmaleimide was added to the buffer to preserve ubiquitin conjugation. These additives increased the quality of the blots while also the signal around full length SY1 started to appear as a separate band when the blots were detected with anti-ubiquitin. Since the ubiquitin antibody binds only weakly to ubiquitin, obtaining the desired blot quality for quantification was impossible using this approach. Therefore, a new strategy was followed. For this, myc-tagged ubiquitin was expressed in the different strains. Since this allowed us to detect ubiquitin indirectly using a myc antibody, we could work independent of the weak binding ubiquitin antibodies. Two immunoprecipitation were performed in parallel, one time SY1 was precipitated and in the other immunoprecipitation all myc tagged proteins were precipitated. With this new strategy, the resulting blots could be used for quantification. First of all, these blots show that SY1 is indeed ubiquitinated when expressed in the different UPS mutants, which is in line with previous research (Li & Guo, 2009) . Moreover, this suggests that the UPS is important for SY1 processing, as was suggested before (Lee et al., 2002). This is in agreement with previous studies that suggested that the dysfunction of the proteasome is associated with the onset and development of neurodegenerative diseases (McNaught & Jenner, 2001). We further discovered that almost 3x more SY1 is ubiquitinated in *ubc4*Δ than in the WT strain. The aforementioned hypothesis concerning the increased SY1 toxicity of in *ubc4*Δ (Ubc4p being more effective in interacting with the proteasome and inducing a stress response) is in conflict with the observed increase in SY1 ubiquitination when *UBC4* is absent. Instead, this result suggests that the Ubc5p is more efficient in inducing a stress response. Perhaps, it is the accumulation of

ubiquitinated proteins that has a toxic effect because the UPS cannot cope with the burden of an excess of ubiquitinated proteins. Perhaps a too efficient stress response is self-destructive when SY1 is overexpressed. Taken together, these results suggest that more SY1 ubiquitination is linked with an increase in small deleterious inclusions and a growth reduction. The fact that the WT and *ltn1*Δ do not show this hypothetic toxic stress response, is somewhat contradictory. However, it is possible that when both *UBC4* and *UBC5* are present only Ubc4p is activated. At the moment no clear conclusions can be drawn from the results and therefore the experiments should be repeated in order to get more reliable and hopefully unambiguous results. None of the other strains showed a significant difference in SY1 ubiquitination compared to the WT. Therefore, the growth reduction in *pre9*Δ upon SY1 expression is probably not due to exceptional SY1 ubiquitination but rather due to the activity of the proteasome. Moreover, previous research states that both MG-132 and PR-619 cause an increase in the abundance of ubiquitinated proteins within 24h (Seiberlich et al., 2012). In contrast with these findings, even though using similar concentrations of inhibitors, we saw no significant difference in ubiquitination of SY1 when the inhibitors were present. Therefore, also these experiments should be repeated with more transformants to be able to draw more reliable conclusions.

To study the ubiquitination of SY1 in more detail in the future it would be interesting to overexpress Parkin, one of the E3 ubiquitin ligases of SY1, and to see what the effect of its overexpression is on the amount of ubiquitinated SY1 in the different strains. Research has shown that this ubiquitination process is impaired in the familial PD forms. Moreover, it has been suggested that Parkin is required for the formation of Lewy bodies (Chung et al., 2001). Additionally, it has been shown that Parkin does not ubiquitinate α-syn. Therefore, it would be interesting to investigate the effect of Parkin overexpression on the amount of ubiquitinated α-syn as well. Furthermore, it would be interesting to overexpress SIAH since this ubiquitin ligase ubiquitinates both SY1 and α-syn (Nagano et al., 2003). Moreover, it was shown in previous research that SY1 phosphorylation by glycogen kinase 3β decreases the amount of ubiquitinated SY1 in HEK cells (Avraham et al., 2005). Therefore, it would be interesting to investigate the amount of ubiquitinated SY1 in the *mds1*Δ strain, in which the yeast orthologue of glycogen kinase 3β has been deleted.

Since we expect that Ubc5p takes over the function of Ubc4p upon *UBC4* deletion we wanted to create a double mutant strain, lacking both *UBC4* and *UBC5*, and investigate its effect on SY1 toxicity and ubiquitination. However, we failed to create this double deletion strain in the commonly used BY4741 background because the double mutant is not viable in this background. Fortunately, we received this double deletion and the according WT, *ubc4*Δ and *ubc5*Δ from Mark Hochstrassers's group. In this background the mutant was viable, however the strain suffered from a serious growth impairment. The growth defect is probably due to the fact that the double mutant is expected to have serious defects in the ubiquitination machinery and protein degradation as was indicated by previous research (Tongaonkar et al., 2000). Since working in a different background can also change the phenotype of

our SY1 model, the newly transformed strains were first used for growth analysis and analysis of inclusion formation (Franssens et al., 2010). In general these strains grew slower than the strains from the BY4741 background. As expected, the growth of the double mutant strain *ubc4*Δ*ubc5*Δ was drastically diminished compared to the other strains, highlighting the importance of a good working ubiquitin machinery. Moreover, SY1 expression caused an additional and significant growth reduction in all strains except for the WT. Interestingly, in this case the *UBC5* deletion seems to be more toxic than the *UBC4* deletion. In this way, the growth reduction upon SY1 expression was more pronounced in the *ubc5*Δ strain than in the *ubc4*Δ. This is in contrast with our previously performed experiments in the BY4741 background for which we discovered that *ubc4*Δ is more toxic. Possibly, this difference is due to the different background. We should keep in mind that there was a lot of variation between the different transformants of the *ubc5*Δ strain and therefore this might not give a good representation of the real situation. Also in the WT and the double mutant a lot of variation was found between the different transformants, hence complicating the analysis. We repeated this experiment to get more consistent results but again we witnessed a lot of variation in the growth of the different transformants of each strain. Since the cells of the MHY-series precipitated very quickly, it is possible that we did not start from the same OD_{600nm} in the different transformants and that this is the reason for the observed variation.

In addition to the growth analysis, the MHY series were also subject to a study concerning inclusion formation. Therefore the strains were transformed with fluorescently labeled SY1 and the according empty vector. Compared to the BY4741 background the ratio small over large aggregates was more or less switched in the WT, *ubc4*Δ and *ubc5*Δ. Furthermore, the % inclusion positive cells was lower than in the BY4741 background (about 35% in the WT of the MHY background compared to 50% in the BY4741 background). In this genetic background the WT had about 60% small and 40% large aggregates (80% large and 20% small in the BY4741 background) after 48h of growth. A significant increase in % small aggregates was discovered for *ubc4*Δ whereas a not significant and smaller increase was discovered for *ubc5*Δ. No inclusion positive cells were seen in the double mutant at 48h of growth. Therefore, the cultures were grown further and after 96h of growth the cells were counted again. The same trends were seen at 96 of growth, however there were no more significant differences compared to the WT. Interestingly, in the *ubc4*Δ*ubc5*Δ strain, inclusions were present after 96h of growth however only in 9% of the cells. Moreover, the percentages of small and large aggregates were respectively 45% and 55%. These findings are unexpected since we hypothesise that a higher incidence of small aggregates is linked to a higher cytotoxicity. Hence, even more small foci were expected in the double mutant than in the single E2 conjugating enzyme deletions. Since we observed that this double mutant, especially when SY1 is expressed, is almost not viable, it is possible that only cells that formed suppressors were able to grow. If this is the case, this will give us a completely wrong view concerning aggregate formation in the double mutant. Therefore, a good future experiment would entail inserting a plasmid in the double deletion strain that expresses the Ubc4p from

a repressible promotor. In this way, the strain can survive just as a *ubc5*Δ strain until we repress the promotor at a certain point during growth. This will result in downregulation of Ubc4p expression resulting in the actual double mutant phenotype. In this way, we can also see if SY1 expression indeed results in a more toxic phenotype.

In the second part of our study we wanted to investigate the influence of protein degradation components on α-syn biology in yeast. Therefore, WT yeast cells were transformed with native α-syn and the corresponding empty vector. After verifying the α-syn expression, cells were subjected to growth analysis. As observed in our study and previously reported by other groups (Outeiro & Lindquist, 2003; Zabrocki et al., 2005), α-syn has a negative effect on the growth of yeast. In addition, the host lab already investigated the effect of α-syn expression in UPS mutants including *ubc4*Δ, *ubc5*Δ and *pre9*Δ. In all these strains a similar growth reduction upon α-syn expression was seen as for the WT strain, which suggests that these genes have no influence on the α-syn toxicity. In this study we also investigated α-syn toxicity in the *ltn1*Δ strain. We discovered that the toxic effect of α-syn on the growth is aggravated in *ltn1*Δ compared to the WT. This interesting finding suggests that Ltn1p, a RING domain ubiquitin ligase, is important in α-syn toxicity. Interestingly, this protein was also important in the toxicity of Htt103Q (unpublished data). The experiment should be repeated with more transformants to be sure the results are reliable. Moreover, it would be interesting to investigate the ubiquitination level of α-syn in the different strains in a similar way as was done for SY1.

It was previously described that α-syn expression increases the amount of cytosolic stress and necroptosis (Franssens et al., 2013; Swinnen et al., 2011). Since previous work in the host lab experienced problems to detect this increase in ROS upon α-syn expression this was also a point of focus for us. Therefore, the amount of PI and DHE positive cells were measured in WT cells expressing α-syn after 36 hours of growth. At first, we faced similar problems i.e. the empty vector cells experienced as much or even more cytosolic stress as the cells expressing α-syn. However, when we performed this experiment at an earlier timepoint (12h) we measured more DHE and PI positive cells when α-syn was expressed than for the corresponding empty vector, which is in line with both our expectations and published work. The results after 36 and 60 hours of growth can be explained by the possibility that the toxic effect is mainly present during exponential growth or by the fact that α-syn expressing cells grow much slower. As a result of the slower growth, it is possible that α-syn expressing cells are still growing exponentially when the empty vectors are already in the more stressful stationary phase and therefore can exceed the ROS levels of the α-syn expressing cells. We performed this experiment using two different types of α-syn expressing plasmids and discovered that when pYX212T-SYN is transformed into yeast cells instead of pGGE181-SYN that the toxic effect of α-syn is more stable. Also cells transformed with pYX212T-SYN resulted in a more pronounced growth reduction than cells transformed with pGGE181-SYN when both were compared to their corresponding empty vectors. Therefore, in future experiments we recommend using the pYX212T-SYN plasmid and corresponding empty vector for research con-

cerning α-syn.

We also studied α-syn inclusion localization for the WT and the *ltn1*Δ strain by expressing fluorescently labeled α-syn in the strains. The results indicate that for both strains α-syn inclusions are found close to the nucleus and to the vacuole. This could mean that both IPOD and JUNQ like inclusions are formed. However, before drawing conclusions this should be evidenced further using the aformentioned Atg8 and Sec63 proteins, markers for respectively IPOD and JUNQ. When only one large inclusion was present it was often located close to the periphery and nucleus, suggesting that in this case only the JUNQ-like compartment was present. Possibly, only when the cell cannot cope with the burden of misfolded ubiquitinated proteins, they are directed to IPOD. In the future it is important to investigate the ubiquitination of α-syn in a similar way as was done for SY1 in order to strengthen the hypothesis of α-syn being initially directed to JUNQ.

7. Conclusion

In this study we were able to show that SY1 is ubiquitinated which might indicate that its processing is dependent on the UPS machinery. This is encouraged by the fact that some of the UPS mutant strains (*ubc4*Δ and *pre9*Δ) showed an enhanced growth reduction upon SY1 expression compared to the WT. The toxic effect of SY1 in the different strains was more pronounced when a deubiquitination enzyme inhibitor was added to the growth medium. Moreover, the addition of the inhibitor increased the ratio of small to large inclusions in all studied strains. Interestingly, the most small aggregates were found in the *ubc4*Δ and *pre9*Δ strain. Therefore, we suggest that an increase in small inclusions results in a more toxic phenotype. Another finding that supports the idea of the UPS being linked to SY1 toxicity, is that SY1 ubiquitination was enhanced in yeast lacking *UBC4* compared to the WT strain. Possibly, the UPS cannot cope with the burden of an overload of ubiquitinated SY1 resulting in the observed toxicity. Furthermore, the fact that both α-syn and SY1 were found in close proximity to the nucleus and the vacuole suggests that both proteins can be found in JUNQ as well as IPOD inclusions. Even though we know that α-syn has a toxic effect on yeast cells, an enhanced α-syn toxicity was discovered in the *ltn1*Δ strain compared to the WT, suggesting a role for the RING domain ubiquitin ligase in the regulation of the α-syn toxicity. No such increase in α-syn toxicity was reported for the other UPS mutant strains (*ubc4*Δ, *ubc5*Δ, and *pre9*Δ).

In conclusion, these results provide a strong indication that protein degradation components and especially ubiquitination might play a role in the aggregation management of SY1 and α-syn. Moreover, using the optimized ubiquitin detection approach, we will be able to get a better insight in the mechanisms underlying the aggregation management of the PD associated proteins SY1 and α-syn and further clarify the link with the UPS.

Bibliography

Aguilaniu, H., Gustafsson, L., Rigoulet, M., & Nyström, T. (2003, March). Asymmetric inheritance of oxidatively damaged proteins during cytokinesis. *Science (New York, N.Y.)*, *299*(5613), 1751–1753.

Ahn, M., Kim, S., Kang, M., Ryu, Y., & Doohun Kim, T. (2006, August). Chaperone-like activities of α-synuclein: α-Synuclein assists enzyme activities of esterases. *Biochemical and Biophysical Research Communications*, *346*(4), 1142–1149.

Avraham, E., Szargel, R., Eyal, A., Rott, R., & Engelender, S. (2005, December). Glycogen synthase kinase 3β modulates synphilin-1 ubiquitylation and cellular inclusion formation by SIAH: implications for proteasomal function and Lewy body formation. *Journal of Biological Chemistry*, *280*(52), 42877–42886.

Bagola, K., & Sommer, T. (2008, November). Protein Quality Control: On IPODs and Other JUNQ. *Current Biology*, *18*(21), 1019–1021.

Balch, W. E., Morimoto, R. I., Dillin, A., & Kelly, J. W. (2008, February). Adapting Proteostasis for Disease Intervention. *Science (New York, N.Y.)*, *319*(5865), 916–919.

Barbeau, A. (1969). L-Dopa therapy in Parkinsons Disease - a critical review of 9 years experience. *Canadian Medical Association Journal*, *101*(13), 791–800.

Bassett, D. E., Boguski, M. S., & Hieter, P. (1996, February). Yeast genes and human disease. *Nature*, *379*(6566), 589–590.

Bennett, M. C., Bishop, J. F., Leng, Y., Chock, P. B., Chase, T. N., & Mouradian, M. M. (1999, November). Degradation of α-synuclein by proteasome. *Journal of Biological Chemistry*, *274*(48), 33855–33858.

Benov, L., Sztejnberg, L., & Fridovich, I. (1998, November). Critical evaluation of the use of hydroethidine as a measure of superoxide anion radical. *Free radical biology & medicine*, *25*(7), 826–831.

Bonifácio, M. J., Palma, P. N., Almeida, L., & Soares-da Silva, P. (2006, December). Catechol-O-methyltransferase and its inhibitors in Parkinson's disease. *CNS Drug Reviews*, *13*(3), 352–379.

Botstein, D., Chervitz, S. A., & Cherry, J. M. (1997, August). Yeast as a model organism. *Science (New York, N.Y.)*, *277*(5330), 1259–1260.

Büttner, S., Delay, C., Franssens, V., Bammens, T., Ruli, D., Zaunschirm, S., ... Winderickx, J. (2010, October). Synphilin-1 enhances α-synuclein aggregation in yeast and contributes to cellular stress and cell death in a Sir2-dependent manner. *PloS one*, *5*(10), 13700–13700.

Chandra, S., Gallardo, G., Fernández-Chacón, R., & Schlüter, O. M. (2005). α-Synuclein cooperates with CSPα in preventing neurodegeneration. *Cell*, *123*(3), 383–396.

Chen, P., Johnson, P., Sommer, T., Jentsch, S., & Hochstrasser, M. (1993). Multiple ubiquitin-conjugating enzymes participate in the *in vivo* degradation of the yeast MATα2 repressor. *Cell*, *74*(2), 357–369.

Choi, P., Ostrerova-Golts, N., Sparkman, D., Cochran, E., Lee, J. M., & Wolozin, B. (2000, August). Parkin is metabolized by the ubiquitin/proteosome system. *Neuroreport*, *11*(12), 2635–2638.

Chung, K. K., Zhang, Y., Lim, K. L., Tanaka, Y., Huang, H., Gao, J., ... Dawson, T. M. (2001, October). Parkin ubiquitinates the α-synuclein-interacting protein, synphilin-1: implications for Lewy-body formation in Parkinson disease. *Nature medicine*, *7*(10), 1144–1150.

Eldridge, A. G., & Brien, T. O. a. (2009, June). Therapeutic strategies within the ubiquitin proteasome system. *Cell Death & Differentiation*, *17*(1), 4–13.

Engelender, S., Kaminsky, Z., Guo, X., Sharp, A. H., Amaravi, R. K., Kleiderlein, J. J., ... Ross, C. A. (1999, May). Synphilin-1 associates with α-synuclein and promotes the formation of cytosolic inclusions. *Nature Genetics*, *22*(1), 110–114.

Eyal, A., & Engelender, S. (2006, September). Synphilin isoforms and the search for a cellular model of lewy body formation in Parkinson's disease. *Cell cycle (Georgetown, Tex.)*, *5*(18), 2082–2086.

Foury, F. (1997, August). Human genetic diseases: a cross-talk between man and yeast. *Gene*, *195*(1), 1–10.

Franssens, V., Boelen, E., Anandhakumar, J., Vanhelmont, T., Büttner, S., & Winderickx, J. (2010, May). Yeast unfolds the road map toward α-synuclein-induced cell death. *Cell Death & Differentiation*, *17*(5), 746–753.

Franssens, V., Bynens, T., Van den Brande, J., Vandermeeren, K., Verduyckt, M., & Winderickx, J. (2013). The benefits of humanized yeast models to study Parkinson's disease. *Oxidative medicine and cellular longevity*, *2013*(2), 9–9.

Gallagher, P. S., Oeser, M. L., Abraham, A.-c., Kaganovich, D., & Gardner, R. G. (2013, December). Cellular maintenance of nuclear protein homeostasis. *Cellular and Molecular Life Sciences*, *71*(10), 1865–1879.

Garrett, R. H., & Grisham, C. M. (2010). *Biochemistry* (4th ed.). University of Virginia: Mary Finch.

Gietz, R. D., Schiestl, R. H., Willems, A. R., & Woods, R. A. (1995, April). Studies on the transformation of intact yeast cells by the LiAc/SS-DNA/PEG procedure. *Yeast*, *11*(4), 355–360.

Greggio, E., Bisaglia, M., Civiero, L., & Bubacco, L. (2011). Leucine-rich repeat kinase 2 and α-synuclein: intersecting pathways in the pathogenesis of Parkinson's disease? *Molecular Neurodegeneration*, *6*(1).

Ii, K., Ito, H., Tanaka, K., & Hirano, A. (1997, January). Immunocytochemical co-localization of the proteasome in ubiquitinated structures in neurodegenerative diseases and the elderly. *Journal of Neuropathology & Experimental Neurology*, *56*(2), 125–131.

Imai, Y., Soda, M., & Takahashi, R. (2000, November). Parkin suppresses unfolded protein stress-induced cell death through its E3 ubiquitin-protein ligase activity. *Journal of Biological Chemistry*, *275*(46), 35661–35664.

Ito, T., Niwa, J.-I., Hishikawa, N., Ishigaki, S., Doyu, M., & Sobue, G. (2003, August). Dorfin localizes to Lewy bodies and ubiquitylates synphilin-1. *Journal of Biological Chemistry*, *278*(31), 29106–29114.

Kaeberlein, M., McVey, M., & Guarente, L. (1999, October). The SIR2/3/4 complex and SIR2 alone promote longevity in *Saccharomyces cerevisiae* by two different mechanisms. *Genes & Development*, *13*(19), 1–11.

Kaganovich, D., Kopito, R., & Frydman, J. (2008, August). Misfolded proteins partition between two distinct quality control compartments. *Nature*, *454*(7208), 1088–1095.

Kopito, R. R. (2000, December). Aggresomes, inclusion bodies and protein aggregation. *Trends in cell biology*, *10*(12), 524–530.

Krüger, R. (2004, September). The role of synphilin-1 in synaptic function and protein degradation. *Cell and Tissue Research*, *318*(1), 195–199.

Kusmierczyk, A. R., Kunjappu, M. J., Funakoshi, M., & Hochstrasser, M. (2008, March). A multimeric assembly factor controls the formation of alternative 20S proteasomes. *Nature Structural & Molecular Biology*, *15*(3), 237–244.

Lee, G., Junn, E., Tanaka, M., Kim, Y. M., & Mouradian, M. M. (2002, September). Synphilin-1 degradation by the ubiquitin-proteasome pathway and effects on cell survival. *Journal of neurochemistry*, *83*(2), 346–352.

Leroy, E., Boyer, R., Auburger, G., Leube, B., Ulm, G., & Mezey, E. (1998). The ubiquitin pathway in Parkinson's disease. *Nature*, *395*(6701), 451–452.

Li, H., & Guo, M. (2009, March). Protein degradation in Parkinson disease revisited: it's complex. *The Journal of clinical investigation*, *119*(3), 442–445.

Lim, K. L., Chew, K. C. M., Tan, J. M. M., Wang, C., Chung, K. K. K., Zhang, Y., ... Dawson, T. M. (2005, February). Parkin mediates nonclassical, proteasomal-independent ubiquitination of synphilin-1: implications for Lewy body formation. *The Journal of Neuroscience*, *25*(8), 2002–2009.

Liu, B., Larsson, L., Caballero, A., Hao, X., Öling, D., Grantham, J., & Nyström, T. (2010, January). The polarisome is required for segregation and retrograde transport of protein aggregates. *Cell*, *140*(2), 257–267.

Liu, B., Larsson, L., Franssens, V., Hao, X., Hill, S. M., Andersson, V., ... Nyström, T. (2011, November). Segregation of protein aggregates involves actin and the polarity machinery. *Cell*, *147*(5), 959–961.

Lowe, J., McDermott, H., Landon, M., Mayer, R. J., & Wilkinson, K. D. (1990, June). Ubiquitin carboxyl-terminal hydrolase (PGP 9.5) is selectively present in ubiquitinated inclusion bodies characteristic of human neurodegenerative diseases. *The Journal of pathology*, *161*(2), 153–160.

Marx, F. P., Holzmann, C., Strauss, K. M., & Li, L. (2003). Identification and functional characterization of a novel R621C mutation in the synphilin-1 gene in Parkinson's disease. *Human molecular Genetics*, *12*(11), 1223–1231.

McNaught, K. S. P., & Jenner, P. (2001, January). Proteasomal function is impaired in substantia nigra in Parkinson's disease. *Neuroscience letters*, *297*(3), 191–194.

Mortimer, R. K., & Johnston, J. R. (1959, June). Life span of individual yeast cells. *Nature*, *183*(4677), 1751–1752.

Mouradian, M. M. (2002, January). Recent advances in genetics and pathogenesis of Parkinson disease. *Neurology*, *58*(2), 179–185.

Nagano, Y., Yamashita, H., Takahashi, T., Kishida, S., Nakamura, T., Iseki, E., ... Matsumoto, M. (2003, December). Siah-1 facilitates ubiquitination and degradation of synphilin-1. *Journal of Biological Chemistry*, *278*(51), 51504–51514.

Neystat, M., Rzhetskaya, M., Kholodilov, N., & Burke, R. E. (2002, June). Analysis of synphilin-1 and α-synuclein interactions by yeast two-hybrid β-galactosidase liquid assay. *Neuroscience letters*, *325*(2), 119–123.

Nyström, T. (2007). A Bacterial Kind of Aging. *PLoS genetics*, *3*(12), 2355–2357.

Nyström, T., & Liu, B. (2013, October). Protein quality control in time and space - links to cellular aging. *FEMS Yeast Research*, *14*(1), 40–48.

Outeiro, T. F., & Lindquist, S. (2003, December). Yeast cells provide insight into α-synuclein biology and pathobiology. *Science (New York, N.Y.)*, *302*(5651), 1772–1775.

Polymeropoulos, M. H., Lavedan, C., Leroy, E., Ide, S. E., Dehejia, A., Dutra, A., ... Nussbaum, R. L. (1997, June). Mutation in the α-synuclein gene identified in families with Parkinson's disease. *Science (New York, N.Y.)*, *276*(5321), 2045–2047.

Pruyne, D., Legesse-Miller, A., Gao, L., Dong, Y., & Bretscher, A. (2004). Mechanisms of polarized growth and organelle segregation in yeast. *Annual review of cell and developmental biology*, *20*(1), 559–591.

Racette, B. A., Aschner, M., Guilarte, T. R., Dydak, U., Criswell, S. R., & Zheng, W. (2012, August). Pathophysiology of manganese-associated neurotoxicity. *NeuroToxicology*, *33*(4), 881–886.

Seiberlich, V., Goldbaum, O., Zhukareva, V., & Richter-Landsberg, C. (2012, November). The small molecule inhibitor PR-619 of deubiquitinating enzymes affects the microtubule network and causes protein aggregate formation in neural cells: Implications for neurodegenerative diseases. *Biochimica et biophysica acta*, *1823*(11), 2057–2068.

Sherman, F. (2002). Getting started with yeast. *Methods Enzymology*, *350*, 3–41.

Sidhu, A., Wersinger, C., & Vernier, P. (2004, April). Does α-synuclein modulate dopaminergic synaptic content and tone at the synapse? *FASEB journal : official publication of the Federation of American Societies for Experimental Biology*, *18*(6), 637–647.

Soto, C. (2003, January). Unfolding the role of protein misfolding in neurodegenerative diseases. *Nature reviews. Neuroscience*, *4*(1), 49–60.

Spillantini, M. G., Schmidt, M. L., Lee, V. M. Y., Trojanowski, J. Q., Jakes, R., & Goedert, M. (1997, August). α-Synuclein in Lewy bodies. *Nature*, *388*(6645), 839–840.

Swinnen, E., Büttner, S., Outeiro, T. F., Galas, M.-C., Madeo, F., Winderickx, J., & Franssens, V. (2011, October). Aggresome formation and segregation of inclusions influence toxicity of α-synuclein and synphilin-1 in yeast. *Biochemical Society transactions*, *39*(5), 1476–1481.

Szargel, R., Rott, R., & Engelender, S. (2008, January). Synphilin-1 isoforms in

Parkinson's disease: regulation by phosphorylation and ubiquitylation. *Cellular and Molecular Life Sciences*, *65*(1), 80–88.

Szargel, R., Rott, R., Eyal, A., Haskin, J., Shani, V., Balan, L., ... Engelender, S. (2009, April). Synphilin-1A inhibits seven in absentia homolog (SIAH) and modulates α-synuclein monoubiquitylation and inclusion formation. *Journal of Biological Chemistry*, *284*(17), 11706–11716.

Takahara, T., & Maeda, T. (2012, July). Transient Sequestration of TORC1 into Stress Granules during Heat Stress. *Molecular Cell*, *47*(2), 242–252.

Takalo, M., Salminen, A., & Soininen, H. (2013). Protein aggregation and degradation mechanisms in neurodegenerative diseases. *American Journal of Neurodegenerative Diseases*, *2*(1), 1–14.

Tongaonkar, P., Chen, L., Lambertson, D., Ko, B., & Madura, K. (2000, June). Evidence for an interaction between ubiquitin-conjugating enzymes and the 26S proteasome. *Molecular and Cellular Biology*, *20*(13), 4691–4698.

Towbin, H., Staehelin, T., & Gordon, J. (1979, September). Electrophoretic transfer of proteins from polyacrylamide gels to nitrocellulose sheets: procedure and some applications. *Proceedings of the National Academy of Sciences of the United States of America*, *76*(9), 4350–4354.

Van Zeebroeck, G., Rubio-Texeira, M., Schothorst, J., & Thevelein, J. M. (2014, July). Specific analogues uncouple transport, signalling, oligo-ubiquitination and endocytosis in the yeast Gap1 amino acid transceptor. *Molecular microbiology*, *93*(2), 213–233.

Volles, M. J., & Lansbury, P. T. (2007, March). Relationships between the sequence ofα-synuclein and its membrane affinity, fibrillization propensity, and yeast toxicity. *Journal of molecular biology*, *366*(5), 1510–1522.

Winzeler, E. A., Shoemaker, D. D., Astromoff, A., Liang, H., Anderson, K., Andre, B., ... Davis, R. W. (1999, August). Functional characterization of the *S. cerevisiae* genome by gene deletion and parallel analysis. *Science (New York, N.Y.)*, *285*(5429), 901–906.

Wong, E. S. P., Tan, J. M. M., Soong, W. E., Hussein, K., Nukina, N., Dawson, V. L., ... Lim, K. L. (2008, May). Autophagy-mediated clearance of aggresomes is not a universal phenomenon. *Human Molecular Genetics*, *17*(16), 2570–2582.

Xie, Y.-Y., Zhou, C.-J., Zhou, Z.-R., Hong, J., Che, M.-X., Fu, Q.-S., ... Hu, H.-Y. (2010, January). Interaction with synphilin-1 promotes inclusion formation of α-synuclein: mechanistic insights and pathological implication. *FASEB journal : official publication of the Federation of American Societies for Experimental Biology*, *24*(1), 196–205.

Zaarur, N., Meriin, A. B., Gabai, V. L., & Sherman, M. Y. (2008, October). Triggering aggresome formation. Dissecting aggresome-targeting and aggregation signals in synphilin 1. *Journal of Biological Chemistry*, *283*(41), 27575–27584.

Zabrocki, P., Bastiaens, I., Delay, C., Bammens, T., Ghillebert, R., Pellens, K., ... Winderickx, J. (2008, October). Phosphorylation, lipid raft interaction and traffic of α-synuclein in a yeast model for Parkinson. *Biochimica et Biophysica Acta (BBA) - Molecular Cell Research*, *1783*(10), 1767–1780.

Zabrocki, P., Pellens, K., Vanhelmont, T., Vandebroek, T., Griffioen, G., Wera, S.,

... Winderickx, J. (2005, March). Characterization of α-synuclein aggregation and synergistic toxicity with protein tau in yeast. *The FEBS journal*, *272*(6), 1386–1400.

Zhang, Y., Gao, J., Chung, K. K. K., Huang, H., Dawson, V. L., & Dawson, T. M. (2000, November). Parkin functions as an E2-dependent ubiquitin– protein ligase and promotes the degradation of the synaptic vesicle-associated protein, CDCrel-1. *Proceedings of the National Academy of Sciences of the United States of America*, *97*(24), 13354–13359.

Zhou, C., Slaughter, B. D., Unruh, J. R., & Eldakak, A. (2011). Motility and segregation of Hsp104-associated protein aggregates in budding yeast. *Cell*, *147*(5), 1186–1196.

Zimmerman, D. W. (2004). A note on preliminary tests of equality of variances. *British Journal of Mathematical and Statistical Physiology*, *57*, 173–181.

A. Addendum

A.1 Materials

A.1.1 *S. Cerevisiae* growth media

Rich medium YPD - 1 L

peptone	20 g
yeast extract	10 g
MilliQ	950 mL
40 % glucose	50 mL

For solid medium add 15 g agar and adjust pH to 6.5 using KOH

SD (Minimal medium) - 1 L

NH_4SO_4	5 g
Yeast nitrogen base without AA and growth factors	1.9 g
Complete supplement mixture (CSM) missing AA of choice	see table
MilliQ	950 mL
40 % glucose	50 mL

For solid medium add 15 g agar and adjust pH to 6.5 using KOH

CSM	amount
lacking histidine	770 mg L^{-1}
lacking leucine	690 mg L^{-1}
lacking uracil	770 mg L^{-1}

A.1.2 Alternative *S. Cerevisiae* media

Stock medium - 100 mL

Bactopeptone	2 g
Yeast extract	1 g
H_2O	until 50 mL
Glycerol 100 %	26.1 mL
Adjust volume until 100 mL	

Sporulation medium - 500 mL

KAc	5 g
$KHCO_3$	0.5 g
Agar	7 g
pH 6 with HCl	

All media were autoclaved before use in order to make them sterile.

A.1.3 buffers

Sample buffer 1x

Tris pH 8	50 mM
SDS	2 %
Bromophenol blue	0.1 %
Glycerol	10 %
* β-mercaptoethanol	10 mM

* add just before use

Stripping buffer

SDS	2 %
Tris-HCl pH 6,8	62.5 %
β-mercaptoethanol	100 mM

adjust to desired volume with H_2O.

Running buffer (5X): 1 L

Tris-HCl	15.1 g
Glycine	94 g
SDS	5 g
in water	

Blotting buffer (1X) 2 L

Methanol	400 mL
5X running buffer	400 mL
in water	

Lysis buffer (10 mL)

Table A.1: The content of the optimized lysis buffer used for immunoprecipitation

Component	**Stock concentration**	**Amount (for** 10 mL **final volume)**
HEPES-NaOH (pH 7.5)	500 mM	800 µL
NaCl	1.2 M	1 mL
EDTA	1 M	10 µL
Protease inhibitor (40 µg mL^{-1} aprotinin, 40 µg mL^{-1} leupeptin, 20 µg mL^{-1} pepstatin A)	/	1 tablet
CHAPS	3 %	1 mL
NaF	1 M	500 µL
β-glycerophosphate	1 M	100 µL
MilliQ H_2O	/	6.085 mL
PR-619	40 mM in DMSO	5 µL
N-ethylmaleimide	powder	0.01 g

TBS (1X): 1 L

Tris	25 mM = 87.7 g
NaCl	1.50 M = 30.28 g

adjust pH to 7.6 using HCl

TBST (1X)

Tris	25 mM
NaCl	1.5 M
Tween 20	0.05 %

adjust pH to 8 using HCl

Blocking buffer - 50 mL

Skim milkpowder	2.5 g
in 50 mL TBST	
= 5 % milk solution	

* For the antibody containing milk solutions the correct dilution of antibody (see table 4.4 on page 22) is made in 5 % milk solution.

PBS (1X)

NaCl	137 mM
KCl	2.7 mM
$Na_2HPO_4 \cdot 2\,H_2O$	10 mM
KH_2PO_4	2 mM

Filter the solution using 0.2 µm filter

PBS (1X) + 2 % Tween 20: 50 mL

Tween 20	1 mL
PBS (10X)	5 mL
H_2O	44 mL

PBS (1X) + 0.02 % Tween 20: 50 mL

PBS (1X) + 2 % Tween 20	500 µL
PBS (1X)	49.5 mL

TE buffer (1X)

EDTA	1 mM
Tris-HCl	10 mM

adjust pH to 8

TAE buffer (10x) - 10 L

0.5 M EDTA	200 mL
Tris	484 g
Acetic acid	114 mL

adjust pH to 8 and adjust to a final volume of 10 L with H_2O

Loading buffer (DNA) (6X) - 50 mL

Tris 1 M pH 8	12.5 mL
SDS 10 %	5 g
Bromophenol blue 0.5 %	0.25 g
Glycerol	50 %
in water	

A.2 Solutions

PCl - 100 mL **- pH 8**

Phenol	50 mL
Chloroform	48 mL
Isoamylalcohol	2 mL

APS 10 % **-** 20 mL

APS	2 g
in water, autoclave	

SDS 10 % **-** 500 mL

SDS	50 g
in water, autoclave	

Tris-HCl 1 M **-** 500 mL **- pH 8.8**

Tris	60.57 g
in water, adjust pH to 8.8 with HCl, autoclave	

Tris-HCl 0.25 M **-** 500 mL **- pH 6.8**

Tris	15.14 g
in water, adjust pH to 6.8 with HCl, autoclave	

EDTA 0.5 M **-** 100 mL **- pH 8**

EDTA	14.612 g
in water, autoclave	

NaCl 1.2 M **-** 500 mL

NaCl	35.063 g
In water, autoclave	

Glucose 40 % **-** 1 L

Glucose	400 g
in water, autoclave	

PEG 3350 50 % **-** 250 mL

PEG 3350	125 g
in water, autoclave	

LiAC 1 M **-** 250 mL

LiAc	25.5 g
in water, autoclave	

HEPES/NaOH 0.5 M **-** 100 mL

HEPES	11.9 g
in water, adjust pH to 7.5 with NaOH	

CHAPS 3 % **-** 100 mL

CHAPS	3 g
in water, autoclave	

β**-Glycerophosphate** 1 M **-** 10 mL

β-Glycerophosphate	2.16 g
in water, autoclave	

NaF 1 M **-** 100 mL

NaF	4.2 g
in water, autoclave	

Deubiquitinating enzyme inhibitor PR-619 40 mM **in DMSO**

PR-619	5 mg
in DMSO	560 µL

Proteasome inhibitor MG-132 10 mM **in DMSO**

MG-132	4.756 mg
in DMSO	1 mL

A.2.1 Transformation

Yeast cells from used strains
Microcentrifuge
LiAc 0.1 M
ssDNA (salmon)
Plasmid of choice
Sterile H_2O
PLI-mix (1mL 1 M LiAc, 1 mL H_2O, 8 mL 3350 PEG 50 %)
Vortex
Shaking waterbad (42 °C)
Selective agar medium

A.2.2 Protein extraction

Heat block (95 °C)
Sample buffer 5x (see section A.1.3)
Table centrifuge
Minimal medium (see section A.1.1)

A.2.3 Immunoprecipitation

Heat block (95 °C)
Sample buffer 1x (see section A.1.3)
Table centrifuge
Lysis buffer (see section A.1.3)
Tween 20
Dynabeads protein G
anti-Sy1 antibody
Rotator
1x PBS
Magnet holder
ice
spectrophotometer
BSA ($10\,\mathrm{mg\,mL^{-1}}$)
MP fastprep machine
-80 °C freezer
-20 °C freezer
Selective medium
Incubator 30 °C
Fast prep tubes
Microcentrifuge tubes
Glass beads
Pierce 660nm Protein assay reagent
Beckman DXT 880 Multimode Detector
Plate shaker

A.2.4 Fluorescence-activated cell sorting

PBS (1X) (A.1.3)
Spectrophotometer
DHE dye ($2.5\,\mathrm{mg\,mL^{-1}}$)
PI dye
Plate shaker
Incubator (30 °C)
Table centrifuge
Guava machine
Microtiter plate

Staining solutions 4x

DHE 4x solution: 1 µL of the stock DHE dye (5 mM) (in 1 mL PBS (1X).
PI 4x solution: 1 µL the stock PI dye ($2.5\,\mathrm{\mu g\,mL^{-1}}$) in 1 mL PBS (1X).

A.2.5 Agarose gel electrophoresis

Agarose
TAE buffer (0.5X)
Microwave
Holder
Comb
Erlenmeyer
Gel electrophoresis running block
Loading Dye (6x)
DNA Ladder
Ethidiumbromide

A.2.6 Fluorescence microscopy

DAPI-staining

Eppendorf tubes
Table centrifuge
PBS 1X
100 % EtOH
DAPI dye
Yeast cultures
Fluorescence microscope

CMAC-staining

HEPES solution (10 mM HEPES, pH 7.4 containing 5 % glucose)
Eppendorf tubes
Table centrifuge
CMAC dye
Yeast cultures
Fluorescence microscope

A.2.7 Western blotting

Gels

The gels used for the SDS-PAGE are made of a running and a stacking gel consisting of the following components:

Running gel:

acrylamide/bisacrylamide	3.34 mL
Tris 1 M, pH 8.8	3.75 mL
SDS 10 %	100 µL
H_2O	2.75 mL
APS 10 %	100 µL
TEMED	30 µL

Stacking gel:

acrylamide/bisacrylamide	0.75 mL
Tris 0.25 M, pH 6.8	2.5 mL
SDS 10 %	50 µL
H_2O	1.5 mL
APS 10 %	30 µL
TEMED	10 µL

Amounts are given for 3 gels

SDS-PAGE

heat block (95 °C)
Gels
Sample buffer 1x (see section A.1.3)
Precision Plus Protein All Blue Standards Ladder (Biorad)
Isopropanol
milliQ
Biorad SDS equipment
Falcon tubes
Running buffer (see section A.1.3)

Blotting

Immobilon-PVDF membranes (millipore)
Methanol
Blotting cassette
Tank
Holder
Blotting buffer (see section A.1.3)
Biorad Blotting equipment
Watmann paper
Ice

Immunodetection

TBST (see section A.1.3)
Blocking buffer (see section A.1.3)
ECL-kit
Biospectrum Multispectral imaging system, UVP ® VisionWorks software

A.2.8 Tetrad analysis

MilliQ H_2O
Lyticase ($2\,mg\,mL^{-1}$)
Microcentrifuge tubes
Incubator
Spores
Micromanipulator
YPD plates
Geneticin $150\,\mu g\,mL^{-1}$

A.2.9 PCR

Phenol-chloroform 1:1
Fastprep MP
Fastprep tubes
1x TE buffer, pH 8
H_2O
2.5 mM dNTPS
$5\,U\,\mu L^{-1}$ KAPA Taq DNA polymerase
10x KAPA Taq Reaction Buffer
Primers ($0.1\,\mu g\,mL^{-1}$)
Genomic DNA of interest (from PCI extraction)

A.3 Risk analysis

The functional biology laboratory is a class I laboratory (L1). This means that the organisms (*S. Cerevisiae* BL1 type) and substances we work with have low biological, environmental and health risks. The Good laboratory practices (GLP) and recommendations of the Health-Safety-Environment department from the KU Leuven are applicable for all experimental work. Washing hands before and after the experiments is a must. Furthermore it's required to wear a lab coat, gloves and glasses and to close windows and doors during experimental procedures. Eating, drinking and smoking are never allowed. The fume hood must be clean and disinfected before starting an experiment. Inocultations and manipulations are performed under the flow. Another requirement is to work in an organized manner and not to leave unused tools in the working area. This reduces the risk of contamination. After the experiments, biological and chemical waste needs to be disposed of correctly using the appropriate waste vessels.

We use UV-light (carcinogen), electrodes (electric shock), LiAc (irritating) and yeast extract (possible allergen). Furthermore, we use some compounds that are considered not or little dangerous such as ROS-dihydroethidium, DAPI, CMAC, Tween 20, PEG 3350, Sodium dodecyl sulphate, EDTA, PVDF membranes, Tris-HCl, antibodies and horseradish peroxidase.

Finally, we use some chemicals that are more toxic or dangerous (E3/E4/E5) than the aforementioned and require adapted safety precautions: Acrylamide/bisacrylamide (E4) is carcinogenic, irritating and can have toxic effects after inhalation. β-mercaptoethanol (E4) is deadly if inhaled and causes acute toxicity. TEMED (E3) is a flammable fluid and has toxic effects after inhalation and after being swallowed. Propidium iodide (PI) (E3) is also toxic which means that inhalation should be prevented. Methanol (E4) is highly flammable. Furthermore do not inhale, swallow or let it come in contact with your skin (toxic effects). Also ethanol (E3) is highly flammable. APS (ammoniumpersulfate) (E3) causes acute toxicity, eye and skin irritation and can be harmful if swallowed. Isopropanol (E3) is a flammable substance and irritates the eyes without proper ventilation. Glacial acetic acid (E3) is also flammable. Sodium fluoride (E5) is irritating for eyes and skin and is toxic when swallowed. Phenol-chlorophorm (1:1) (E4) is toxic when making contact with the skin or when swallowed (carcinogen). Moreover, it is deadly if inhaled. N-ethylmaleimide (E4) is deadly when swallowed, can cause severe skin burning and eye injury. Some of these chemicals such as isopropanol and β-mercaptoethanol require a well-ventilated working place. As such, working with these compounds requires a fume hood. If one swallows one of these more dangerous chemicals, one should contact the poison center. If there is contact with the skin make sure that one washes off the skin with water and takes polluted clothes off. After inhalation immediately secure access to fresh air and if necessary, contact a doctor [3].

[3] Databank gevaarlijke stoffen. KU Leuven: https://webwsps.aps.kuleuven.be/irj/portal/desktop/BIG

A.4 Statistics using Prism 6

Table A.2: Overview of the t-tests and their indications used for growth curve analysis

Sign of significance (α=0.05)	**t-test data**	**t-test type**	**Transformants included**
*	between EV and SY1 transformants of red strain/condition	Welch's t-test	All
*	between EV and SY1 transformants of black strain/condition	Welch's t-test	All
**	between EV transformants of black strain/condition and EV transformants of red strain/condition	Welch's t-test	All
**	between SY1 transformants of black strain and SY1 transformants of red strain	Welch's t-test	All

A Welch's t-test is more robust than a students t-test when there is uncertainty about the equality of variances. This together with the fact that preliminary tests of equality of variances often worsen the reliability of the t-test's outcome supports the use of the Welch's t-tests during our analysis (Zimmerman, 2004). Moreover, when performing t-tests we assume that we work with populations that have a normal distribution. In practice, it is hard to perform tests for normality due to the small sample sizes.

FUNCTIONAL BIOLOGY
SECTION OF MOLECULAR PHYSIOLOGY OF PLANTS AND MICRO-ORGANISMS
Kasteelpark Arenberg 31 bus 2433
3001 LEUVEN, BELGIË
tel. + 32 16 32 15 16
fax + 32 16 32 19 67
joris.winderickx@bio.kuleuven.be
www.kuleuven.be